ANALYSIS OF TRF1 FUNCTION IN ALTERNATIVE LENGTHENING OF TELOMERES ACTIVITY

ANALYSIS OF THE ROLE OF TRF1 PHOSPHORYLATION AND TRF1 DOMAIN STRUCTURE IN ALTERNATIVE LENGTHENING OF TELOMERES ACTIVITY

By FLORENCE WILSON, B.Sc (Hon)

A Thesis Submitted to the School of Graduate Studies in Partial Fulfillment of the Requirements for the Degree Master of Science

McMaster University MASTER OF SCIENCE (2014) Hamilton, Ontario (Biology)

TITLE: Analysis of the Role of TRF1 Phosphorylation and TRF1 Domain Structure in ALT activity

AUTHOR: Florence Wilson, B.Sc (Hon)

SUPERVISOR: Dr. Xu-Dong Zhu

NUMBER OF PAGES: xiii, 178

Abstract

Telomeres are heterochromatic DNA-protein structures that protect the ends of linear chromosomes from being recognized as sites of DNA damage and help maintain genomic integrity. The shelterin complex that binds telomeres is vital for regulating telomere length and function, disruption of which can lead to ageing and tumorigenesis. About 90% of human cancers activate telomerase to maintain telomere length, which allows these cells to have unlimited proliferation. The remaining 10% of cancers use a telomerase-independent mechanism that relies on homologous recombination for telomere synthesis, known as alternative lengthening of telomeres or ALT. TRF1, a component of the shelterin complex that binds directly to telomeric DNA, has been implicated in telomere maintenance in both telomerase-positive and negative cancer cells. The function of TRF1 is regulated in part by post-translational modifications, such as phosphorylation. TRF1 phosphorylation at T371 has been implicated in regulating TRF1 functions in mitosis and in the repair of DNA double strand breaks in telomerase-positive cells. The results presented in this thesis demonstrate that TRF1 phosphorylation at T371 is also important in ALT cells and is regulated by DNA damage response factors. T371 phosphorylation is required for the functional assembly of ALT-associated PML bodies and the production of C-circles, which are hallmarks of ALT cancer cells. The results presented in this thesis also suggest that the dimerization and DNA binding capabilities of TRF1 are required for the functional assembly of ALT-associated PML bodies. The work presented here identifies a novel role of TRF1 in ALT activity, which provides further insight into telomere regulation mechanisms in this subset of cancer.

Acknowledgements

I would like to thank my supervisor Dr. Xu-Dong Zhu for her continual support and guidance throughout my graduate studies. Dr. Zhu has provided me with excellent training in many molecular and cellular biology techniques, as well as in data analysis and the critical assessment of other published works. I am very grateful for all of her help and encouragement, and for pushing me to accomplish more than I ever thought I could.

I also owe thanks to the other members of my supervisory committee, Dr. Peter Whyte and Dr. Bagwati Gupta, for their time and assistance.

I would also like to thank other members of the Zhu lab who assisted me with my projects. From teaching me new techniques, to helping me troubleshoot experiments, your assistance was much appreciated. Thank you for being there to keep the lab environment fun and join me for coffee breaks. I wish you all the best of luck in the future.

Thank you to my friends around the Biology department, around campus and outside McMaster who helped keep me grounded and relieved the stress of grad school. You helped me overcome the many challenges I faced and helped keep my spirits up. I would especially like to thank Ben for his support, for teaching me about other areas of science and for making my grad school experience much more fulfilling.

Finally, I would like to thank my family for their continual support, encouragement and love. I would not be where I am today without you.

Table of Contents

List of Figures

List of Abbreviations

53BP1	p53 binding protein 1
ADP	Adenine diphosphate
ALT	Alternative lengthening of telomeres
APB	ALT-associated PML body
ASF1	anti-silencing factor 1
ATM	Ataxia telangiectasia mutated
ATP	Adenosine triphosphate
ATR	Ataxia telangiectasia Rad3-related
BLM	Bloom
BRCA	Breast cancer
BRCT	BRCA1 C terminus
BrdU	Bromodeoxyuridine
CDK	Cyclin-dependent kinase
ChIP	Chromatin immunoprecipitation
Chk	Checkpoint kinase
CK	Casein kinase
CtIP	CTBP-interacting protein
DAPI	4,6-diamindino-2-phenylindole
D-loop	Displacement loop
DMEM	Dulbecco's modified Eagle's media
DMSO	Dimethyl sulfoxide
DNA	Deoxyribonucleic acid
DNA-PK	DNA-dependent protein kinase
DSB	Double strand break
dsDNA	Double stranded DNA
ECTR	Extrachromosomal telomere repeat
ERCC1	Excision repair cross-complementation group 1
EXO	Exonuclease
FISH	Fluorescence in situ hybridization
G1	Gap1
G2	Gap2
GNL3L	Guanine nucleotide binding protein-like 3
HJ	Holliday Junction
HR	Homologous recombination
hTERT	Human telomerase reverse transcriptase
hTR	Human telomerase RNA
IF	Immunofluorescence
IR	Ionizing radiation
Kb	Kilobase
KD	Knockdown
kDa	Kilodalton
MDC1	Mediator of DNA damage checkpoint protein 1

Mre11	Meiotic recombination 11
MRN	Mre11-Rad50-Nbs1
Nbs1	Nijmegen Breakage syndrome 1
NHEJ	Non-homologous end joinging
NIMA	Never-In-Mitosis A
NuRD	Nucleosome remodeling and histone deacetylation
OB	Oligosaccharide/oligonucleotide binding
P	Phospho
PAGE	Polyacrylamide gel electrophoresis
PBS	Phosphate buffered saline
PD	Population doubling
Pin2	Protein interacting with NIMA-2
Plk	Polo-like kinase
PML	Promyelocytic leukemia
PNA	Peptide nucleic acid
POT1	Protein of telomeres 1
PRMT	Protein arginine methyltransferase
Rap1	Repressor/Activator protein 1
RNA	Ribonucleic acid
RNF	Ring finger
RPA	Replication protein A
RTEL1	Regulator of telomere elongation helicase 1
S	Synthesis
SDS	Sodium dodecyl sulfate
sh	Short Hairpin
si	Small interfering
Siah	Seven in absentia homolog
sm	Silent mutation
ssDNA	Single stranded DNA
SUMO	Small ubiquitin-related modifier
TAH1	Telomere-associated homeobox-containing protein 1
TDM	Telomeric-DNA containing double minute chromosomes
TIF	Telomere dysfunction-induce focus
TIN2	TRF1 interacting protein 2
T-loop	Telomeric loop
TPP1	TINT1/PTOP/PIP1
TRAP	Telomere repeat amplification protocol
TRF1	Telomere repeat binding factor 1
TRF2	Telomere repeat binding factor 2
TRFH	TRF homology
T-SCE	Telomere-sister chromatid exchange
V	Vector
WCE	Whole cell extract
WRN	Werner

WT	Wild type
XPF	Xeroderma pigmentosum group F
Xrcc	X-ray repair complementing defective repair in Chinese hamster

CHAPTER 1 INTRODUCTION

1.1 Telomeres and Telomere Length Maintenance

1.1.1 Telomere Structure

Telomeres are dynamic heterochromatic DNA-protein structures located at the ends of linear chromosomes. They protect the ends of DNA from being recognized as sites of DNA damage and help maintain genomic integrity (Denchi & de Lange, 2007; Karlseder, 1999; Takai et al., 2003; van Steensel et al., 1998). Mammalian telomeres are composed of double-stranded tandem repeats of the sequence TTAGGG, as well as a single-stranded 3' G-rich overhang (Cheng et al., 1989; de Lange et al., 1990; Henderson & Blackburn, 1989; Makarov et al., 1997; McElligott & Wellinger, 1997; Meyne et al., 1989; Moyzis et al., 1988; Wright et al., 1997). This hexameric G-rich telomeric sequence is evolutionarily conserved throughout many eukaryotes (Palm & de Lange, 2008; Sfeir et al., 2009). In humans, this repeating sequence ranges from 10 to 15 kilobase (kb) pairs in length at birth, but can be up to 50kb in laboratory rats or mice (Allsopp et al., 1992; de Lange et al., 1990; Harley et al., 1990; Kipling & Cooke, 1990; Palm & de Lange, 2008).

Telomeric DNA is coated in a six-subunit complex known as shelterin, composed of TRF1, TRF2, POT1, TPP1, TIN2 and Rap1 (Figure 1.1). The three main functions of shelterin are to protect chromosome ends from DNA repair mechanisms, to distinguish chromosome ends from DNA breaks elsewhere in the genome and to regulate telomere function and maintenance (Palm & de Lange, 2008). The disruption of shelterin from telomeres produces dysfunctional telomeres that are recognized damaged DNA,

contributing to genome instability, ageing and tumorigenesis (Hockemeyer et al., 2005; McKerlie & Zhu, 2011; Mitchell et al., 2009; Sfeir & de Lange, 2012; Sfeir et al., 2009; Takai et al., 2003; van Steensel et al., 1998; Wang et al., 2004). The binding of this complex to telomeres helps form a higher order t-loop structure (Amiard et al., 2007; Doksani et al., 2013; Griffith et al., 1999; Stansel et al., 2001). This t-loop configuration is formed when the single-stranded 3' overhang loops back on the telomere and displaces a complementary sequence in the double-stranded telomere region (Griffith et al., 1999). A large double-stranded loop is formed with a short region of single-stranded DNA exposed within the loop, known as the displacement loop or D-loop (Griffith et al., 1999). Sequestering the chromosome end in a t-loop is thought to provide a physical barrier against DNA damage repair machinery that would otherwise target exposed DNA ends for repair (Doksani et al., 2013; Griffith et al., 1999).

1.1.2 The End Replication Problem

Most human somatic cells are limited by the number of times they can divide before senescence occurs. This is known as the Hayflick limit and is due to telomere shortening (Hayflick, 1965). Since DNA polymerase can only operate in the 5' to 3' direction, leading and lagging strands are formed during DNA replication, with the lagging strands synthesized discontinuously in small Okazaki fragments (Okazaki et al., 1968). DNA polymerase requires a short RNA primer with a 3'-OH group to start synthesizing an Okazaki fragment. These primers are subsequently degraded and replaced with DNA which is ligated together. However, when the last RNA primer on the lagging strand is removed, a gap forms and there is no free 3'-OH group for DNA polymerase to

use (Levy et al., 1992; Olovnikov, 1971, 1973; Watson, 1972). This results in gradual chromosome shortening with each round of replication, a process known as the end replication problem (Greider & Blackburn, 1987; Olovnikov, 1971, 1973; Watson, 1972). The last RNA primer is located randomly about 70 to 100 nucleotides from chromosome ends, meaning that a length of DNA longer than the RNA primer is lost with each cell division (Chow et al., 2012). Once telomeres shorten to less than 1kb, cells can become irreversibly senescent and are no longer able to divide (Baird & Kipling, 2004; Blasco et al., 1997; Counter et al., 1992). The telomere-imposed limit on the number of times a cell can divide is thought to act as a tumour suppressing mechanism by preventing uncontrolled cell proliferation (Olovnikov, 1971, 1973; Palm & de Lange, 2008); however, the loss of telomeric DNA is correlated with ageing (de Lange et al., 1990; Harley et al., 1990; Hastie et al., 1990). Since telomeres act as a protective cap or buffer region for the rest of the chromosome, cells with longer telomeres are able to go through more cell divisions than cells with shorter telomeres. Cancer cells are able to divide indefinitely and keep their telomeres long by using certain telomere lengthening mechanisms.

1.1.3 Telomere Lengthening Mechanisms

All cancer cells have acquired a mechanism to prevent telomere loss associated with each cell division. About 90% of cancer cells activate telomerase, a reverse transcriptase enzyme responsible for adding telomeric DNA to the ends of chromosomes (Greider & Blackburn, 1985). In telomerase-positive cells, the telomerase ribonucleoprotein extends telomeres by recognizing and binding to the 3' G-rich overhang by its complementary

CCCUAA sequence in the RNA subunit, adding TTAGGG repeats to telomere ends (Blackburn et al., 1989; Greider & Blackburn, 1985, 1987, 1989; Morin, 1989). This addition of DNA thus compensates for the DNA lost during replication. Unlike DNA polymerase, telomerase extension of telomeres does not require an RNA primer, but rather can extend directly from the 3' end of the chromosome (Blackburn et al., 1989; Greider & Blackburn, 1985, 1987, 1989). Telomerase activity is not only restricted to immortal cancer cells, but is also found in germ cells and stem cells, which have elevated proliferative and self-renewal capacities and require long-term viability throughout an individual's lifetime (Broccoli et al., 1995; Cifuentes-Rojas & Shippen, 2012; Kim et al., 1994; Lee et al., 1998).

The remaining 10% of cancers are telomerase-negative and use DNA recombination to maintain their telomere length, in a process known as *a*lternative *l*engthening of *t*elomeres (ALT) (Bryan et al., 1995; Henson et al., 2002; Muntoni & Reddel, 2005), which will be discussed in more detail shortly.

1.2 The Shelterin Complex

The individual protein components of the shelterin complex each play important roles in telomere regulation. TRF1 and TRF2 bind as homodimers to double-stranded telomeric DNA (Bianchi et al., 1997; Bilaud et al., 1997; Broccoli et al., 1997b; Chong et al., 1995; Fairall et al., 2001; Shen et al., 1997; Smogorzewska et al., 2000; van Steensel & de Lange, 1997) and POT1 binds the single-stranded 3' G-rich overhang (Baumann & Cech, 2001; Loayza et al., 2004). TRF1 and TRF2 are both negative regulators of telomere length and have roles in end protection (Ancelin et al., 2002; Celli & de Lange, 2005; de

Lange, 2005; Iwano et al., 2004; Karlseder, 1999; Karlseder et al., 2002; Liu et al., 2004a; Martínez et al., 2009; McKerlie & Zhu, 2011; Sfeir et al., 2009; Smogorzewska et al., 2000; Takai et al., 2010; van Steensel & de Lange, 1997; van Steensel et al., 1998; Wang et al., 2004). TRF1 and TRF2 do not interact directly, but are joined together by TIN2, which also interacts with TPP1 (Broccoli et al., 1997b; Chen et al., 2008c; Fairall et al., 2001; Houghtaling et al., 2004; Kim et al., 2004, 1999a; Ye et al., 2004a; Zhu et al., 2000). TPP1 plays a role in telomerase regulation at telomeres through its recruitment of POT1 to the 3' overhang (O'Connor et al., 2006; Ye et al., 2004b). Rap1 forms a heterodimer with TRF2 in a 1:1 stoichiometric ratio (Li et al., 2000; Zhu et al., 2000). The TRF2/Rap1 complex binds double-stranded DNA and plays a role in the prevention of non-homologous end-joining (NHEJ) at telomeres (Bae & Baumann, 2007; van Steensel et al., 1998).

1.2.1 Telomere Repeat Binding Factor 1 (TRF1)

TRF1 was the first telomere protein identified in mammals (Zhong et al., 1992; Chong et al., 1995) and is transcribed from band q13 of chromosome 8 (Broccoli et al., 1997a). TRF1 is an essential gene since the lack of TRF1 is embryonically lethal (Iwano et al., 2004; Karlseder et al., 2003). TRF1 is a 56 kDa protein that contains an N-terminal acidic domain, a TRF homology (TRFH) homodimerization domain, a flexible linker region and a C-terminal SANT/Myb-like DNA binding domain (Broccoli et al., 1997b; Fairall et al., 2001). TRF1 binds as a homodimer to double stranded telomeric DNA in both interphase and mitosis (Bianchi et al., 1997; Chong et al., 1995; van Steensel & de

Lange, 1997). The flexible linker region in TRF1 allows it to bend and connect relatively distant regions of telomeric DNA (Bianchi et al., 1999; Griffith et al., 1998).

Pin2 is an isoform of TRF1 which is derived from the same gene *PIN2/TRF1* (Shen et al., 1997). It was identified in a yeast two-hybrid screen through its interaction with NIMA (*n*ever-*i*n-*m*itosis *A*) mitotic kinase (Lu et al., 1996). Pin2 and TRF1 are identical in sequence apart from a 20 amino acid deletion in the linker region of Pin2, generated through alternative splicing (Shen et al., 1997). It is possible that this structural difference between TRF1 and Pin2 affects their function at telomeres. Both Pin2 and TRF1 homo- and heterodimers can localize to telomeres, but Pin2 is expressed at about a 5 to 10 fold higher level than TRF1 (Shen et al., 1997).

1.2.2 Telomere Repeat Binding Factor 2 (TRF2)

TRF1 and TRF2 have several similarities and are likely paralogous (Bilaud et al., 1997; Broccoli et al., 1997b). They have structural similarities and are both able to bind to double-stranded telomeric DNA, but they contain different domains, have different functions and interact with different proteins (Chen et al., 2008c; Palm & de Lange, 2008). TRF1 and TRF2 both contain Myb-type domains which bind to double-stranded telomeric DNA, as well as TRFH domains, through which homodimerization occurs (Bianchi et al., 1997; Bilaud et al., 1997; Broccoli et al., 1997b; Chong et al., 1995; Fairall et al., 2001; Shen et al., 1997; Smogorzewska et al., 2000; van Steensel & de Lange, 1997). However, TRF1 and TRF2 are unable to directly interact with each other (Broccoli et al., 1997b; Fairall et al., 2001; Zhu et al., 2000).The main structural difference between these two proteins is that TRF1 contains an acidic N-terminal domain

whereas TRF2 contains a basic N-terminal domain that is rich in glycines and arginines (Broccoli et al., 1997a, 1997b; Chong et al., 1995; Mitchell et al., 2009).

The main function of TRF2 is to protect telomeres from being recognized as damaged DNA (Celli & de Lange, 2005; Karlseder, 1999; van Steensel et al., 1998). The flexibility of the hinge region in TRF2 aids in its ability to form t-loop structures (Stansel et al., 2001). If TRF2 is not present in cells, the 3' G-rich overhang is degraded, which is through to prevent t-loop formation (Celli & de Lange, 2005; Stansel et al., 2001; van Steensel et al., 1998). The exposed overhang is recognized as a double-strand break via activation of the ATM and p53 DNA damage response pathway and telomere fusions occur in an attempt to repair the damage, leading to cellular senescence or apoptosis (Celli & de Lange, 2005; Iwano et al., 2004; Karlseder, 1999; Karlseder et al., 2002; van Steensel et al., 1998). The presence of TRF2 on telomeres prevents overhang loss, thus preventing NHEJ repair of chromosome ends and fusions (Zhu et al., 2003). ERCC1/XPF is involved in nucleotide excision repair (Sijbers et al., 1996). TRF2 and ERCC1/XPF associate at telomeres and the endonuclease activity of ERCC1/XPF is involved in processing the 3' overhang (Zhu et al., 2003). In cells expressing a dominant negative allele of TRF2 ($TRF2^{\Delta B \Delta M}$), ERCC1/XPF degrades the 3' overhangs and cells develop telomere fusions. This suggests that TRF2 protects telomeric overhangs from ERCC1/XPF processing and NHEJ repair (Zhu et al., 2003). TRF2 is also a negative regulator of telomere length, but unlike TRF1, this is in a telomerase-independent manner. Telomere length decreases when TRF2 is overexpressed in either telomerase-positive or telomerase-negative cells, and conversely, shRNA knockdown of TRF2 results

in telomere elongation (Karlseder et al., 2002; Smogorzewska et al., 2000; Takai et al., 2010). TRF2 methylation by the protein arginine methyltransferase PRMT1 is also important in regulating its function in telomere length maintenance and genomic stability (Mitchell et al., 2009).

1.2.3 TRF1-Interacting Nuclear protein 2 (TIN2)

Located centrally in the shelterin complex, TIN2 interacts with TRF1, the TRF2/Rap1 complex and TPP1, acting as a bridge to stabilize these components (Houghtaling et al., 2004; Liu et al., 2004a; O'Connor et al., 2006; Ye & de Lange, 2004; Ye et al., 2004a). TIN2 was identified through a yeast two-hybrid screen where the C-terminus of TIN2 containing an FxLxP motif was found to interact with the TRFH domain of TRF1 (Kim et al., 1999a). The N-terminus of TIN2 interacts with a hinge domain region in TRF2 (Chen et al., 2008c; Kim et al., 2004). Expression of truncated TIN2 proteins that cannot interact with either TRF1 or TRF2 results in telomere deprotection, which is accompanied by elevated levels of γH2AX and 53BP1 foci at telomeres, indicating a DNA damage response (Kim et al., 2004). In addition, cells lacking functional TIN2 show reduced levels of TRF2, TRF1 and Rap1 at telomeres, indicating that TIN2 is important for the localization and stability of other shelterin components and also for telomere protection and length control (Kim et al., 2004; Ye et al., 2004a). In telomerase-positive cells, TIN2 acts as a negative regulator of telomerase-dependent telomere elongation by mediating the function of TRF1 (Kim et al., 1999a). Expression of TIN2 truncation mutants that can still interact with TRF1 results in telomere elongation (Kim et al., 1999a). Additionally, telomerase-positive cells depleted

for TIN2 via shRNA show telomere elongation, resembling the phenotype of TRF1 depletion (Ye & de Lange, 2004). TIN2 influences the TRF1-tankyrase 1 interaction by preventing tankyrase 1 from modifying TRF1, thus stabilizing TRF1 on telomeres (Ye & de Lange, 2004). Since TIN2 is a central scaffolding protein in the shelterin complex, its stability can regulate other proteins in the complex. The E3 ligase Siah2 is responsible for the ubiquitination of TIN2, targeting TIN2 to the proteasome for degradation (Bhanot & Smith, 2012).

1.2.4 Repressor/Activator Protein 1 (Rap1)

Identified in a yeast-two hybrid screen, human Rap1 (hRap1) associates with the shelterin complex through interaction with TRF2 since it is unable to bind DNA itself (Li & Lange, 2003; Li et al., 2000). TRF2 and hRap1 are found in a ratio of approximately 1:1 (Zhu et al., 2000). The TRF2/Rap1 complex plays a role in the prevention of NHEJ at telomeres (Bae & Baumann, 2007; Li & Lange, 2003; Sarthy et al., 2009; van Steensel et al., 1998). Rap1 has also been identified as a repressor of homology directed repair (HDR) at telomeres (Sfeir et al., 2010). Telomeres lacking Rap1 undergo an elevated level of HDR, but do not contain detectable TIFs, unlike when either TRF2 or POT1 are removed and TIFs are formed (Sfeir et al., 2010).

1.2.5 Protection of Telomeres 1 (POT1)

Human POT1 was identified through sequence homology with the *Schizosaccharomyes pombe* protein (Baumann & Cech, 2001). POT1 is connected to the shelterin complex through its interaction with TPP1 (Liu et al., 2004b; Ye et al., 2004b). The interaction between POT1 and TPP1 greatly enhances the ability of POT1 to localize

to and protect telomeres from fusions and from the induction of DNA damage responses and dysfunctional telomere-induced foci (Hockemeyer et al., 2007; Wang et al., 2007; Xin et al., 2007). The N-terminus of POT1 contains two OB-fold domains, allowing it to bind to the single-stranded 3' G-rich overhang at telomeres (Baumann & Cech, 2001; Kelleher et al., 2005; Lei et al., 2004; Loayza & Lange, 2003). The interaction between POT1 and ssDNA has been demonstrated both *in vitro* through gel shift assays (Baumann & Cech, 2001; Kelleher et al., 2005) and *in vivo* through ChIP assays (Loayza & Lange, 2003). POT1 can also bind to the single-stranded DNA within the D-loop (Loayza & Lange, 2003; Palm & de Lange, 2008).

It has been proposed that the TRF1 complex mediates POT1 binding to telomeres, since longer telomeres are capable of binding more TRF1 and therefore capable of binding more POT1 (Loayza & Lange, 2003). POT1 may act to relay information from the TRF1 complex to the telomere terminus where telomerase activity is regulated (Loayza & Lange, 2003). ChIP analysis showed that a reduction in TRF1 at telomeres due to tankyrase 1 overexpression results in less POT1 bound to telomeres (Loayza & Lange, 2003). In addition, a mutant POT1 lacking the OB-fold is unable to bind to telomeres and causes rapid telomere elongation, even though TRF1 levels are unaffected (Loayza & Lange, 2003). These results demonstrate the intricate interactions between TRF1 and POT1 required for telomere length regulation.

POT1 also plays an important role in repressing the ATR-mediated DNA damage response pathway, partially through its exclusion of RPA from telomeres (Denchi & de Lange, 2007; Gong & de Lange, 2010; Takai et al., 2011). The ATR pathway is activated

in response to single stranded DNA, making POT1 an ideal suppressor of this pathway at telomeres (Denchi & de Lange, 2007). POT1 has been reported to interact with the RecQ helicases WRN and BLM (Opresko et al., 2005) and to aid in the dissociation of telomeric G-quadruplexes (Zaug et al., 2005), potentially facilitating recombination and telomere replication.

1.2.6 TPP1 (TINT1/PTOP/PIP1)

TPP1 is known formerly as TINT1, PTOP and PIP1 since it was discovered by three separate groups (Houghtaling et al., 2004; Liu et al., 2004b; Ye et al., 2004b). TPP1 has no DNA binding activity itself (Wang et al., 2007; Xin et al., 2007), but links POT1 to TIN2 (Abreu et al., 2010; Takai et al., 2010, 2011). The OB-fold domain at the N-terminus of TPP1 is essential for the recruitment of telomerase to telomeres and thus for telomere elongation in telomerase-positive cells (Xin et al., 2007; Zhong et al., 2012).

1.3 Telomeres and the DNA damage response

The structure of telomeres, including the shelterin complex, t-loop and accessory factors, helps to prevent chromosome ends from being recognized as broken or damaged DNA. DNA is constantly exposed to damaging agents, including reactive oxygen species, ionizing radiation, ultraviolet radiation and chemicals. DNA double strand breaks (DSBs) are a harmful consequence of this exposure and must be repaired efficiently and accurately to maintain genome integrity. The two major pathways involved in the repair of DSBs are non-homologous end joining (NHEJ) and homologous recombination (HR) (Figure 1.2) (Liang et al., 1998; Rouet et al., 1994). The choice between NHEJ and HR is controlled by two main tumour suppressor proteins, 53BP1 and BRCA1. These proteins

have an antagonistic relationship, with 53BP1 promoting NHEJ and BRCA1 promoting HR (Bouwman et al., 2010; Bunting et al., 2010; Cao et al., 2009; Dimitrova et al., 2008; Escribano-Díaz et al., 2013; Moynahan et al., 1999; Nakamura et al., 2006; Schultz et al., 2000; Scully et al., 1997; Xu et al., 2001). It has been suggested that deprotected telomeres bound by 53BP1 have increased mobility, which increases the probability that telomeres will become close enough to fuse through NHEJ (Dimitrova et al., 2008). The antagonistic relationship between 53BP1 and BRCA1 was first discovered in mice. Expression of a mutant BRCA1 allele (a deletion of exon 11, $Brca1^{\Delta 11/\Delta 11}$) in mice resulted in tumorigenesis, chromosomal abnormalities and embryonic lethality (Xu et al., 2001). Deleting 53BP1 in addition to BRCA1 was able to rescue many of these defects, but an elevated level of genomic instability was still present (Cao et al., 2009). The relationship between 53BP1 and BRCA1 is specific, as depletion of 53BP1 is unable to rescue cells lacking Xrcc2 or Brca2, which are two other important HR proteins (Bouwman et al., 2010; Bunting et al., 2010).

The telomeric structure helps prevent DNA damage responses by repressing the activation of the two main DNA damage response kinases, ATM and ATR (Griffith et al., 1999; Guo et al., 2007; Takai et al., 2003). The presence of DSBs in a cell activates the ATM kinase, while single stranded DNA activates ATR (Shiloh, 2003; Zhou & Elledge, 2000). Both kinases are also activated when telomeres reach a critically short length, possibly due to an insufficient amount of shelterin at telomeres (Guo et al., 2007; Karlseder, 1999; Takai et al., 2003; Vaziri et al., 1997). The phosphorylation and activation of Chk1 and Chk2 via ATM and ATR can result in cell cycle arrest and p53

activation, leading to inhibition of cell division (Bartek & Lukas, 2003; Palm & de Lange, 2008).

The accumulation of protein complexes at DNA sites can be visualized through cytological techniques and are termed "foci". When DNA damage and repair proteins accumulate at dysfunctional telomeres, the resulting foci are known as telomere dysfunction-induced foci or TIFs (Takai et al., 2003).

1.3.1 Homologous Recombination

Homologous recombination can occur in response to DNA lesions but is also used as a telomere maintenance mechanism in ALT cells. HR is predominantly an error-free pathway and involves the pairing and exchange of two homologous DNA molecules (Chapman et al., 2012; Moynahan & Jasin, 2010; San Filippo et al., 2008). HR is limited to S and G2 phases, since cells are enriched with sister chromatids at this time, providing the template DNA necessary for this process (Liang et al., 1998). Using HR to repair DNA when sister chromatids are available helps prevent unnecessary mutagenesis. Defects in HR are associated with genome instability and a predisposition to cancer; for example, humans expressing a defective or mutated version of the HR protein BRCA1 show elevated levels of breast and ovarian cancer (Easton et al., 1993; Szabo & King, 1995; Tirkkonen et al., 1997; Tomlinson et al., 1998).

An overview of the HR process is shown in Figure 1.2. An early step in HR involves the binding of the Mre11-Rad50-Nbs1 (MRN) complex to DNA ends (Carson et al., 2003; Nelms & Petrini, 1998; Petrini, 1999). Following this, the ATM phosphoinositide-3-kinase is recruited and activated by MRN (Falck et al., 2005; Jazayeri et al., 2006; Lee

& Paull, 2004; Uziel et al., 2003; You et al., 2005). ATM and MRN regulate each other's activity through a positive feedback loop (Jazayeri et al., 2006; Lee & Paull, 2005; Lim et al., 2000; Wu et al., 2007). One of the initial responses of ATM is to phosphorylate histone H2AX on S139, forming γH2AX, and leading to the recruitment of other repair factors (Burma et al., 2001; Paull et al., 2000; Rogakou et al., 1998; Takai et al., 2003). Next, the mediator and scaffold protein MDC1 is recruited through binding to γH2AX, which in turn promotes binding of the E3 ubiquitin ligase RNF8 (Chapman et al., 2012; Huen et al., 2007; Lukas et al., 2004; Stucki et al., 2005). Then, the recruitment and interaction of 53BP1 and BRCA1 promotes the appropriate repair pathway (Chapman et al., 2012; Huen et al., 2007). The nuclease CTBP-interacting protein (CtIP) is phosphorylated at S327 by cyclin-dependent kinases (CDKs) in G2 phase (Yu & Chen, 2004). Once CtIP is phosphorylated it can interact with BRCA1, which has E3 ubiquitin ligase activity. This allows BRCA1 to ubiquitinate CtIP and enhance its DNA association (Yu et al., 2006). CtIP phosphorylation also promotes its interaction with MRN, required for end resection (Chen et al., 2008a; Paull, 2010; Sartori et al., 2007). The combined action of the CtIP-MRN complex, in conjunction with BLM and EXO1 nucleases, helps promote nucleolytic end-resection and the production of single stranded DNA (Chapman et al., 2012; Gravel et al., 2008; Nimonkar et al., 2011; Sartori et al., 2007). Replication protein A (RPA) binds to the single stranded DNA produced by resection, stabilizes the DNA and protects it from degradation (Alani et al., 1992; Coverley et al., 1992). Rad51 displaces RPA and forms a nucleoprotein filament wrapped around the single stranded DNA (Liu et al., 2010; New et al., 1998). Rad51 recombinase is stimulated by a direct

interaction with Rad52 (Milne & Weaver, 1993; Shen et al., 1996) and invades the complementary strand of DNA, searching for a "donor" homologous sequence to use as a template (Baumann & West, 1998). This process forms a displacement loop (D loop) (Radding, 1978). Rad54 appears to stimulate topological changes in this invasion, including the introduction of negative supercoils into DNA (Petukhova et al., 1999; Tan et al., 1999) and disassembling Rad51 filaments from dsDNA (Solinger et al., 2002). DNA synthesis occurs through the action of DNA polymerase δ and the processivity factor PCNA, extending the 3' end of the invading strand using the donor strand as a template (Li et al., 2009). Nucleotides that were lost through the initial resection are also replaced at this point, followed by Holliday junction resolution and ligation of DNA ends (Constantinou et al., 2001; Duckett et al., 1988; Heyer et al., 2010; Liu et al., 2004c). Depending on how the intermediates of the HR process are resolved, either crossover or non-crossover products can be formed (San Filippo et al., 2008). It is important that the correct resolution is chosen, depending on the situation; crossing over is essential in meiotic cells but it is avoided in mitotic cells, since this may increase mutations such as translocations (Chapman et al., 2012).

1.3.2 Non-Homologous End Joining

The NHEJ repair pathway is much more error-prone than HR, since DNA ends are directly ligated, which frequently results in deletions and insertions at the break site (Chapman et al., 2012; Liang et al., 1998; Lieber, 2010; Rouet et al., 1994). NHEJ is the main form of DNA repair in mammalian cells since it occurs more rapidly than HR and is active throughout the cell cycle, favoured especially in G1 cells (Burma et al., 2006; Mao

et al., 2008). As shown in Figure 1.2, this process begins similarly to HR. The activation of ATM and MRN at a DNA break triggers the accumulation of γH2AX, which leads to the recruitment of other repair factors and 53BP1 promotes the NHEJ pathway. The next complex to bind the break site is DNA-dependent protein kinase (DNA-PK) holoenzyme, composed of a Ku70/80 heterodimer and a catalytic subunit (Gottlieb & Jackson, 1993). The Ku70/80 heterodimer component of this complex holds DNA ends together (Burma et al., 2006; Falzon et al., 1993; Walker et al., 2001). The binding of Ku to dsDNA ends recruits and activates the catalytic subunit of DNA-PK (DNA-PKcs) (Dynan & Yoo, 1998; Gottlieb & Jackson, 1993). The nuclease Artemis is also recruited, and its phosphorylation by DNA-PKcs activates its 5' to 3' endonuclease activity, enabling Artemis to process DNA ends if they are not compatible to be ligated directly (Ma et al., 2002; Moshous et al., 2001). If a gap is formed by resection of the break, DNA polymerases fill the gap and DNA ligase IV joins the DNA ends together, while XRCC4 helps stabilize and stimulate ligase IV (Burma et al., 2006; Grawunder et al., 1997; Modesti et al., 1999).

1.4 Alternative Lengthening of Telomeres

Besides serving as a DNA damage repair mechanism, HR can also occur at telomeres and is used as a telomere lengthening mechanism in some cells. Most cancer cells express telomerase through transcriptional up-regulation (Shay & Bacchetti, 1997), but a subset of tumours are telomerase-negative and use DNA recombination to maintain their telomere length (Dunham et al., 2000; Londoño-Vallejo et al., 2004; Lundblad & Blackburn, 1993). This mechanism is known as alternative lengthening of telomeres

(ALT) (Bryan et al., 1995; Henson et al., 2002; Muntoni & Reddel, 2005). In ALT cells, telomeres have been observed to undergo several types of HR, including homologous recombination at the t-loop, telomere-sister chromatid exchange, recombination between the telomere and interstitial DNA sites, and recombination with extrachromosomal telomere repeats (Palm & de Lange, 2008). There are several main characteristics of ALT cells that distinguish them from telomerase-positive cells; a heterogeneous telomere length distribution, elevated telomere-sister chromatid exchange (T-SCE) events, the presence of ALT-associated promyelocytic leukemia bodies (APBs) and extrachromosomal telomere repeats (ECTRs). The majority of ALT cells display all of these characteristics and thus operate in the canonical ALT pathway. Although very rare, it is also possible for cells to exhibit ALT activity, but lack one or more of these characteristics, referred to as the non-canonical ALT pathway (Chung et al., 2012). This may suggest that multiple ALT mechanisms of telomere regulation exist (Muntoni & Reddel, 2005).

ALT is activated in cancers of neuroepithelial origin, such as astrocytomas, and of mesenchymal origin, including soft tissue sarcomas and osteosarcomas (Henson et al., 2005). The prognostic outcome of ALT tumours appears to vary with cell type (Muntoni & Reddel, 2005). The astrocytoma glioblastoma multiforme is the most common and most malignant form of brain cancer in humans (Darefsky et al., 2012). Although treatment options have improved greatly in the past two decades, patient prognosis is still poor, with a mean survival time of several months to two years after diagnosis (Darefsky et al., 2012; Hakin-Smith et al., 2003).

Just as telomerase activity exists normally in germ cells and stem cells but is upregulated in telomerase-positive tumours, it has been proposed that ALT is a normal telomere maintenance mechanism, but that ALT regulation is lost in ALT-positive tumours, leading to overly active and unscheduled HR (Muntoni & Reddel, 2005). Similar to telomerase activation, ALT activation also requires the loss of normal p53 tumour suppressor function (Mekeel et al., 1997; Rogan et al., 1995; Stampfer et al., 2003). It is also possible that reduced telomere protection caused by loss of the shelterin complex may increase recombination at telomeres and promote ALT; for example, low levels of TRF2 at telomeres have been found in some ALT cell lines (Cesare et al., 2009). When ALT cells are fused with telomerase-positive cells or with normal fibroblasts, ALT activity is repressed and telomerase is activated, suggesting that a loss of normal suppressor function may trigger ALT activity (Cesare et al., 2009; Perrem et al., 1999).

Another interesting phenotype of ALT cells is the presence of spontaneous telomere dysfunction in the absence of exposure to DNA damage. Metaphase chromosomes in untreated ALT cells show γH2AX staining predominantly at telomeres, with a signal at either one or both sister chromatid ends. This staining pattern is referred to as metaphase TIFs or meta-TIFs (Cesare et al., 2009). Spontaneous meta-TIFs occur more frequently in ALT cells, such as GM847, than in telomerase-positive cells and appear to be caused by telomere dysfunction, since similar meta-TIFs can be produced in telomerase-positive cells by overexpressing $TRF2^{\Delta B \Delta M}$ or cells depleted of POT1 (Cesare et al., 2009). The presence of many meta-TIFs in a cell line seems to be correlated with a loss of p53 function, and cell lines with limited or no telomerase activity have a higher abundance of

meta-TIFs (Cesare et al., 2009). Notably, the human ALT osteosarcoma cell line U2OS is the only ALT cell line known to have functional wild-type p53, and U2OS cells have a similar low level of γH2AX meta-TIFs as telomerase-positive cells (Cesare et al., 2009). Even though most ALT cells display a high number of meta-TIFs, there are very few spontaneous end-to-end telomere fusions in these cells, suggesting that the telomere dysfunction causing meta-TIFs is distinct from that causing fusions (Cesare et al., 2009). The number of meta-TIFs in GM847 cells can be reduced by overexpressing TRF2 (Cesare et al., 2009). Since ALT cells have a low level of TRF2 protein compared to the amount of telomeric DNA, this change may be due to rescuing the level of TRF2 relative to telomeric DNA, rather than inhibiting the DNA damage response at telomeres (Cesare et al., 2009).

1.4.1 Extrachromosomal Telomere Repeats

The presence of nuclear extrachromosomal telomere repeats (ECTRs), often in the form of circles, is used as a marker for ALT cells. The t-loop formation at telomeres has been described as an intermediate structure in homologous recombination (Jiang et al., 2007). When HR occurs at the t-loop and the Holliday junction (HJ) is resolved, an excised telomeric circle or linear fragment and a truncated telomere are produced (Cesare & Griffith, 2004; Lustig, 2003; Muntoni & Reddel, 2005; Wang et al., 2004). Telomeric circles may occur as a by-product of normal mechanisms that trim long telomeres to regulate telomere length (Pickett et al., 2009). T-loop resolution frequently results in telomeric rapid deletion (TRD) events (Li & Lustig, 1996; Palm & de Lange, 2008; Wang et al., 2004). These sudden lengthening and shortening events help explain why ALT cells

show such heterogeneity in telomere length, with lengths ranging from <1 to >50kb (Bryan et al., 1995; Rogan et al., 1995). Holliday junction resolution depends on the resolvase activity of XRCC3, as well as on Nbs1 (Liu et al., 2004c; Wang et al., 2004). The helicase WRN has also been implicated in the branch migration step of t-loop HR (Li et al., 2008). Perturbing the end-protection roles of TRF2 and POT1 can produce a situation where ECTRs are formed and T-SCE events occur. In telomerase-positive cells, overexpression of a TRF2 allele with a basic domain deletion ($TRF2^{\Delta B}$) can result in circle formation through t-loop HR, indicative of the role of TRF2 in forming t-loops and inhibiting Holliday junction resolution (Wang et al., 2004). Inhibition of POT1 function in telomerase-positive cells can also induce t-loop resolution and T-SCE events (Opresko et al., 2005; Wu et al., 2006). Although ALT cells show elevated levels of HR at telomeres, there does not appear to be an increase in recombination throughout the genome (Bechter et al., 2003, 2004; Cho et al., 2014).

ALT cells contain several forms of telomeric circles (Figure 1.3); t-circles are relaxed double-stranded circles with nicks in both strands, whereas C-circles and G-circles are both partially single-stranded, self-priming circles, containing either C-rich or G-rich ssDNA (Cesare & Griffith, 2004; Henson et al., 2009). C-circles have been reported to be the most reliable marker for ALT activity (Henson et al., 2009). C-circles are specific to ALT cells, whereas t-circles can be induced in telomerase-positive cells (Cesare & Griffith, 2004; Henson et al., 2009; Wang et al., 2004; Wu et al., 2006). The appearance of C-circles is associated with ALT activation and the level of C-circles tends to correlate with the level of ALT activity (Henson et al., 2009). The ALT-positive subclonal cell line

C3-c16 (created from WI38-VA13/2RA cells expressing functional hTR but catalytically inactive hTERT) is a telomerase-negative cell line that is devoid of APBs, t-circles and length heterogeneity, yet telomere length is still maintained (Cerone et al., 2005). C-circles are present in this cell line, suggesting that C-circles could be a reliable indicator of ALT activity, regardless of other ALT characteristics (Henson et al., 2009).

It is thought that telomeric circles are used as a template for telomere elongation through rolling-circle amplification. The 3' G-rich single-stranded telomeric overhang pairs with complementary bases in C-circles and G-circles and uses the overhang as a primer and the circle as a template sequence (Henson et al., 2002; Nabetani & Ishikawa, 2011; Natarajan & McEachern, 2002). Since t-circles have nicks in both DNA strands, they are only able to undergo one round of rolling-circle amplification, unless these nicks are ligated (Henson et al., 2009; Wang et al., 2004). The process of rolling-circle amplification has been used *in vitro* to amplify telomeric DNA (Henson et al., 2009), supporting the role of ECTRs in telomere regulation.

1.4.2 Telomere-Sister Chromatid Exchanges

Recombination at telomeres can also result in telomere-sister chromatid exchange (T-SCE) where leading and lagging strand sequences are exchanged (Londoño-Vallejo et al., 2004). It has been suggested that these events are specific to ALT cells (Londoño-Vallejo et al., 2004), but some telomerase-positive cells and cells with short or damaged telomeres may also show elevated T-SCE (Jin & Ikushima, 2004; Wang et al., 2005). Therefore T-SCE may not always be a reliable indicator of ALT activity (Henson & Reddel, 2010).

In contrast to telomeric circle formation, overexpression of the TRF2$^{\Delta B}$ allele in telomerase-positive cells does not result in elevated T-SCE events, indicating that the basic domain of TRF2 is not required for TRF2 to repress this process (Celli et al., 2006). Since telomeres contain repetitive DNA sequences, it is possible for sister telomeres to find homologous sites at various locations along the telomere, possibly resulting in unequal exchange. Unequal T-SCEs can be detrimental to genomic integrity, as one sister telomere could lose DNA to the other, resulting in daughter cells with either elongated or shortened telomeres (Celli et al., 2006; Palm & de Lange, 2008). Cell cycle arrest is possible in a cell with one short telomere, so the daughter cell that receives the shorter telomere would soon senesce or die (Hemann et al., 2001). Although this seems detrimental to the cell population, the cell with the longer telomere now has increased proliferative potential, ultimately immortalizing these cells (Muntoni & Reddel, 2005).

Recombination can also occur between a telomere and an internal TTAGGG-like sequence within the chromosome, which may be how telomeric-DNA containing double minute chromosomes (TDMs) form (Zhu et al., 2003). The endonuclease complex ERCC1/XPF, likely recruited to telomeres through an interaction with TRF2, may help prevent this aberrant event from occurring by cleaving an intermediate HR structure (Zhu et al., 2003). WRN helicase has also been proposed to reduce T-SCE and prevent TDMs from forming by repressing the formation of recombination intermediates (Laud et al., 2005).

1.4.3 ALT-Associated PML Bodies

Homologous recombination occurs in late S and G2 phase and this is correlated with the presence of ALT-associated PML bodies (APBs) (Wu et al., 2000a). APBs are defined as the co-localization of telomeric DNA, telomere-binding proteins and other proteins involved in recombination within promyelocytic leukemia (PML) nuclear bodies (Grobelny et al., 2000; Pickett et al., 2009; Yeager et al., 1999). Despite this true definition, cytological experiments most often use the localization of a single telomere-binding protein or recombination factor within the PML body as an indicator of APBs. PML bodies are present in both telomerase-positive and ALT cells, but the clusters of chromosome ends in these bodies is only associated with ALT activity and only occurs in a subset of PML bodies (Henson et al., 2005; Yeager et al., 1999). Telomeric clusters at APBs tend to have a greater signal intensity than telomeres not at APBs (Henson & Reddel, 2010; Yeager et al., 1999). Bringing telomeres in close proximity within PML bodies is thought to facilitate recombination between homologous sequences, but the details of this process are still unknown (Draskovic et al., 2009). There is a strong correlation between APBs and ECTRs in ALT cells, regardless of whether these characteristics are elevated or reduced. For example, cells depleted for the histone chaperone anti-silencing factor 1 (ASF1) show elevated levels of APBs and ECTRs (O'Sullivan et al., 2014), whereas cells depleted for the telomere-associated homeobox-containing protein 1 (TAH1) show reduced levels of APBs and ECTRs (Feng et al., 2013). This further suggests that telomeric recombination occur at APBs.

There are various techniques for scoring APBs, including counting the number of cells with at least one APB showing clustered proteins or telomeric DNA of increased signal intensity localized completely within the PML body (Henson et al., 2005; Jiang et al., 2005; Laud et al., 2005; Wang et al., 2013; Zhong et al., 2007), the number of cells with APBs of small or large size (Fasching et al., 2007), the number of APBs per cell (Cho et al., 2014; Conomos et al., 2012; Feng et al., 2013), or using 3D computer scanning technology to record APB co-localizations (Osterwald et al., 2012; Pickett et al., 2009; Potts & Yu, 2007). The APB scoring technique that is used could potentially influence the experimental outcome, so it is crucial that an appropriate technique is chosen, that the results it produces are reproducible, and that the technique is documented accurately so that data can be interpreted accordingly.

PML bodies are mobile nuclear organelles found in various cell types. These hollow shell structures range in size from 0.25 to 1μm in diameter (Lang et al., 2010). The shell thickness of PML bodies varies between 50 to 100nm and is independent of APB size (Lang et al., 2010). Between 5 to 30 PML bodies can be found within a cell nucleus at a given time, depending on the cell type, phase of the cell cycle and stimuli that are present (Chung et al., 2012). The proteins PML and Sp100 are the main structural components of PML bodies. Both of these proteins contain SUMO interacting motifs and are post-translationally sumoylated (Chung et al., 2012; Hecker et al., 2006). PML bodies have a variety of functions, including transcription regulation (Vallian et al., 1997; Xie et al., 1993), an apoptotic role (Wang et al., 1998), viral genome replication (Maul et al., 1993) and they are potential sites of RNA accumulation and transcription factor storage (Doucas

et al., 1999; LaMorte et al., 1998). In ALT cells, PML bodies are involved in DNA repair and transiently associate with many cellular factors, providing a nuclear sub-compartment with ideal catalytic conditions for reactions to take place (Chung et al., 2012; Draskovic et al., 2009; Lallemand-Breitenbach & de Thé, 2010). During mitosis, the PML protein scaffold becomes highly dynamic and de-sumoylated, leading to breakdown of the structure (Everett et al., 1999; Lang et al., 2010). Thus, APBs are not present in mitotic cells and the co-localization of telomeric DNA with PML is only visible from early G1 to late G2 phase (Draskovic et al., 2009). Under normal circumstances, APBs are enriched in late S and G2 phase when DNA recombination is most active (Grobelny et al., 2000; Perrem et al., 2001). A proposed model for APB formation is through a sequential assembly mechanism. An initial sumoylation of telomere proteins by MMS21 may promote the recruitment of a PML and Sp100 structural scaffold, which is required for the subsequent recruitment of DNA repair and HR proteins, such as Nbs1 and Rad51 (Chen et al., 2008b; Chung et al., 2011; Jiang et al., 2007). The PML scaffold also appears to promote telomere clustering and recombination within the APB (Cho et al., 2014; Chung et al., 2011; Draskovic et al., 2009).

DNA synthesis occurs at APBs, shown by the incorporation of the thymidine analogue bromodeoxyuridine (BrdU) in late S and G2 phase cells (Grobelny et al., 2000; Wu et al., 2000a). DNA synthesis at APBs depends on ATM and ATR activity (Nabetani et al., 2004) and on the localization of the entire MRN complex and BRCA1 at APBs (Wu et al., 2003), suggesting that DNA damage signaling is coupled to the ALT pathway. When APB formation is inhibited, the telomeres in ALT cells progressively shorten,

further suggesting that DNA synthesis occurs at these sub-nuclear structures (Jiang et al., 2005). Once telomere elongation at APBs is complete, it is thought that the PML body and telomeres dissociate, or de-sumoylation of the APB structure results in disassembly of the complex (Brouwer et al., 2009).

A variety of proteins involved in the DNA damage response and HR repair of DSBs in telomerase-positive cells are also found at APBs in ALT cells. The HR proteins Rad51, Rad52, RPA (Yeager et al., 1999), Nbs1, Mre11, Rad50, BRCA1 (Wu et al., 2003) and the RecQ helicases WRN and BLM (Cesare & Reddel, 2010; Henson et al., 2002) localize to APBs, as well as the entire shelterin complex (Wu et al., 2000a, 2003; Yeager et al., 1999) and the phosphorylated histone variant γH2AX (Cesare et al., 2009; Nabetani et al., 2004). Although these factors are found at both DNA damage foci and APBs, it is important to note that these complexes form independently and are structurally distinct (Wu et al., 2003). For example, phosphorylation of Nbs1 at S343 by ATM is critical for its role in the DNA damage response (Lim et al., 2000; Wu et al., 2000b), but this site does not appear important for the localization of Nbs1 to APBs (Wu et al., 2003). Furthermore, Rad51 is essential for the HR repair of DSBs, but there is no effect on APB formation when ALT cells are depleted of Rad51 (Potts & Yu, 2007; Tarsounas et al., 2004).

Each component of the MRN complex is important for APB formation and ALT activity (Jiang et al., 2007; Zhong et al., 2007). A functional Nbs1 protein is required for APB formation and a direct interaction between Nbs1 and the PML body component Sp100 may promote its early localization to APBs (Naka et al., 2002; Wu et al., 2000a;

Zhong et al., 2007). Overexpressing Sp100 sequesters the MRN complex away from APBs and inhibits telomeric DNA and telomere-binding proteins from localizing to PML bodies, which prevents APB formation (Jiang et al., 2005). Deleting the N-terminal BRCT domain of Nbs1, but not the CR2 Mre11 interaction domain, abrogates the ability of Nbs1 to localize to APBs (Wu et al., 2003). This suggests that Nbs1 localizes to APBs independently of Mre11 (Wu et al., 2003). However, Nbs1 is required for the subsequent recruitment of Mre11, Rad50 and BRCA1 to APBs, but it is not required for the localization of TRF1 or Rad51 (Wu et al., 2003), despite the ability of Nbs1 to bind directly to TRF1 (Wu et al., 2000a). In addition, shRNA-mediated knockdown of MRN proteins results in less APB formation as well as decreased telomere length (Zhong et al., 2007). These data suggest that Nbs1 and the MRN complex have a role in telomere maintenance in ALT cells.

PML and the shelterin proteins TRF1, TRF2, TIN2 and Rap1 are also required for APB formation, but Sp100 is dispensable (Jiang et al., 2007). Through tethering experiments, researchers have been able to form APBs *de novo*. Tethering GFP-tagged PML to *lacO*-labeled telomeres resulted in the recruitment of Sp100 to these sites and the formation of APB-like structures (Chung et al., 2011). In addition, tethering GFP-tagged TRF1, TRF2, Nbs1, Rad51 and the SUMO E3 ligase MMS21 to *lacO*-labeled telomeres resulted in the recruitment of endogenous PML protein to these sites forming bona fide APBs (Chung et al., 2011).

It has been suggested that ALT telomere clustering can occur independently of BRCA1 (Cho et al., 2014), but whether RPA has a role in APB formation has yet to be

determined. Although there are no reports on a requirement for ATM in APB formation, it appears that ATM is required for DNA synthesis at APBs (Nabetani et al., 2004). The NHEJ factor 53BP1 shows partial co-localization with APBs, but it is not required for telomere clustering or for APB formation (Cho et al., 2014; Jiang et al., 2007; Osterwald et al., 2012).

1.4.4 Chromatin Remodeling in ALT

Several studies have identified an important role of chromatin remodeling in ALT activity. It has been proposed that altering the heterochromatic state of telomeres by creating an "open" configuration may allow HR between telomeres to occur more easily, thus regulating telomere length and APB formation in ALT cells (Conomos et al., 2013). Similarly, it is possible that a "closed" chromatin configuration is involved in repressing ALT activity (Benetti et al., 2007a, 2007b; Gonzalo et al., 2006). Correlations have been found between ALT activity and mutations in the SWI/SNF-family ATP-dependent helicase ATRX and the death domain-associated protein DAXX (Schwartzentruber et al., 2012). It is possible that disruption of ATRX-DAXX function interferes with the incorporation of the histone H3 variant H3.3 at telomeres, disrupting the heterochromatic state of telomeres, which results in increased HR (Chung et al., 2012; Heaphy et al., 2011; Schwartzentruber et al., 2012). The histone chaperone anti-silencing factor 1 (ASF1) has also been implicated in ALT activity, as depletion of both ASF1 paralogs resulted in an upregulation of ALT characteristics, including APBs, ECTRs and T-SCE events (O'Sullivan et al., 2014). In addition, interaction of the nucleosome remodeling and histone deacetylation (NuRD) complex with the zinc-finger protein ZNF827 at telomeres

has been shown to promote chromatin remodeling and recombination of telomeric DNA in ALT cells (Conomos et al., 2014). Telomeric histone deacetylation by the NuRD-ZNF827 complex results in chromatin compaction and is associated with increased ALT activity, as evident by increased levels of APBs, C-circles and T-SCE events (Conomos et al., 2014). Therefore, although the regulation of telomeric chromatin state is not well understood, it appears that ALT activity is highly dependent on this intricate process, and it is possible that ALT activity may be partially a result of deregulated chromatin organization.

1.5 TRF1 Function and Post-Translational Modifications

1.5.1 TRF1 and Telomere Maintenance

The shelterin protein TRF1 has a wide variety of roles in the cell, including telomere protection, telomere length regulation, telomere resolution during mitosis and signalling in the DNA damage response. TRF1 is important for telomere protection, evident in cells lacking TRF1 that show elevated levels of telomere fusions (Iwano et al., 2004; Martínez et al., 2009; McKerlie & Zhu, 2011; Sfeir et al., 2009). TRF1 is also required for the replication of telomeric DNA, perhaps by recruiting BLM and RTEL1 helicases to replication forks (Sfeir et al., 2009), as well as in mitosis, where TRF1 regulates sister telomere resolution (Dynek & Smith, 2004; McKerlie & Zhu, 2011) and mitotic spindles (Nakamura et al., 2002; Shen et al., 1997). Although the role of TRF1 in telomerase-positive cells has been investigated extensively, little work has been done regarding its role in telomerase-negative or ALT cells.

TRF1 is well known for its role as a negative regulator of telomerase-dependent telomere elongation. TRF1 limits the accessibility of telomerase to telomeres, thus regulating telomere length (Ancelin et al., 2002; Smogorzewska & de Lange, 2004; Smogorzewska et al., 2000; van Steensel & de Lange, 1997). When the poly(ADP-ribose) polymerase tankyrase 1 binds to TRF1, TRF1 dissociates from telomeres, is ubiquitinated and degraded by the proteasome, resulting in telomere elongation (Chang et al., 2003; Cook et al., 2002; Her & Chung, 2009; Smith & de Lange, 2000; Smith, 1998). The overexpression of TRF1 in telomerase-positive cells results in a gradual loss of telomere length, whereas the same cells expressing a dominant-negative form of TRF1 that lacks DNA-binding activity leads to a progressive increase in telomere length (Smogorzewska et al., 2000; van Steensel & de Lange, 1997). Telomere repeat amplification protocol (TRAP) assays have shown that TRF1 does not affect telomerase expression, which illustrates that TRF1 works through a *cis*-acting regulatory pathway (Ancelin et al., 2002; Smogorzewska et al., 2000; van Steensel & de Lange, 1997). Similar mechanisms of telomerase-mediated control of telomere length also exist in yeast. Rap1 in *S. cerevisiae* and Taz1 in *S. pombe* also act as negative regulators of telomerase-dependent telomere elongation *in cis* (Cooper et al., 1997; Marcand, 1997).

1.5.2 Post-translational modifications of TRF1

The stability, localization and DNA binding affinity of TRF1 is regulated by various post-translational modifications, including phosphorylation, ubiquitination, sumoylation and PARsylation (Walker & Zhu, 2012). TRF1 contains many serine and threonine residues, allowing it to be targeted by various kinases. Ten phosphorylation sites have

been studied quite extensively (Figure 1.4). Cyclin B-dependent kinase 1 (Cdk1) phosphorylates serine/threonine sites with a Ser/Thr-Pro (S/TP) consensus sequence (Kennelly & Krebs, 1991). Cdk1 phosphorylates several sites on TRF1, including T149, T344 and T371. Phosphorylation of TRF1 at T149 occurs in mitosis and allows TRF1 to interact with the prolyl isomerase PIN1 through its TRFH domain (Lee et al., 2009). PIN1 binds and isomerizes S/TP motifs (Shen et al., 1998). The interaction of PIN1 with TRF1 impairs the ability of TRF1 to bind telomeres, leading to TRF1 degradation (Lee et al., 2009). Cdk1 has also been shown to phosphorylate T344 *in vitro* (Wu et al., 2008) and T371 both *in vitro* and *in vivo* (McKerlie & Zhu, 2011; Wu et al., 2008).

Previous studies that have investigated the TRF1 phosphorylation site T371 have been exclusively in telomerase-positive cells. About 5% of endogenous TRF1 is phosphorylated at T371 by Cdk1, referred to as (pT371)TRF1 (McKerlie & Zhu, 2011). This phosphorylation is upregulated upon mitotic entry, but is also present at a low level in interphase cells (McKerlie & Zhu, 2011). The chromatin binding ability of TRF1 has a significant impact on its function at telomeres. T371 phosphorylation negatively regulates the ability of TRF1 to bind DNA. This is shown by differential salt extraction experiments where wild type TRF1 is predominantly chromatin-bound (420mM KCl fraction) whereas phosphorylated (pT371)TRF1 is predominantly chromatin-free (150mM KCl fraction) (McKerlie & Zhu, 2011). Phosphorylation at this site only occurs on TRF1 that is unbound from DNA, which stabilizes TRF1 and prevents its degradation (McKerlie & Zhu, 2011). T371 phosphorylation upon mitotic entry is associated with telomere de-protection and the accumulation of γH2AX at telomeres, labeling these sites

as damaged (McKerlie & Zhu, 2011). When Cdk1 activity decreases in telophase, TRF1 is dephosphorylated at T371, allowing TRF1 to re-bind telomeres in late mitosis (McKerlie & Zhu, 2011). Creating a phosphomimic point mutation at T371 by replacing threonine with aspartic acid (T371D) acts as a permanent phosphorylation and thus cannot be dephosphorylated upon mitotic exit. This mutation impairs the ability of TRF1 to bind DNA which results in sister telomere fusions, anaphase bridges and lagging chromosomes (McKerlie & Zhu, 2011). Conversely, a non-phosphorylatable alanine point mutation at T371 (T371A) prevents the release of TRF1 from DNA in early mitosis and blocks sister telomere resolution (McKerlie & Zhu, 2011). Together, these results suggest that T371 phosphorylation is important for the resolution of sister chromatids in mitosis. Cells depleted for TRF1 show an increased level of telomere loss and the expression of either T371A or T371D in TRF1-depleted cells further promoted this loss (McKerlie & Zhu, 2011). Expression of T371D also produced defects in cell proliferation, suggesting that telomere uncapping and fusions promoted apoptosis (McKerlie & Zhu, 2011). Defects in telomere replication can produce telomere doublets, where two telomeric DNA signals are present at a single metaphase chromatid end (Martínez et al., 2009; Sfeir et al., 2009). Cells depleted for TRF1 show increased telomere doublets, but the introduction of T371A or T371D mutants into these cells was able to suppress this phenotype to a level comparable to wild type TRF1 (McKerlie & Zhu, 2011). These findings suggest that phosphorylation at T371 is not involved in telomere replication.

Phosphorylated (pT371)TRF1 is also involved in the DNA damage response (McKerlie et al., 2013). Although phosphorylation at T371 has been shown to promote

TRF1 dissociation from telomeres (McKerlie & Zhu, 2011), phosphorylated (pT371)TRF1 is predominantly chromatin-bound after exposure to ionizing radiation (McKerlie et al., 2013). Immunofluorescence using a phospho-specific anti-pT371 antibody shows that this form of TRF1 localizes to IR-induced DNA damage foci and co-localizes with the DSB damage markers 53BP1 and γH2AX (McKerlie et al., 2013). These damage foci occur independently of telomeric DNA, implicating TRF1 in a non-telomeric role (McKerlie et al., 2013). The point mutation R425V in the Myb-like DNA binding domain of TRF1 prevents TRF1 from binding to telomeric DNA (Fairall et al., 2001; McKerlie & Zhu, 2011; McKerlie et al., 2013). Although TRF1-R425V cannot localize to telomeres, this mutant forms IR-induced DNA damage foci, suggesting that unbound TRF1 is recruited to sites of DNA damage (McKerlie et al., 2013). The use of I-SceI reporter constructs specific to NHEJ and HR in cells expressing T371 mutants showed that phosphorylation at T371 was important for HR-mediated repair of DNA (McKerlie et al., 2013). The formation of (pT371)TRF1 IR-induced foci at DSBs was reduced in cells lacking functional ATM, MRN or BRCA1, but foci formation was upregulated in cells lacking 53BP1 or the 53BP1 effector Rif1, further suggesting that (pT371)TRF1 is important for the HR repair of DSBs (McKerlie et al., 2013). Since ALT cells are known to employ an HR mechanism of telomere length maintenance, (pT371)TRF1 may be involved in this process.

TRF1 is also targeted by the ATM kinase which phosphorylates Ser-Gln (SQ) sites (Kim et al., 1999b). ATM interacts with and phosphorylates TRF1 at S219 following exposure to ionizing radiation (Kishi et al., 2001). However, mutating S219 does not

affect TRF1-DNA interactions (Wu et al., 2007) and thus does not affect telomere length (Kishi et al., 2001). ATM also phosphorylates TRF1 at S274 and S367 independent of DNA damage, which may negatively regulate the ability of TRF1 to bind to telomeres (McKerlie et al., 2012; Wu et al., 2007). TRF1 phosphorylated at S367 targets it to subnuclear proteasome centres for degradation (McKerlie et al., 2012). Expression of a phosphomimic mutation at this site (S367D) abrogates TRF1 binding to telomeres, promotes TRF1 degradation, telomerase-dependent telomere elongation and the formation of telomere doublets, suggesting that S367 phosphorylation is important for regulating telomere length, replication and stability (McKerlie et al., 2012).

The serine-threonine kinases AKT, Aurora A, CK2 and Plk1 also phosphorylate TRF1. AKT phosphorylates T273 of TRF1 *in vitro* (Chen et al., 2009). Overexpressing AKT upregulates the level of TRF1 and causes telomere shortening (Chen et al., 2009). Aurora A phosphorylates TRF1 at S296 *in vitro* and is involved in regulating mitosis and chromosomal stability (Ohishi et al., 2010). Casein kinase 2 (CK2) phosphoylates T122 of TRF1 *in vitro* (Kim et al., 2008). CK2 phosphorylation is required for TRF1 to dimerize and bind DNA and therefore regulates TRF1 stability (Kim et al., 2008). Polo-like kinase 1 (Plk1) also phosphorylates TRF1 at S435 *in vitro*, which enhances TRF1 binding to telomeres (Wu et al., 2008).

Post-translational modifications are important for controlling cellular processes and this is no exception in ALT cells. Sumoylation, the covalent attachment of small ubiquitin-related modifier (SUMO) proteins, is a highly dynamic and reversible process that is vital for genome integrity. Sumoylation occurs through a similar enzymatic

cascade to ubiquitination, but it does not usually trigger protein degradation (Chung et al., 2012). Sumoylation can influence protein localization, such as nuclear transport, protein-protein interactions, the stabilization of protein complexes and transcriptional repression (Müller et al., 2001). PML bodies are nuclear hotspots for sumoylated protein complexes (Müller et al., 2001). Modification of PML and Sp100 proteins by SUMO is required for APB formation (Potts & Yu, 2007; Sternsdorf et al., 1997). The SUMO E3 ligase MMS21 is part of the SMC5/6 complex and localizes to APBs in late S and G2 phase (Andrews et al., 2005; Potts & Yu, 2005, 2007; Zhao & Blobel, 2005). MMS21 induces the sumoylation of the shelterin proteins TRF1, TRF2, TIN2 and Rap1, which is required for APB formation (Chung et al., 2011; Potts & Yu, 2007). The sumoylation of these four shelterin proteins does not seem to be regulated by a DNA damage response, as their level of sumoylation is unaffected by exposure to ionizing radiation (Potts & Yu, 2007). The requirement of TRF1 and TRF2 sumoylation for APB formation may suggest that shelterin sumoylation is required for interaction with the SUMO binding domain of PML (Draskovic et al., 2009; Potts & Yu, 2007). In fact, TRF1 and the PML isoform PML3 are known to directly interact (Yu et al., 2010). It has also been proposed that sumoylation is required for APBs to persist in the cell, rather than for their initial formation, since telomere clustering has also been observed in G1 phase (Draskovic et al., 2009). MMS21 is also required for HR, as mouse and human ALT cells depleted of MMS21 by siRNA show reduced T-SCE events (Potts & Yu, 2007).

1.5.3 The Role of TRF1 in ALT

There are various connections between TRF1 and the ALT pathway. Although the sumoylation of TRF1 is required for APB formation, the involvement of other post-translational modifications of TRF1 in ALT activity has yet to be investigated. TRF1 is able to initiate *de novo* APB formation (Chung et al., 2011) and an interaction between TRF1 and Nbs1 was discovered through yeast two-hybrid assays (Wu et al., 2000a). The C-terminus of Nbs1 interacts directly with full length TRF1 and this complex localizes to PML bodies in S and G2 phase where it appears to bind telomeric DNA (Wu et al., 2000a). Despite the ability of TRF1 to interact with Nbs1, this interaction is not required for Nbs1 to localize to APBs (Wu et al., 2003) and TRF1 shows no binding affinity for the other components of the MRN complex, Mre11 and Rad50 (Wu et al., 2000a). In addition, it has been reported that the overexpression of a TRF1 allele that is unable to bind DNA (TRF1ΔMyb) does not significantly affect the localization of Nbs1 to APBs.

It is clear that post-translational modifications of proteins are important for ALT activity, and also that phosphorylation is important for regulating the functions of TRF1 in telomere maintenance. Previous work on the T371 phosphorylation site identified a role for TRF1 at DNA damage sites away from telomeres, as well as in sister chromatid resolution in mitosis, suggesting that one phosphorylation site can have various diverse functions (McKerlie et al., 2013). As mentioned, phosphorylated (pT371)TRF1 requires several components of the HR pathway to facilitate the repair of DSBs. The HR pathway is also used in cancer cells that rely on the alternative lengthening of telomeres

mechanism for telomere length control. This relationship is interesting and may suggest that phosphorylated (pT371)TRF1 is also involved in some aspects of ALT activity.

1.6 Objectives and Significance

TRF1 has been investigated quite extensively in telomerase positive cells, and although there are connections between TRF1 and the ALT pathway, the functional significance of TRF1 in ALT cells is not well understood. It is clear that the phosphorylation of TRF1 at T371 is important for the HR-mediated repair of DSBs induced by DNA damaging agents (McKerlie et al., 2013) and that ALT cells rely on HR mechanisms for telomere regulation. Based on this, it was proposed that phosphorylated (pT371)TRF1 also plays a role in ALT activity.

There are two main aims of this thesis: 1) an analysis of the role of TRF1 phosphorylation at T371 in ALT activity; and 2) investigating the TRF1 domain structure in ALT activity. Multiple approaches were used to address these aims, including the use of a phospho-specific antibody against (pT371)TRF1, cell lines expressing phosphomimic or non-phosphorylatable T371 mutants within either full length TRF1 or truncated forms of TRF1, and the disruption of various DNA damage response components known to be involved in ALT pathways. The major findings presented in this thesis include characterizing the activity of phosphorylated (pT371)TRF1 in ALT cells, along with the involvement of several DNA damage factors in this process. In addition, mutational analysis of the TRF1 domain structure uncovered separate functions for the Myb and dimerization domains of TRF1 in APB assembly, providing more mechanistic insight into how APB formation occurs.

The distinct characteristics of ALT cells compared to telomerase-positive cells provides several targets that may be exploited for cancer therapeutics, since repressing the ALT mechanism results in senescence and apoptosis of ALT cells (Perrem et al., 1999). Telomerase-inhibitor treatments are commonly used to target telomerase-positive tumours, but a possible implication of this could be ALT activation and the development of ALT tumours (Muntoni & Reddel, 2005). Understanding the ALT pathway and the requirements of ALT cells is therefore important to provide cancer therapy options and improve patient survival. The work presented in this thesis has identified several factors that are important for ALT activity, which could be potential targets for cancer therapeutics.

Figure 1.1. The Shelterin Complex. A schematic diagram of the interactions between the six protein subunits in the human shelterin complex and their association with telomeric DNA (Modified from Palm & de Lange, 2008).

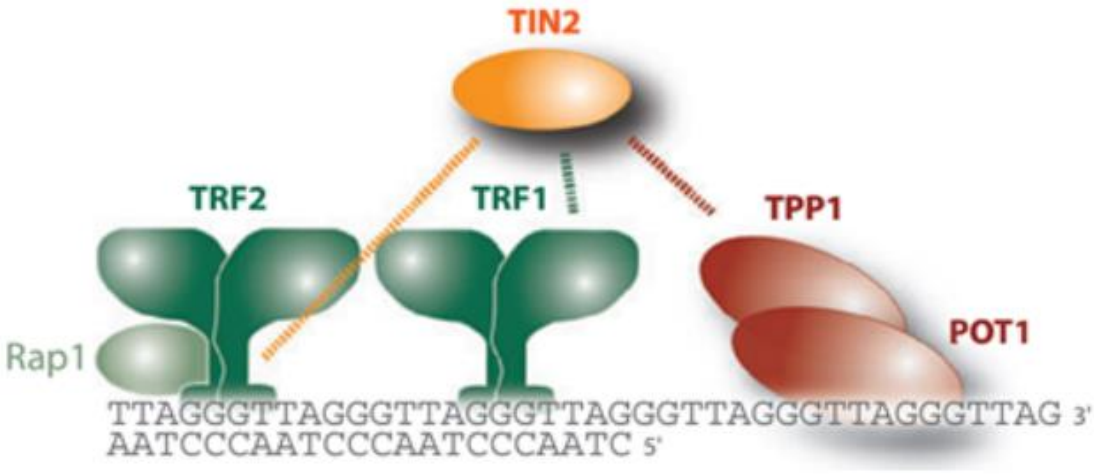
TIN2
TRF2
TRF1
TPP1
POT1
Rap1
TTAGGGTTAGGGTTAGGGTTAGGGTTAGGGTTAGGGTTAG 3'
AATCCCAATCCCAATCCCAATC 5'

Figure 1.2. The DNA Damage Response. A schematic diagram of the DNA damage response that occurs when a double strand break is generated. The Homologous Recombination and Non-Homologous End Joining pathways are depicted. A description of proteins and every step of the pathways are described in the text. Proteins are not drawn to scale and interactions are representations only. Damaged DNA is shown in black and homologous DNA is shown in red.

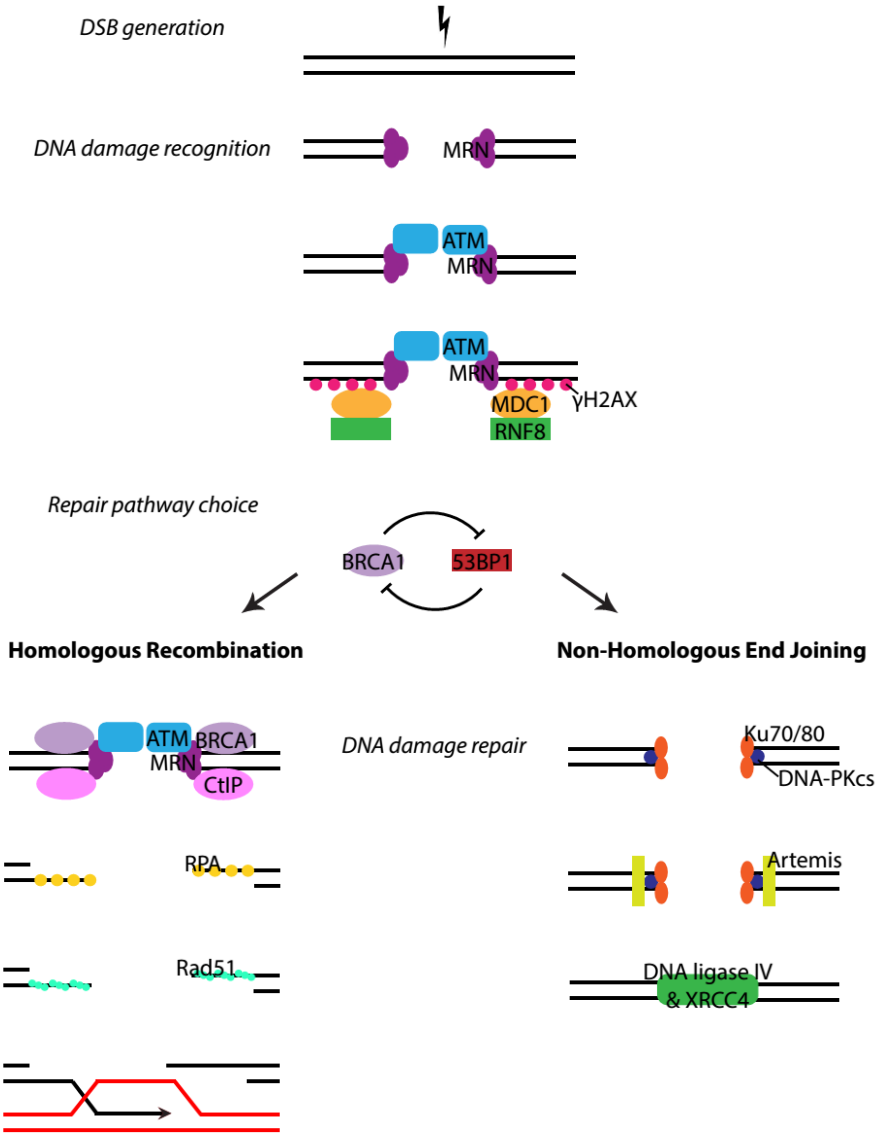
DSB generation
DNA damage recognition
MRN
ATM
MRN
ATM
MRN
MDC1
RNF8
γH2AX
Repair pathway choice
BRCA1
53BP1
Homologous Recombination
Non-Homologous End Joining
ATM
BRCA1
MRN
CtIP
DNA damage repair
Ku70/80
DNA-PKcs
RPA
Artemis
Rad51
DNA ligase IV
& XRCC4

Figure 1.3. Telomeric Circles. A schematic diagram of forms of telomeric circles, including t-circles, C-circles and G-circles. The G-strand is shown in grey and the C-strand is shown in black (Henson & Reddel, 2010).

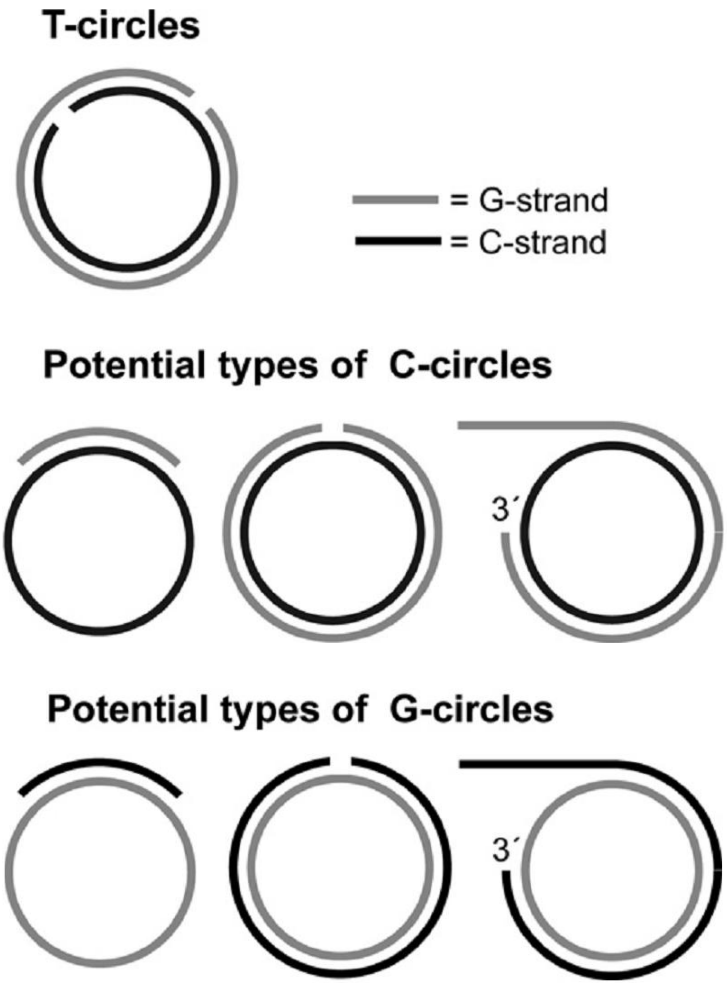
T-circles
= G-strand
= C-strand
Potential types of C-circles
3´
Potential types of G-circles
3´

Figure 1.4. TRF1 Structure and Phosphorylation Sites. A schematic diagram of the major domains of TRF1 and the locations of phosphorylation sites. The first and last amino acids of TRF1 are indicated. Diagram is not drawn to scale.

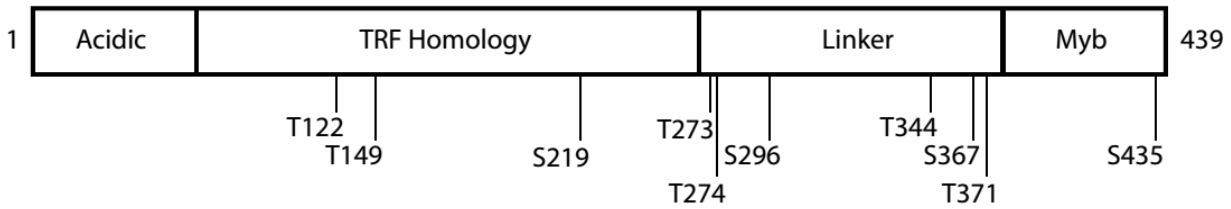
1
Acidic
TRF Homology
Linker
Myb
439
T122
T149
S219
T273
T274
S296
T344
S367
T371
S435

CHAPTER 2 MATERIALS AND METHODS

2.1 Plasmids and Antibodies

Expression constructs for shTRF1 and the TRF1 mutant alleles T371A, T371D, R425V, R425V-T371A and R425V-T371D have been previously described (McKerlie & Zhu, 2011; McKerlie et al., 2013). The shRNA constructs used for shATM, shBRCA1 and sh53BP1 have also been previously described (McKerlie et al., 2013). John Walker generated all TRF1 truncation mutant constructs through PCR using wild type TRF1 as a template. Primer sequences for all alleles will be made available upon request by contacting Xu-Dong Zhu.

The phospho-specific anti-pT371 antibody has been previously described (McKerlie & Zhu, 2011; McKerlie et al., 2013). Antibodies against TRF1, TRF2, TIN2 and Rap1 were gifts from Titia de Lange, Rockefeller University. Anti-Nbs1 antibody was provided by John Petrini, Memorial Sloan-Kettering Cancer Center. Antibodies obtained commercially were c-Myc (9E10, Calbiochem), Cyclin A (Abcam), rabbit anti-PML (Abcam), mouse anti-PML (Santa Cruz), γH2AX (Upstate), histone H2AX (Upstate), BRCA1 (MS110, Abcam), RPA32 (9H8, Abcam), 53BP1 (BD Biosciences), ATM (Novus) and γ-tubulin (GTU88, Sigma).

2.2 Cell Culture and Drug Treatments

All parental cell lines, including Phoenix A, GM847 and U2OS, were grown in DMEM media containing 5% FBS, 20mM L-glutamine, 100U/ml penicillin, 0.1mg/ml streptomycin, and 1% non-essential amino acids. Cells stably expressing pRS constructs

were grown in the presence of 2µg/ml puromycin and cells stably expressing pWZL constructs were grown in 90µg/ml hygromycin. Cells expressing both pRS and pWZL constructs were grown in media containing either puromycin or hygromycin, alternating every two weeks. All cells were grown in incubators at 37°C with 5% CO_2 and 100% humidity.

The Invitrogen Lipofectamine 2000 protocol was used for plasmid DNA transfection into Phoenix amphotropic retroviral packaging cells. Phoenix cells were seeded 24h prior to transfection on 6cm plates at $2x10^6$ cells per plate. GM847 and U2OS target cells were seeded onto 10cm plates at the time of transfection at $7x10^5$ cells per plate. Retroviral infections were carried out as previously described to generate stable cell lines (Karlseder et al., 2002; Zhu et al., 2003). GM847 pRS and pRS-shTRF1 cell lines were made by Michael Gurecki.

For GM847 long term growth curves, cells were counted using a Beckman Z1 Coulter® Particle Counter and $5x10^5$ cells were seeded on 10cm plates every 4 days. The total number of population doublings (PDs) was calculated from the formula $2^n a = b$, where "a" is the initial number of cells, "b" is the final number of cells and "n" is the number of PD. Therefore $n = (\log b - \log a)/\log 2$ and the total PD is the sum of all n-values at that time point.

For all drug treatments, drugs were mixed with fresh media and applied to cells for the indicated treatment times for each experiment. The Mre11 inhibitor Mirin (Sigma, M9948) was used at 100µM, the ATM inhibitor KU55933 (Sigma, K4104) was used at

20µM and the DNA PK inhibitor NU7026 (Sigma, N1537) was used at 20µM. DMSO was used in an equal volume to the inhibitors.

2.3 Protein Extracts, Differential Salt Extraction of Chromatin and Immunoblotting

Protein extracts were collected as described (McKerlie et al., 2013). Cells were trypsinized, washed with media containing 5% FBS and counted. Cells were spun at 1000rpm for 5min at 4°C and the pellet was washed with 1ml cold 1xPBS. Cells were spun at 3000rpm for 2min at 4°C and the pellet was resuspended in buffer C-420 (20 mM HEPES buffer (pH 7.9), 25% glycerol, 5 mM MgCl, 0.2% Nonidet P-40, 1 mM DTT, 1 mM phenylmethylsulfonyl fluoride, 1 µg/ml of aprotinin, 10 µg/ml of peptatin, 1 µg/ml of leupeptin and 420 mM KCl) to obtain $2x10^4$ cells/µl and incubated on ice for 30min. Cells were spun at 14,000rpm for 10min at 4°C and the supernatant was resuspended in 2x Laemmli buffer to obtain 10,000cells/µl.

Differential salt extraction of chromatin was performed essentially as described (McKerlie et al., 2013; Ye & de Lange, 2004). Briefly, cells were trypsinized, washed with media containing 5% FBS and counted. Cells were spun at 1000rpm for 5min at 4°C and the pellet was washed with 1ml cold 1xPBS. Cells were spun at 3000rpm for 2min at 4°C and the pellet was resuspended in buffer C-150 (20 mM HEPES buffer (pH 7.9), 25% glycerol, 5 mM MgCl, 0.2% Nonidet P-40, 1 mM DTT, 1 mM phenylmethylsulfonyl fluoride, 1 µg/ml of aprotinin, 10 µg/ml of peptatin, 1 µg/ml of leupeptin and 150 mM KCl) to obtain $2x10^4$ cells/µl and incubated on ice for 15min. Cells were spun at 3000rpm for 5min at 4°C and the supernatants containing soluble cytoplasmic and nucleoplasmic proteins were collected (150mM KCl fractions). Pellets were resuspended in buffer C-420

(as above, but containing 420mM KCl) to obtain $2x10^4$ cells/µl and incubated on ice for 15min. Cells were spun at 14,000rpm for 10min at 4°C and the supernatants containing chromatin-bound proteins were collected (420mM KCl fractions). Both fractions were resuspended in 2x Laemmli buffer to obtain $1x10^4$ cells/µl. The final pellets were sonicated in Laemmli buffer to obtain $1x10^4$ cells/µl. The whole cell extract was process in parallel, where the cell pellet obtained after the initial PBS wash was directly sonicated in Laemmli buffer.

Immunoblotting was performed as described previously (McKerlie et al., 2013; van Steensel et al., 1998). Unless otherwise stated, protein extracts were fractionated on 8% SDS-PAGE gels and transferred to nitrocellulose membranes which were immunoblotted with the antibodies indicated.

2.4 Immunofluorescence and Fluorescence *in-situ* Hybridization

Immunofluorescence (IF) was performed essentially as described previously (Batenburg et al., 2012; McKerlie et al., 2013; Mitchell et al., 2009). Cells were grown on glass coverslips, rinsed with 1xPBS and fixed in 3% paraformaldehyde with 300mM sucrose in 1xPBS for 10min at room temperature (RT). Cells were washed twice with 1xPBS for 5min each and permeabilized in 0.5% Triton X-100 buffer (20mM Hepes-KOH pH7.9, 50mM NaCl, 3mM $MgCl_2$, 300mM sucrose) for 10min at RT. Cells were washed twice with 1xPBS for 5min each and stored in 1xPBS with 0.02% sodium azide at 4°C. Fixed cells were blocked with PBG (0.2% fish gelatin, 0.5%BSA, 1xPBS) for 30min and incubated with 50µl of primary antibody diluted in PBG for 2h at RT. Coverslips were washed three times in PBG, then incubated with 50µl of secondary antibody

(TRITC or FITC) diluted 1:250 in PBG for 45min at RT in the dark. Coverslips were washed three times in PBG and incubated with 50µl of DAPI diluted in PBG (100ng/ml) for 5min at RT, followed by three washes in 1xPBS. Coverslips were placed cell-side down on embedding media (90% glycerol/10% PBS containing 1mg/ml p-phenylene diamine) on slides and sealed with nail polish.

Immunofluorescence - Fluorescence in-situ Hybridization (IF-FISH) was performed essentially as described (Batenburg et al., 2012; McKerlie et al., 2013). Cells grown on coverslips were fixed in 2% paraformaldehyde in 1xPBS for 10min at RT. Cells were washed twice in 1xPBS for 5min each, and stored in 1xPBS with 0.02% sodium azide at 4°C. Coverslips were blocked with IF-FISH blocking solution (1mg/ml BSA, 3% goat serum, 0.1% TritonX-100, 1mM EDTA pH8.0 in 1xPBS) for 30min at RT. Cells were incubated with 50µl primary antibody diluted in blocking solution for 2h at RT and washed in 1xPBS three times for 5min each. Cells were incubated with 50µl secondary antibody diluted in blocking solution for 45min at RT in the dark and washed in 1xPBS three times for 5min each. Cells were fixed again in 2% paraformaldehyde in 1xPBS for 5min at RT and washed twice in 1xPBS. Cells were dehydrated consecutively in 70%, 95% and 100% ethanol for 5min each. Coverslips were placed cell-side down on a drop of hybridizing solution (70% formamide, 0.5% blocking reagent, 10mM Tris pH7.2, and 1:1000 FITC-TelC PNA probe) on slides and denatured at 80°C for 4min. Coverslips were incubated overnight at 4°C in the dark. Cells were washed twice in washing solution (70% formamide, 10mM Tris pH7.2) for 15min each, followed by three 5min washes in 1xPBS, with DAPI added to the second wash. Coverslips were dried, embedded and

sealed as described previously. For IF-FISH triple staining, the above IF-FISH protocol was followed, using two primary rabbit and mouse antibodies, followed by the corresponding secondary antibodies Rhodamine anti-rabbit IgG (red) and TRITC anti-mouse IgG (blue). As above, the hybridizing solution contained FITC-TelC (green), but DAPI was omitted from the PBS wash.

A Zeiss Axioplan 2 microscope was used to record all cell images. Pictures were captured with a Hamamatsu C4742-95 camera and processed in Open Lab.

The scoring criteria for immunofluorescence microscopy are described with each experiment. All experiments with multiple cell lines were scored in blind, with at least 500 cells scored in triplicate for each experiment.

2.5 Metaphase Chromosome Spreads

Cells were grown on 10cm plates to 80% confluence. Cells were arrested in nocodazole (0.1µg/µl) at 37°C for 90-180min. Cells were collected by mitotic shake off, counted and spun at 1000rpm for 5min at 4°C. Cell pellets were gently resuspended in pre-warmed (37°C) RSB buffer (10mM Tris-HCl (pH 7.4), 10mM NaCl, 5mM $MgCl_2$) to obtain 3-4x10^6 cells/ml. Cells were incubated in RSB buffer at 37°C for 10min, then placed immediately on ice. Cell droplets of 25µl were pipette onto 22mm square glass coverslips on Whatman paper in the swing-out buckets of the table-top centrifuge (Beckman Coulter Allegra® X-15R). Cells were spun until the centrifuge reached 3000rpm then stopped immediately. Coverslips were rinsed in 1xPBS, fixed in 2% paraformaldehyde in 1xPBS for 10min at RT, washed twice in 1xPBS for 5min each and permeabilized in Trixon X-100 buffer for 10min at RT. Cells were washed in 1xPBS,

blocked in PBG for 30min and incubated with primary and secondary antibodies in PBG as above. Coverslips were stained with DAPI, embedded and sealed as previously described.

2.6 Genomic DNA Isolation and Digestion

Cells were collected by scraping and spun at 1000rpm for 5min at 4°C. Cell pellets were washed in 1ml cold 1xPBS and spun at 3000rpm for 2min at 4°C. Pellets were stored at -80°C until needed and were between 50-100µL in size. Genomic DNA was isolated by phenol-chloroform extraction. Cell pellets were incubated overnight at 37°C in 1ml 1xTNE and 1ml TENS/proteinase K in 15ml phase lock gel heavy tubes. An equal volume of phenol/chloroform/isoamylalcohol (25:24:1) was added and mixed gently at RT for 5min to completely mix the phases. Samples were spun at 3000rpm for 10min at 4°C, the aqueous phase was transferred to a new phase lock tube and an equal volume of phenol/chloroform/isoamylalcohol was added. Samples were mixed and spun again at 3000rpm for 10min at 4°C. The aqueous phase was mixed with 2ml iso-propanol and 220µL 2M NaAc (pH 5.5) and the bundle of genomic DNA was incubated in 300µL 1xTNE with 100µg/ml RNase A for 30min at 37°C. DNA was resuspended using a blue cut tip and incubated for 2h at 37°C. Then, 300µL 1xTENS/proteinase K was added to the DNA, solutions were mixed and incubated at 37°C for 1h. An equal volume of phenol/chloroform/isoamylalcohol was added, samples were mixed well and spun at 13000 rpm at 4°C for 10min. The upper phase was transferred with a blue cut tip to a new tube containing 600µL of iso-propanol and 66µL of 2 M NaAc (pH 5.5). Samples were inverted several times and DNA bundles were dissolved in $T_{10}E_{0.1}$ (pH 8.0).

Genomic DNA was digested with RsaI and HinfI and DNA concentrations were measured in duplicate using Hoechst fluorimetry. DNA concentrations ranged from 100ng/µL to 500ng/µL.

2.7 C-Circle Amplification Assay

C-circle amplification (CCA) assays were performed essentially as described (Henson et al., 2009). RsaI/HinfI digested genomic DNA was ethanol precipitated and resuspended in 10mM Tris (pH 7.6). DNA samples were stored at -80°C until needed. Each 10µl DNA sample was combined with 9.25µl of premix (0.2mg/ml BSA, 0.1% Tween 20, 1mM dATP, 1mM dTTP, 1mM dGTP, 1x φ29 buffer) and either 7.5U ϕ29 DNA polymerase (NEB) or 0.75µl ddH_2O, for a total reaction volume of 20µl. Reactions were incubated at 30°C for 8h, followed by incubation in a 65°C water bath for 20min to inactivate the ϕ29 enzyme. Samples were mixed with Orange-G loading dye and separated on a 0.6% agarose gel in 0.5xTBE at 1.75V/cm for 12-16h. Gels were dried at 50°C for 2h, washed in 2xSSC (0.3M NaCl, 30mM Sodium Citrate) at RT for 30min and blocked with Churchmix (0.5M NaPi pH7.2, 1mM EDTA pH8.0, 7% SDS, 1% BSA) at 37°C for 2h. Gels were incubated with end-labeled ^{32}P-γ-dATP $(CCCTAA)_3$ probe in Churchmix at 37°C overnight. Gels were washed three times in 0.1xSSC (15mM NaCl, 1.5mM Sodium Citrate) at 37°C for 30min each, followed by one 30min wash in 0.1xSSC with 0.1% SDS at 37°C. Gels were rinsed in ddH_2O, exposed to Phosphorimager screens and scanned with a Typhoon imager. Quantification was performed using ImageQuant software. Volume reports were obtained for the bands representing C-circles, which were normalized to the corresponding vector.

2.8 Statistical Analysis

One-way ANOVA and Tukey HSD tests were performed using the statistical software R (R Core Team, 2014). All graphs show mean ± standard deviation. One-way ANOVA and Tukey HSD test results are shown as letters above columns. Means not sharing the same letter are significantly different ($p<0.05$). Refer to Appendix I for all P values.

CHAPTER 3 RESULTS

3.1 APB formation and C-circle formation are dependent upon TRF1

It is known that TRF1 is required for APB formation in ALT cells (Jiang et al., 2007), so this information was used to establish a suitable APB scoring technique. Three main size categories of APBs were established: small punctate telomere-like foci, medium, bright, round foci formed by the clustering of several telomere-like foci, and large, bright, round foci that produced a greater fluorescence signal than either small or medium foci. These categories are based on the size of the telomere or protein signal being used, as the size of the PML ring tends to reflect these sizes. Only the nuclei of interphase cells were scored. In addition, only APBs that showed a distinct PML ring structure with a clear reduction in staining intensity in the middle of the ring and with the co-localizing foci completely surrounded by this ring were counted. A cell that contained at least one APB was considered positive. The co-localization of Rap1 and PML was scored using this method in GM847 cells depleted of TRF1 (pRS-shTRF1) and compared to a vector control (pRS). A significant reduction in the percentage of cells with Rap1 at APBs was only observed for shTRF1 when both medium and large foci were counted (Figure 3.1A). The number of APBs per cell was also recorded, and although a reduction was observed in cells depleted of TRF1 compared to the control, this difference was not significant ($P = 0.091$) (Figure 3.1B). Cells depleted of TRF1 will have a decreased TRF1 protein level within PML bodies. A reduced number of TRF1 molecules at APBs would be evident by a reduction in the size of APBs, as large TRF1 foci could become small

foci, but the total number of APBs per cell may not be significantly changed. Based on these results, all future APB scoring used the initial method outlined, counting cells with at least one medium or large APB co-localization as positive. Although the chosen method of APB scoring is partially subjective and it does not account for co-localizations between small foci and PML, it seems to be the most accurate and reproducible method using the technology available. This scoring method also produced a result consistent with the previous report that the presence of TRF1 is required for APB formation (Jiang et al., 2007).

It is well known that TRF1 is important for APB formation (Jiang et al., 2007; Potts & Yu, 2007; Yu et al., 2010), but its involvement in other aspects of the canonical ALT pathway has not been reported. Since C-circles are a reliable indicator of ALT activity, this ALT phenotype was assessed in cells depleted of endogenous TRF1. A C-circle assay was performed using genomic DNA from GM847 cells stably expressing either a vector (pRS) or shRNA against TRF1 (pRS-shTRF1) (Figure 3.2A). Cells depleted of TRF1 showed a significant reduction in C-circle formation compared to the vector, suggesting that TRF1 is required for this ALT characteristic (Figure 3.2B and 3.2C). The ability of TRF1 to induce C-circle formation was also investigated by overexpressing Myc-tagged TRF1 in GM847 cells (Figure 3.2D). A significant increase in C-circle formation was observed compared to the vector (Figure 3.2E and 3.2F). Altogether, these results support the involvement of TRF1 in C-circle formation in ALT cells.

Figure 3.1. Determination of APB scoring criteria. (**A**) Quantification of indirect immunofluorescence on GM847 pRS and shTRF1 cells with anti-Rap1 and anti-PML antibodies. The percentage of cells with 1 or more Rap1/PML foci co-localizing for the indicated foci sizes is shown. Cells were scored from pictures, with >100 cells in n=3. (**B**) Quantification of the average number of Rap1 and PML foci co-localizing per cell in GM847 pRS and shTRF1 cells. Indirect immunofluorescence used anti-Rap1 and anti-PML antibodies. Cells were scored from pictures, with >100 cells in n=3.

Fig3.1

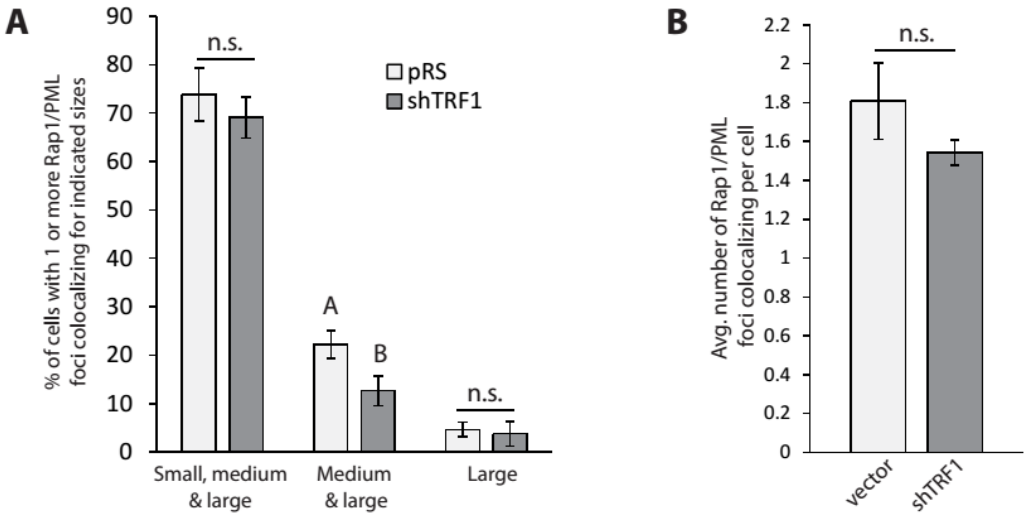
A
% of cells with 1 or more Rap1/PML foci colocalizing for indicated sizes
90
80
70
60
50
40
30
20
10
0
n.s.
pRS
shTRF1
A
B
n.s.
Small, medium & large
Medium & large
Large
B
Avg. number of Rap1/PML foci colocalizing per cell
2.2
2
1.8
1.6
1.4
1.2
1
0.8
0.6
0.4
0.2
0
n.s.
vector
shTRF1

Figure 3.2. C-circle formation depends on TRF1. (**A**) Western analysis of GM847 cells depleted of endogenous TRF1. Immunoblotting was performed with anti-TRF1 or anti-γ-tubulin antibody. The γ-tubulin blot was used as a loading control in this experiment and all subsequent westerns. (**B**) Quantification of the relative ratio of C-circles shown in the gel in (C). C-circle volumes were calculated in ImageQuant5.2. C-circle volumes for ϕ29 lanes were normalized to the vector, which was set to 1. Graph shows mean ± SD for n=3. (**C**) Native C-circle gel on GM847 cells depleted of TRF1. The C-circle areas used for quantification in (B) are indicated. Reactions performed in the absence of ϕ29 enzyme serve as negative controls. (**D**) Western analysis of GM847 cells overexpressing Myc-tagged TRF1 or a vector. Immunoblotting was performed with anti-Myc or anti-γ-tubulin antibody. (**E**) Quantification of the relative ratio of C-circles shown in the gel in (F). Volumes were calculated as previously described. Graph shows mean ± SD for n=3. (**F**) Native C-circle gel on GM847 cells overexpressing TRF1. The C-circle areas used for quantification in (E) are indicated.

Fig3.2

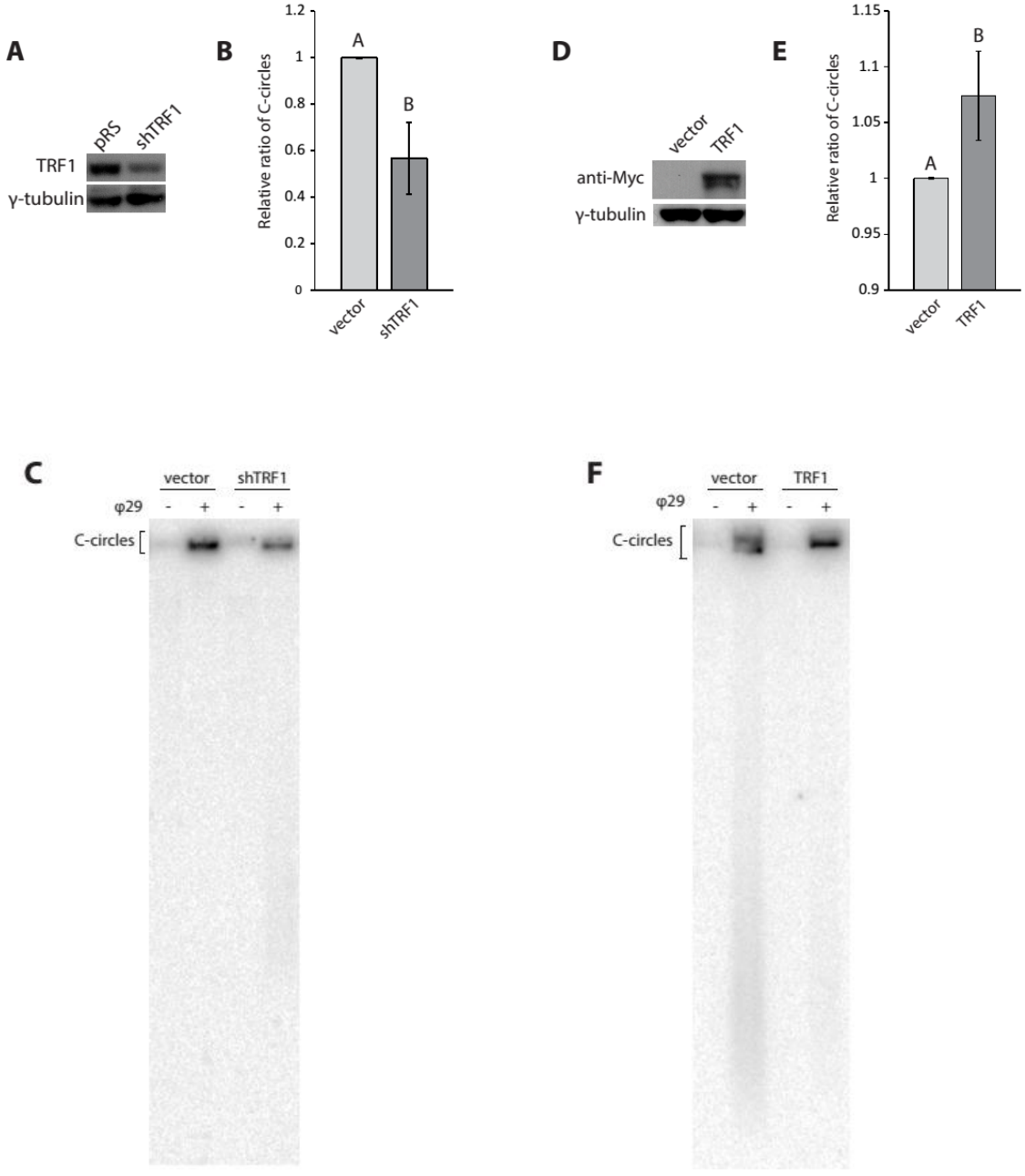
A
pRS
shTRF1
TRF1
γ-tubulin
B
Relative ratio of C-circles
1.2
1
0.8
0.6
0.4
0.2
0
A
B
vector
shTRF1
D
vector
TRF1
anti-Myc
γ-tubulin
E
Relative ratio of C-circles
1.15
1.1
1.05
1
0.95
0.9
A
B
vector
TRF1
C
vector
shTRF1
φ29
- + - +
C-circles
F
vector
TRF1
φ29
- + - +
C-circles

3.2 Phosphorylated (pT371)TRF1 forms a distinct nuclear staining pattern in ALT cells and localizes to APBs dependent upon TRF1

As discussed previously, TRF1 phosphorylated at T371 has been shown to facilitate DNA end resection and the homologous recombination-directed repair of DSBs in telomerase-positive cells (McKerlie et al., 2013). This work and previous work from our lab used an antibody that specifically recognizes TRF1 phosphorylated at T371, referred to as anti-pT371 antibody (McKerlie & Zhu, 2011; McKerlie et al., 2013). This antibody has been previously characterized (McKerlie & Zhu, 2011). To investigate whether phosphorylated (pT371)TRF1 is involved in HR in ALT cells, anti-pT371 antibody was first visualized in these cells.

Analysis of indirect immunofluorescence on GM847 cells using an antibody against endogenous TRF1 showed that 100% of cell nuclei contained bright, punctate TRF1 telomere foci (Figure 3.3A and 3.3B). The anti-TRF1 antibody recognizes full-length, unmodified TRF1, found at all telomeres, hereafter referred to as pan-TRF1. In comparison, analysis of indirect immunofluorescence on GM847 cells with anti-pT371 antibody showed punctate nuclear staining in about 50 to 60% of cells (Figure 3.3A and 3.3B). The anti-pT371 antibody staining included three main patterns in ALT cells (Figure 3.3C). The first type was dim, diffuse, pan-nuclear staining devoid of telomere foci, which represented about 40 to 50% of cells. Phosphorylated (pT371)TRF1 also stained cells with numerous small, bright, punctate nuclear foci that co-localized with telomeres (data not shown). Finally, some cells showed a staining pattern of round foci that were larger and brighter than telomere foci and resembled APBs. These cells tended

to contain about 1 to 6 of these larger APB-like foci and the same cells also contained the small, punctate telomere foci. Cells were considered pT371-positive when they contained five or more bright, telomere foci or had at least one APB-like foci. T371 phosphorylation occurs predominantly in early mitosis, in prophase and metaphase, visualized by a stronger anti-pT371 staining (McKerlie & Zhu, 2011). This more intense staining was also observed in ALT cells, but mitotic cells were not included in scoring experiments, since APBs are disassembled in mitosis.

A differential salt extraction of GM847 cells showed that phosphorylated (pT371)TRF1 was found mainly in the chromatin-free (150mM KCl) fraction with some also present in the chromatin-bound (420mM KCl) fraction (Figure 3.3D). In contrast, total TRF1 and TRF2 were both predominantly chromatin-bound (Figure 3.3D). Histone H2AX was tightly bound to chromatin and found in the pellet fraction (Figure 3.3D), serving as a control for the fractionation protocol.

Taken together, the differences in staining patterns and chromatin-association between TRF1 and phosphorylated (pT371)TRF1 in GM847 cells suggests that phosphorylated (pT371)TRF1 could represent a pool of TRF1 that is distinct from pan-TRF1.

To further investigate if the punctate nuclear staining of phosphorylated (pT371)TRF1 was cell cycle regulated, GM847 cells were costained with anti-pT371 and an antibody against cyclin A, a marker for S and G2 phase cells (Pagano et al., 1992). There was a significant overlap of cells that were both cyclin A-positive and also pT371-positive (Figure 3.4A). About 90% of cyclin A-positive cells were also positive for pT371

foci, and about 80% of pT371-positive cells were also cyclin A-positive (Figure 3.4B). These results suggest that the majority of phosphorylated (pT371)TRF1 is associated with ALT cells in S and G2 phase of the cell cycle.

APBs are defined as the co-localization of telomeric DNA and associated shelterin and repair proteins within a PML body ring (Grobelny et al., 2000; Pickett et al., 2009; Yeager et al., 1999). To confirm that the larger pT371 foci observed were APBs, GM847 cells were co-stained with anti-pT371 and anti-PML antibody, and showed phosphorylated (pT371)TRF1 within PML bodies (Figure 3.4C). Triple staining immunofluorescence-fluorescence *in situ* hybridization (IF-FISH) was also performed on GM847 cells using anti-pT371 antibody, anti-PML antibody and a telomeric DNA-containing peptide nucleic acid (PNA) probe. Phosphorylated (pT371)TRF1 was seen to clearly localize to APBs (Figure 3.4D). Although triple staining IF-FISH is the ideal method to observe APBs, dual indirect immunofluorescence is a more widely used and robust technique. Previous knowledge of the involvement of phosphorylated (pT371)TRF1 in HR, combined with its ability to localize to APBs in ALT cells which employ an HR-mediated telomere maintenance mechanism, suggests that this form of TRF1 could play a role in the HR process in ALT cells.

Both endogenous pan-TRF1 and phosphorylated (pT371)TRF1 localize to APBs, but (pT371)TRF1 is largely localized to telomeres in S and G2 phase cells. To assess whether the different staining patterns also influenced the localization of these proteins to APBs, GM847 cells were co-stained with anti-PML antibody and either anti-TRF1 or anti-pT371 antibodies. No significant difference in the percentage of cells with either

pan-TRF1 or phosphorylated (pT371)TRF1 at APBs was observed (Figure 3.5A), suggesting that both forms of TRF1 show equal levels of APB localization despite their differences in staining patterns.

To confirm that the phospho-specific anti-pT371 antibody is recognizing a form of TRF1, GM847 cells were depleted of endogenous TRF1 and the co-localization of anti-pT371 and anti-PML antibodies at APBs was scored. Cells expressing shTRF1 showed a significant reduction in the localization of (pT371)TRF1 at APBs compared to pRS control cells (Figure 3.5B). The reintroduction of Myc-tagged shTRF1-resistant wild type TRF1 into cells depleted of TRF1 was able to rescue the localization of (pT371)TRF1 to APBs to a level similar to the vector control (Figure 3.5C and 3.5D). These data therefore demonstrate that anti-pT371 antibody is recognizing a form of endogenous TRF1 and is not a result of cross-reactivity, and also that the localization of phosphorylated (pT371)TRF1 to APBs is dependent upon TRF1.

Figure 3.3. Phosphorylated (pT371)TRF1 forms a distinct staining pattern in ALT cells and a portion of (pT371)TRF1 is free of chromatin. (**A**) Indirect immunofluorescence on GM847 cells with anti-TRF1 or anti-pT371 antibodies. Cell nuclei were stained with DAPI in blue. Original magnification x100. (**B**) Quantification of the percentage of GM847 cells positive for the indicated foci. Indirect immunofluorescence was performed with anti-TRF1 or anti-pT371 antibodies as shown in (A). Cells with 5 or more foci were considered positive. Graph shows mean ± SD for >100 cells in n=3. (**C**) Indirect immunofluorescence on GM847 cells with anti-pT371 antibody. Cell nuclei were stained with DAPI in blue. (**D**) Differential salt extraction of chromatin on GM847 cells. Immunoblotting was performed with anti-pT371, anti-TRF1, anti-TRF2 or anti-H2AX antibodies.

Fig3.3

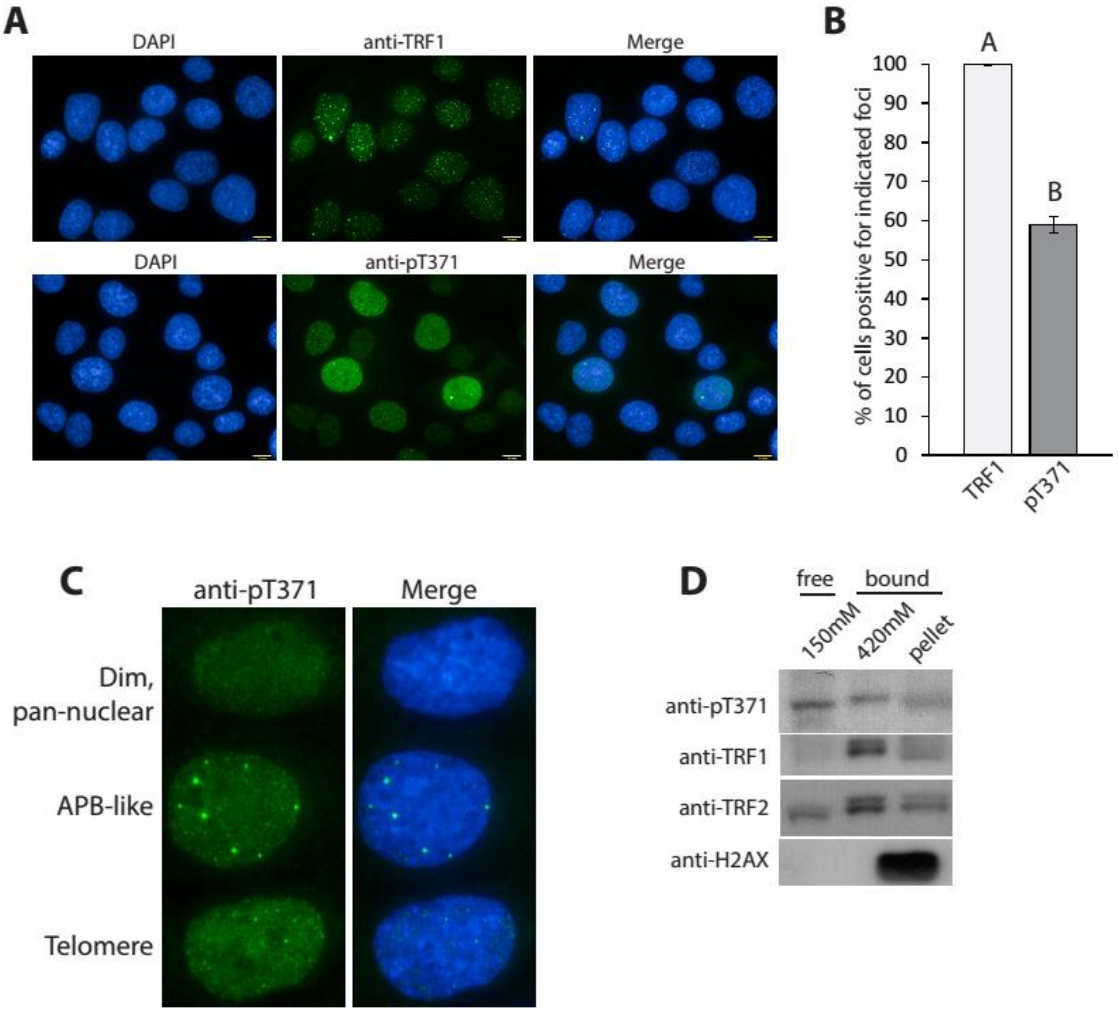
A
DAPI
anti-TRF1
Merge
DAPI
anti-pT371
Merge
B
A
B
% of cells positive for indicated foci
100
90
80
70
60
50
40
30
20
10
0
TRF1
pT371
C
anti-pT371
Merge
Dim, pan-nuclear
APB-like
Telomere
D
free
bound
150mM
420mM
pellet
anti-pT371
anti-TRF1
anti-TRF2
anti-H2AX

Figure 3.4. Phosphorylated (pT371)TRF1 localizes to S and G2 phase cells and is found at APBs. (**A**) Indirect immunofluorescence on GM847 cells with anti-pT371 and anti-cyclin A antibodies. Cell nuclei were stained with DAPI in blue. (**B**) Quantification of the percentage of GM847 cells positive for both pT371 and cyclin A staining as shown in (A). Graph shows mean ± SD for >500 cells in n=3. (**C**) IF-FISH triple staining on GM847 cells using anti-pT371 and anti-PML antibodies in conjunction with a telomeric DNA-containing peptide nucleic acid (PNA) probe. White dashed lines outline the nuclei. (**D**) Indirect immunofluorescence on GM847 cells with anti-pT371 and anti-PML antibodies. Cell nuclei were stained with DAPI in blue. White arrows indicate co-localizations of indicated foci at APBs.

Fig3.4

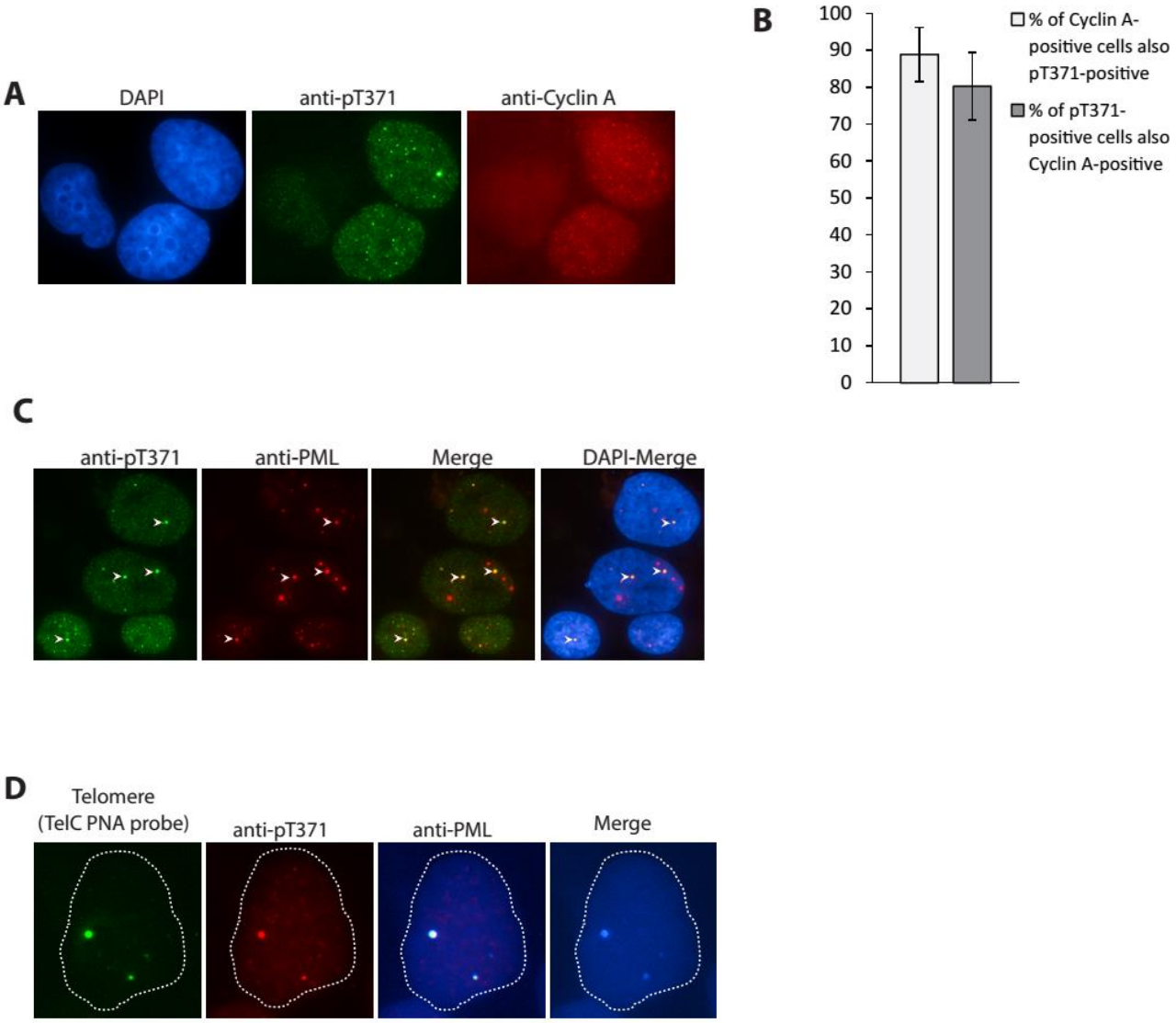
A
DAPI
anti-pT371
anti-Cyclin A
B
100
90
80
70
60
50
40
30
20
10
0
% of Cyclin A-positive cells also pT371-positive
% of pT371-positive cells also Cyclin A-positive
C
anti-pT371
anti-PML
Merge
DAPI-Merge
D
Telomere (TelC PNA probe)
anti-pT371
anti-PML
Merge

Figure 3.5. The localization of phosphorylated (pT371)TRF1 to APBs depends on TRF1. (**A**) Quantification of indirect immunofluorescence on GM847 cells with anti-PML antibody in conjunction with either anti-TRF1 or anti-pT371 antibody. The percentage of cells with TRF1 or (pT371)TRF1 at APBs is indicated. Graph shows mean ± SD for >100 cells in n=3. (**B**) Quantification of indirect immunofluorescence on GM847 cells depleted of endogenous TRF1, stained with anti-pT371 and anti-PML antibodies. The percentage of cells with (pT371)TRF1 at APBs is indicated. Cells were scored from pictures, with >100 cells in n=3. (**C**) Dual indirect immunofluorescence with anti-pT371 and anti-PML antibodies on GM847 cells depleted of endogenous TRF1 and complemented with Myc-tagged shTRF1-resistant wild type TRF1. Cell nuclei were stained with DAPI in blue. White arrows indicate co-localizations of indicated foci at APBs. (**D**) Quantification of indirect immunofluorescence on GM847 cells expressing various constructs as shown in (C). Cells were stained with anti-pT371 and anti-PML antibodies. The percentage of cells with (pT371)TRF1 at APBs is indicated for >500 cells in n=6.

Fig3.5

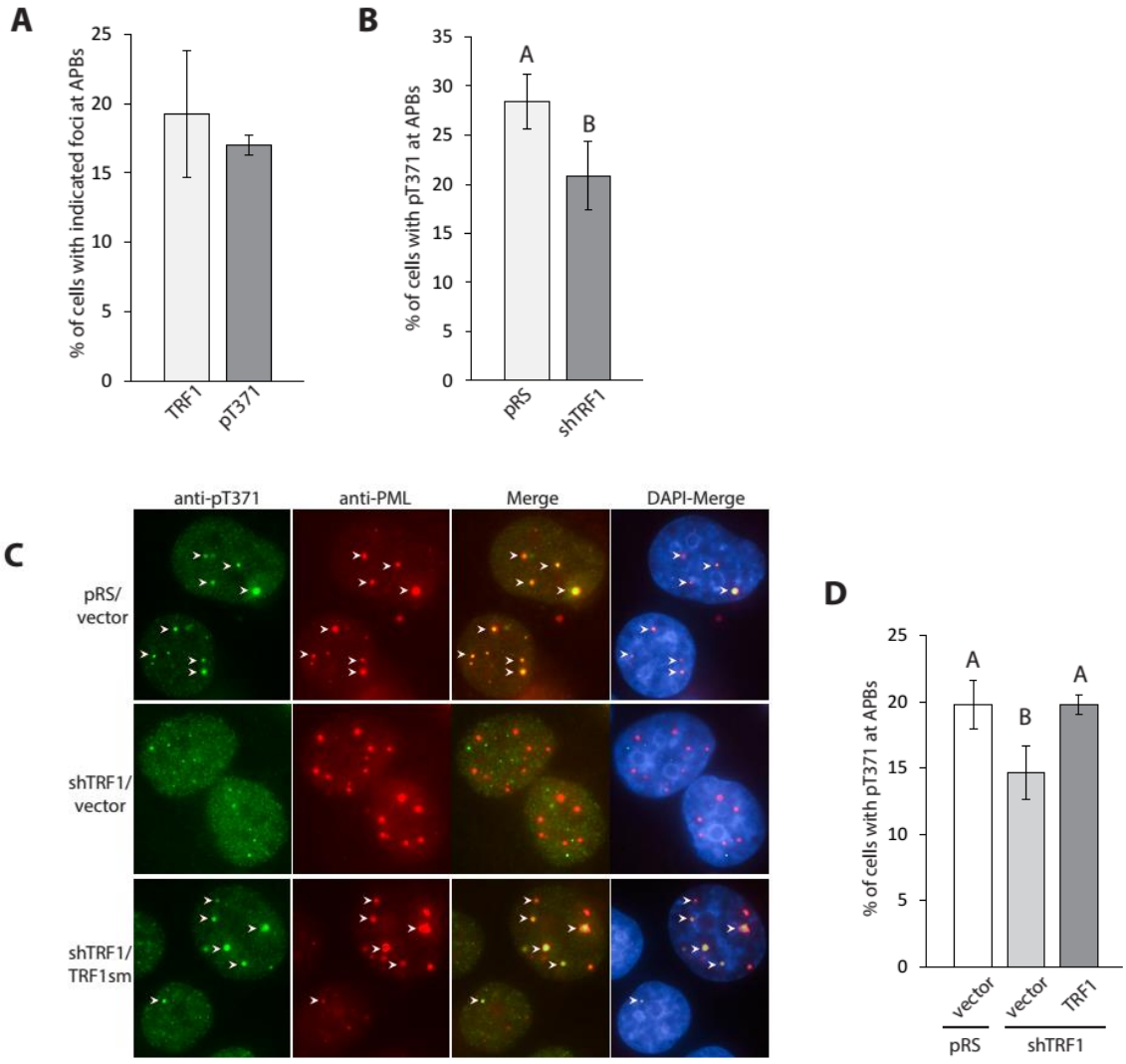
A
% of cells with indicated foci at APBs
25
20
15
10
5
0
TRF1
pT371
B
% of cells with pT371 at APBs
35
30
25
20
15
10
5
0
A
B
pRS
shTRF1
C
anti-pT371
anti-PML
Merge
DAPI-Merge
pRS/
vector
shTRF1/
vector
shTRF1/
TRF1sm
D
% of cells with pT371 at APBs
25
20
15
10
5
0
A
B
A
vector
vector
TRF1
pRS
shTRF1

3.3 Phosphorylated (pT371)TRF1 is associated with the DNA damage marker γH2AX and HR repair proteins at APBs

Previous findings have shown that IR-induced (pT371)TRF1 foci co-localize with the DNA damage marker γH2AX in telomerase-positive cells as part of the process in which phosphorylated (pT371)TRF1 facilitates the HR-mediated repair of DSBs (McKerlie et al., 2013). Since γH2AX shows partial overlap with APBs (Nabetani et al., 2004), the relationship between γH2AX and phosphorylated (pT371)TRF1 was investigated. About 90% of GM847 cells were found to be γH2AX-positive, containing five or more foci, consistent with previous findings that untreated ALT cells show an increased basal level of DNA damage with spontaneous telomere dysfunction (Cesare et al., 2009). About 14% of cells showed γH2AX at APBs, about 17% of cells showed (pT371)TRF1 at APBs, and about 11% of cells showed both γH2AX and (pT371)TRF1 at APBs (Figure 3.6A). Almost 70% of cells with (pT371)TRF1 at APBs also contained γH2AX at APBs, and conversely, almost 80% of cells with γH2AX at APBs also contained (pT371)TRF1 at APBs (Figure 3.6B). Therefore there is a substantial amount of overlap between γH2AX and phosphorylated (pT371)TRF1 at APBs in interphase cells (Figure 3.6C).

To further examine the involvement of phosphorylated (pT371)TRF1 at APBs in ALT cells, its localization compared to the repair proteins BRCA1, RPA and 53BP1 was investigated. Dual indirect immunofluorescence was performed on GM847 cells with anti-pT371 antibody in conjunction with either anti-BRCA1, anti-RPA32 or anti-53BP1 antibodies (Figure 3.6C). Quantification of co-localizations showed an enhanced

association of (pT371)TRF1 with BRCA1 and RPA at APB-like foci compared to 53BP1 (Figure 3.6D). These results suggest that phosphorylated (pT371)TRF1 is associated with HR repair proteins at APBs.

Figure 3.6. Phosphorylated (pT371)TRF1 is associated with the DNA damage marker γH2AX and HR repair proteins at APBs. (**A**) Quantification of indirect immunofluorescence on GM847 cells with anti-pT371 and anti-PML antibodies (column 1), anti-γH2AX and anti-PML antibodies (column 2) or anti-pT371 and anti-γH2AX antibodies (column 3). Graph shows the percentage of cells with the indicated foci co-localizing at APBs for >500 cells in n=3. (**B**) Quantification of the percentage of GM847 cells with the indicated foci co-localizing at APBs. Dual indirect immunofluorescence was performed with anti-pT371 and anti-γH2AX antibodies for >500 cells in n=3. (**C**) Representative images of dual indirect immunofluorescence on GM847 cells stained with the indicated antibodies. Cell nuclei were stained with DAPI in blue. White arrows indicate co-localizations of the indicated proteins at APB-like foci. (**D**) Quantification of the percentage of pT371-positive GM847 cells with the indicated foci co-localizing at APBs. Anti-pT371 antibody was used in conjunction with either anti-RPA32, anti-BRCA1 or anti-53BP1 antibodies. Cells were scored from pictures for >100 cells in n=3.

Fig3.6

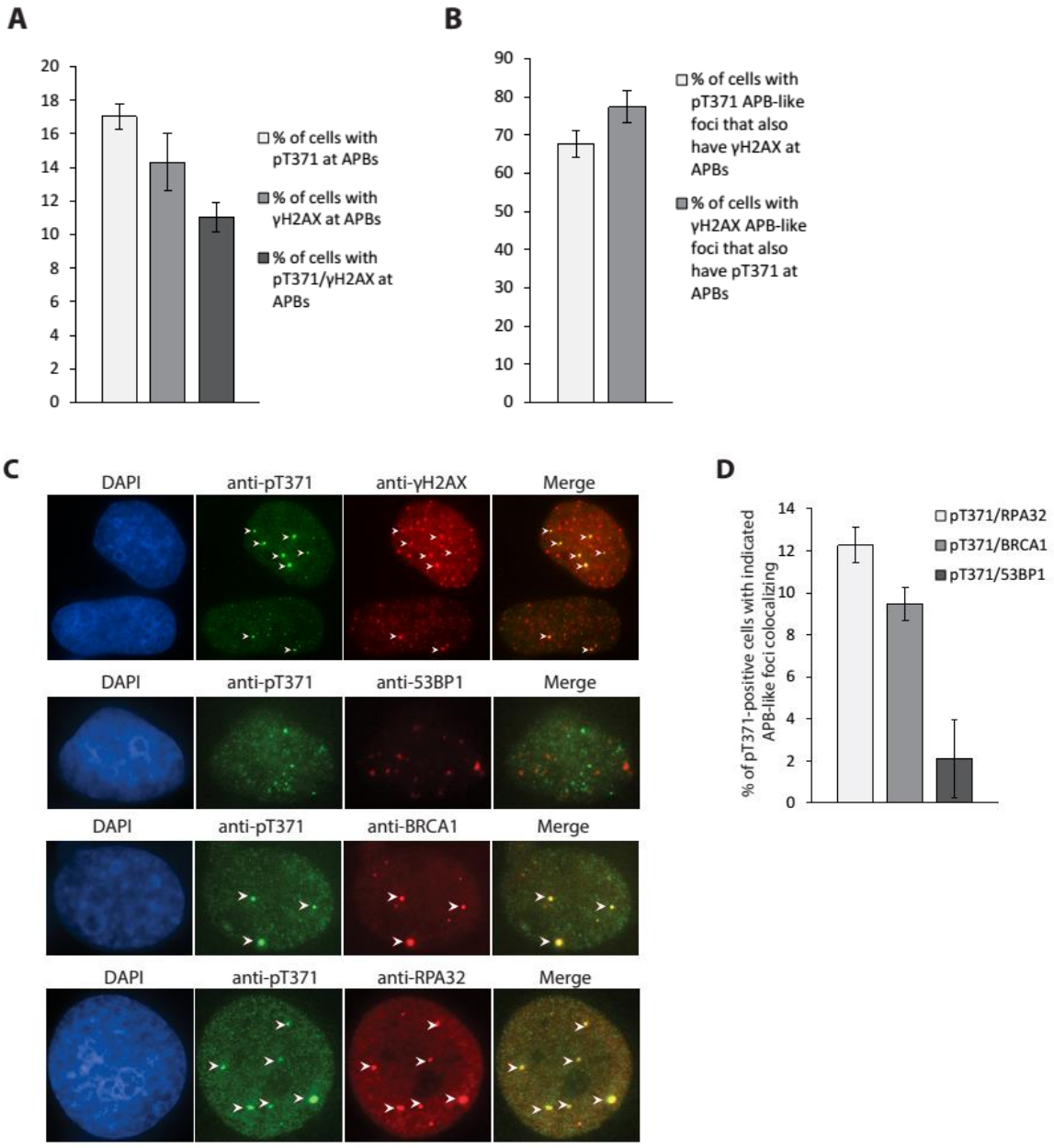
A
20
18
16
14
12
10
8
6
4
2
0
% of cells with pT371 at APBs
% of cells with γH2AX at APBs
% of cells with pT371/γH2AX at APBs
B
90
80
70
60
50
40
30
20
10
0
% of cells with pT371 APB-like foci that also have γH2AX at APBs
% of cells with γH2AX APB-like foci that also have pT371 at APBs
C
DAPI
anti-pT371
anti-γH2AX
Merge
DAPI
anti-pT371
anti-53BP1
Merge
DAPI
anti-pT371
anti-BRCA1
Merge
DAPI
anti-pT371
anti-RPA32
Merge
D
% of pT371-positive cells with indicated APB-like foci colocalizing
14
12
10
8
6
4
2
0
pT371/RPA32
pT371/BRCA1
pT371/53BP1

3.4 Phosphorylated (pT371)TRF1 is associated with the DNA damage marker γH2AX at telomeres in metaphase cells

A previous report has shown that γH2AX forms a unique staining pattern on metaphase chromosomes in ALT cells, with a signal at either one sister chromatid end (chromatid-type) or both sister chromatid ends (chromosome-type), labeling these telomeres as dysfunctional (meta-TIFs) (Cesare et al., 2009). The observation of co-localization of phosphorylated (pT371)TRF1 with γH2AX at APBs in interphase cells prompted an investigation of metaphase chromosomes. Metaphase spreads of GM847 cells were prepared by cytocentrifugation and stained for γH2AX in conjunction with either TRF1, TRF2 or phosphorylated (pT371)TRF1. Both anti-TRF1 and anti-TRF2 antibodies showed clear telomere foci at chromatid ends (Figure 3.7A, 3.7C and 3.7D) and γH2AX staining showed a similar pattern to that described previously, with only a proportion of telomeres being labeled (Figure 3.7B, 3.7C and 3.7D). On some chromosomes that showed a weak or absent telomere signal, a large γH2AX foci was present at this location (Figure 3.7C and 3.7D). Metaphase spreads stained with anti-pT371 antibody showed a remarkably similar pattern to γH2AX, with only a subset of telomeres being labeled and either chromatid-type or chromosome-type staining (Figure 3.7E). Costaining for both (pT371)TRF1 and γH2AX showed significant co-localization, with almost every (pT371)TRF1 foci overlapping with γH2AX foci, even if these foci occurred at interstitial regions (Figure 3.7F). Phosphorylated (pT371)TRF1 was therefore predominantly associated with telomeres that were marked as damage by γH2AX in metaphase.

Figure 3.7. Phosphorylated (pT371)TRF1 is associated with the DNA damage marker γH2AX at telomeres in metaphase cells. (**A**) Representative metaphase spread of GM847 cells stained with anti-TRF1 antibody. Chromosomes were stained with DAPI in blue and white boxes indicate a magnified example for this experiment and all subsequent metaphase spread images. (**B**) Representative metaphase spread of GM847 cells stained with anti-γH2AX antibody. (**C**) Representative metaphase spread of GM847 cells co-stained with anti-TRF1 and anti-γH2AX antibodies. White arrows indicate a telomere lacking a TRF1 signal but containing a γH2AX signal. (**D**) Representative metaphase spread of GM847 cells co-stained with anti-TRF2 and anti-γH2AX antibodies. White arrows indicate sister chromatids lacking TRF2 signals but containing γH2AX signals. (**E**) Representative metaphase spread of GM847 cells stained with anti-pT371 antibody. (**F**) Representative metaphase spread of GM847 cells co-stained with anti-pT371 and anti-γH2AX antibodies.

Fig3.7

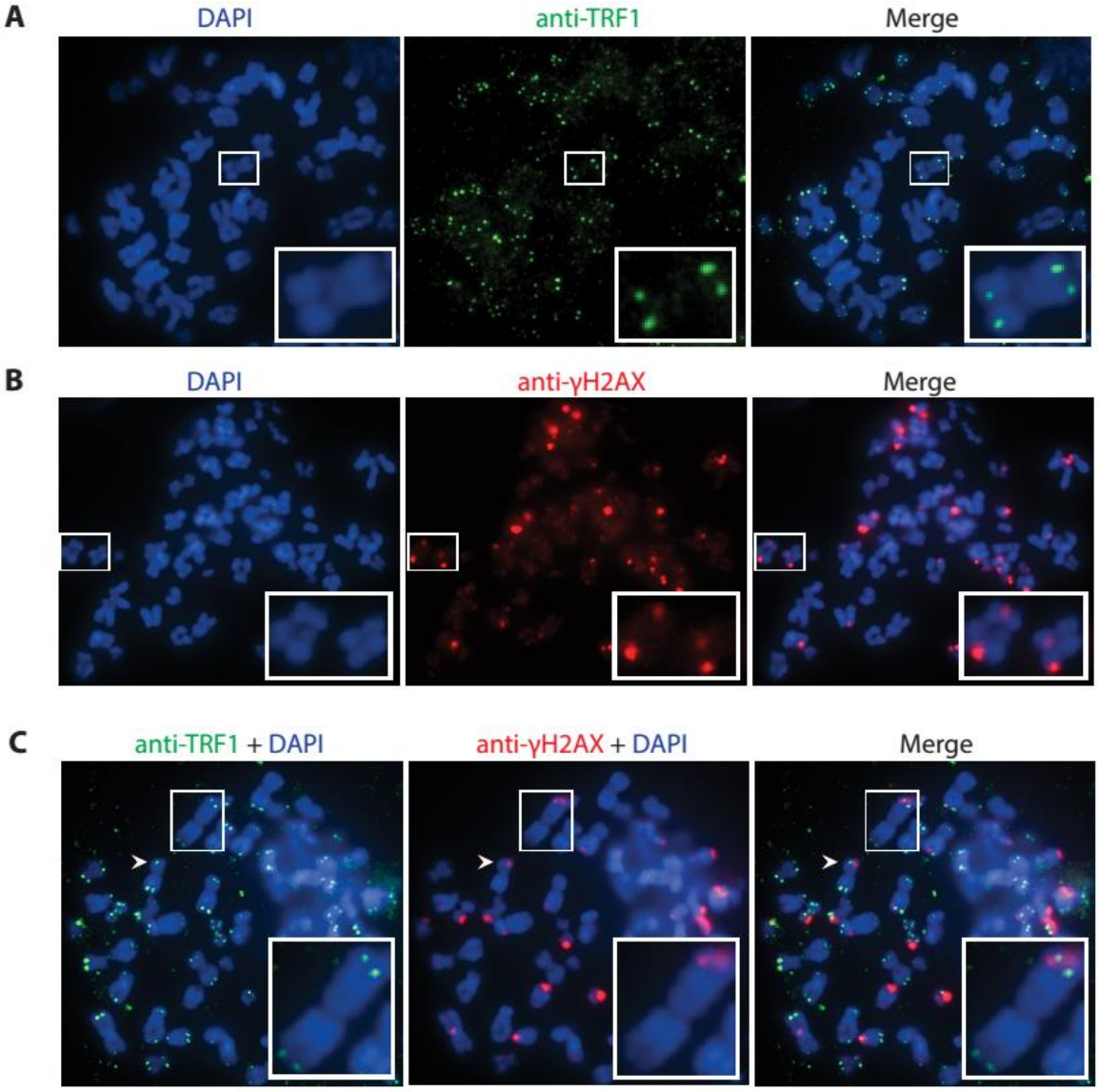
A
DAPI
anti-TRF1
Merge
B
DAPI
anti-γH2AX
Merge
C
anti-TRF1 + DAPI
anti-γH2AX + DAPI
Merge

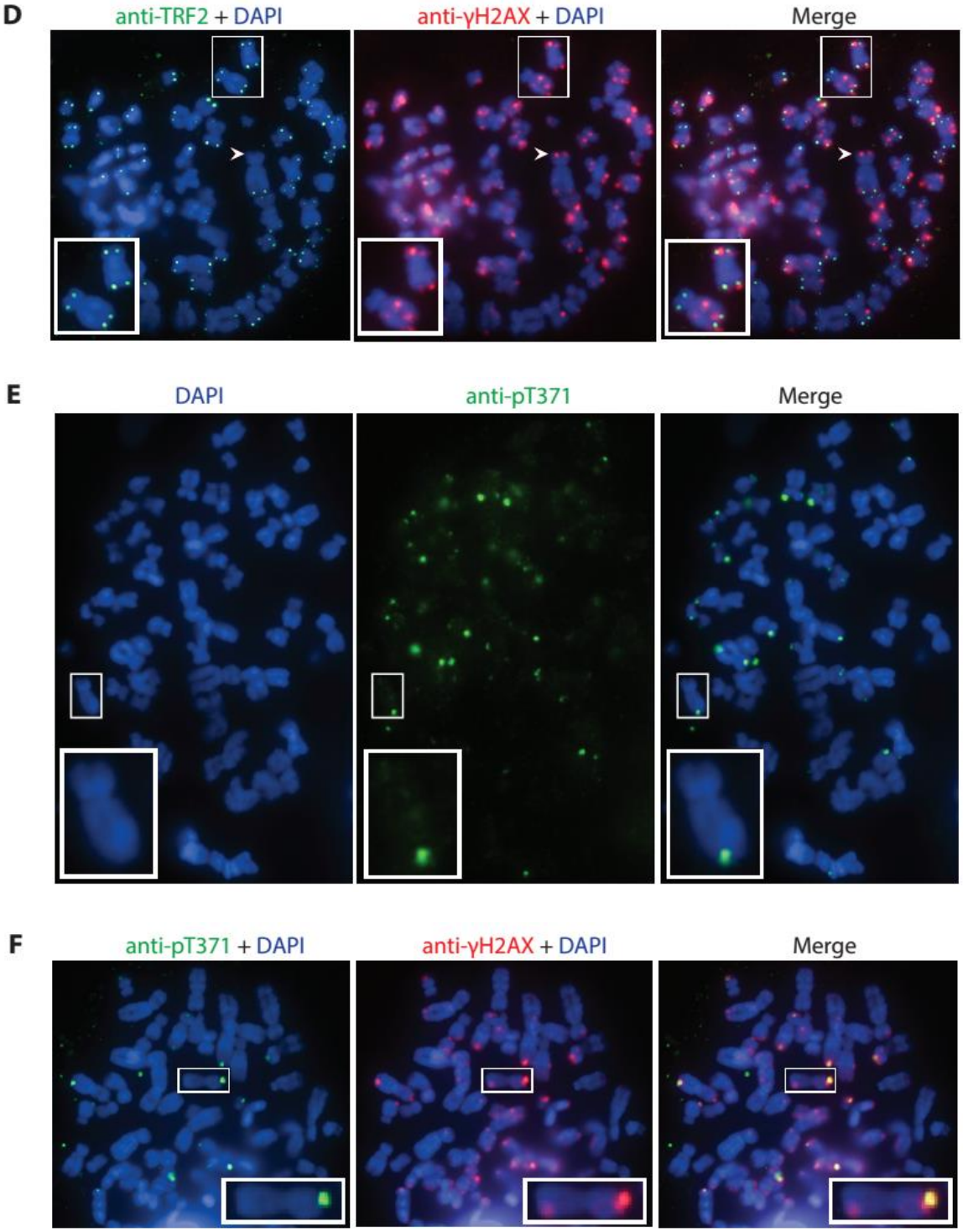
D
anti-TRF2 + DAPI
anti-γH2AX + DAPI
Merge
E
DAPI
anti-pT371
Merge
F
anti-pT371 + DAPI
anti-γH2AX + DAPI
Merge

3.5 The localization of phosphorylated (pT371)TRF1 to APBs is mediated by DNA damage response factors

To further elucidate the involvement of phosphorylated (pT371)TRF1 at APBs, various components of DNA damage response and repair pathways were examined for their role in recruiting (pT371)TRF1 to APBs. Phosphorylated (pT371)TRF1 was first examined in GM847 cells depleted of ATM (Figure 3.8A), BRCA1 (Figure 3.8B) and 53BP1 (Figure 3.8C). A significant reduction in the localization of (pT371)TRF1 to APBs was observed for cells depleted of ATM and BRCA1, but no significant effect was observed for cells depleted of 53BP1 (Figure 3.8D). The percentage of cells positive for pT371 foci was reduced for the knockdown construct sh53BP1-A compared to the pRS vector control, which may explain the slight reduction in the localization of (pT371)TRF1 to APBs for this cell line (Figure 3.8D and 3.8E). No other knockdowns had a significant effect on the percentage of pT371-positive cells (Figure 3.8E). Knockdown of ATM, BRCA1 or 53BP1 did not have a significant effect on the localization of total TRF1 (Figure 3.8F) or TRF2 (Figure 3.8G) to APBs and the total protein levels of (pT371)TRF1 and TRF2 were essentially unchanged (Figure 3.8A, 3.8B and 3.8C). There were no significant changes in the percentage of cells in S and G2 phases as measured by cyclin A staining (Figure 3.8H) or on the percentage of PML-positive cells (Figure 3.8I).

Similarly, U2OS cells depleted of 53BP1 (Figure 3.9A) also showed no significant change in the percentage of cells with (pT371)TRF1 at APBs (Figure 3.9B). The percentage of pT371-positive cells (Figure 3.9C) and the percentage of cells with Rap1 at APBs (Figure 3.9D) were also not significantly affected.

To complement the data obtained from cells depleted of ATM, GM847 cells were treated with an inhibitor of ATM, as well as inhibitors against Mre11 and DNA-PK. KU55933 is a specific inhibitor of ATM kinase activity (Hickson et al., 2004) and NU7026 is specific inhibitor of DNA-PK (Veuger et al., 2004). Mirin is a specific inhibitor of the nuclease activity of Mre11 and prevents the autophosphorylation of ATM on S1981 but does not affect ATM kinase activity (Dupré et al., 2008). Inhibition of these components had little effect on the level of (pT371)TRF1 or TRF2 (Figure 3.10A). There was a significant reduction in the localization of (pT371)TRF1 to APBs for cells treated with inhibitors of ATM and Mre11, but no significant effect was observed for cells treated with the DNA-PK inhibitor compared to the control (Figure 3.10B). The percentage of pT371-positive cells (Figure 3.10C) and the percentage of cells with TRF1 or TRF2 at APBs (Figure 3.10D and 3.10E) were not significantly altered by inhibitor treatments. The percentage of cells in S and G2 phases as measured by cyclin A staining (Figure 3.10F) and the percentage of PML-positive cells (Figure 3.10G) both showed little change upon inhibitor treatments.

U2OS cells were also treated with the inhibitors KU55933 and Mirin. No significant change in the protein level of (pT371)TRF1 was observed after 1h, 2h or 4h inhibitor treatments (Figure 3.11A). The percentage of U2OS cells with (pT371)TRF1 at APBs was significantly reduced upon treatment with either ATM or Mre11 inhibitors (Figure 3.11B). The percentage of pT371-positive cells was unchanged with ATM inhibition, but a significant reduction was observed when Mre11 was inhibited (Figure

3.11C). There was little change in the percentage of cells with Rap1 at APBs following either treatment (Figure 3.11D).

Collectively, these results suggest that the localization of phosphorylated (pT371)TRF1 to APBs is mediated by DNA damage response factors. Localization appears to depend on the presence of functional ATM, Mre11 and BRCA1, but is independent of DNA-PK and 53BP1.

Figure 3.8. The localization of phosphorylated (pT371)TRF1 to APBs in GM847 cells is dependent upon ATM and BRCA1. (**A**) Western analysis of GM847 cells depleted for ATM. Immunoblotting was performed with anti-ATM, anti-pT371, anti-TRF2 and anti-γ-tubulin antibodies. (**B**) Western analysis of GM847 cells depleted for BRCA1. Immunoblotting was performed with anti-BRCA1, anti-pT371, anti-TRF2 and anti-γ-tubulin antibodies. (**C**) Western analysis of GM847 cells depleted for 53BP1. Immunoblotting was performed with anti-53BP1, anti-pT371, anti-TRF2 and anti-γ-tubulin antibodies. (**D**) Quantification of dual indirect immunofluorescence on GM847 cells depleted for ATM, BRCA1 or 53BP1, using anti-pT371 and anti-PML antibodies. The percentage of cells with (pT371)TRF1 at APBs is shown for >1000 cells in n=3. (**E**) Quantification of indirect immunofluorescence on GM847 cells depleted for ATM, BRCA1 or 53BP1, using anti-pT371 antibody. The percentage of pT371-positive cells is shown for >1000 cells in n=3. (**F**) Quantification of dual indirect immunofluorescence on GM847 cells depleted for ATM, BRCA1 or 53BP1, using anti-TRF1 and anti-PML antibodies. The percentage of cells with TRF1 at APBs is shown for >1000 cells in n=3. (**G**) Quantification of dual indirect immunofluorescence on GM847 cells depleted for ATM, BRCA1 or 53BP1, using anti-TRF2 and anti-PML antibodies. The percentage of cells with TRF2 at APBs is shown for >1000 cells in n=3. (**H**) Quantification of the percentage of cyclin A-positive GM847 cells depleted for ATM, BRCA1 or 53BP1. Graph shows results for >1000 cells in n=3. (**I**) Quantification of the percentage of PML-positive GM847 cells depleted for ATM, BRCA1 or 53BP1 for >1000 cells in n=3.

Fig3.8

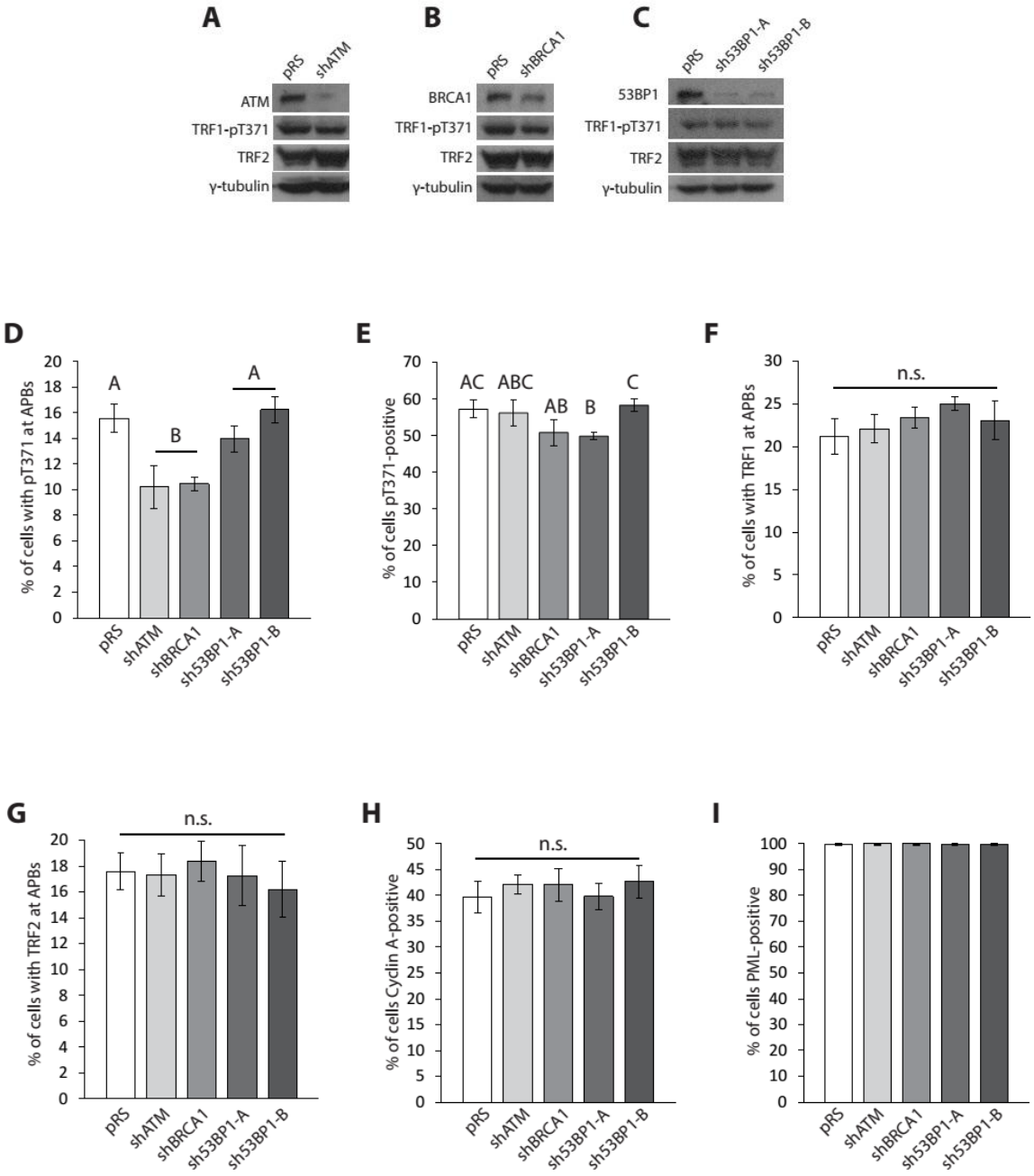
A
pRS
shATM
ATM
TRF1-pT371
TRF2
γ-tubulin
B
pRS
shBRCA1
BRCA1
TRF1-pT371
TRF2
γ-tubulin
C
pRS
sh53BP1-A
sh53BP1-B
53BP1
TRF1-pT371
TRF2
γ-tubulin
D
% of cells with pT371 at APBs
A
B
A
pRS
shATM
shBRCA1
sh53BP1-A
sh53BP1-B
E
% of cells pT371-positive
AC
ABC
AB
B
C
F
% of cells with TRF1 at APBs
n.s.
G
% of cells with TRF2 at APBs
n.s.
H
% of cells Cyclin A-positive
n.s.
I
% of cells PML-positive

Figure 3.9. The localization of phosphorylated (pT371)TRF1 to APBs in U2OS cells is independent of 53BP1. (**A**) Western analysis of U2OS cells depleted for 53BP1. Immunoblotting was performed with anti-53BP1 and anti-γ-tubulin antibodies. (**B**) Quantification of the percentage of U2OS cells depleted for 53BP1 with (pT371)TRF1 at APBs. Dual indirect immunofluorescence was performed with anti-pT371 and anti-PML antibodies for >500 cells in n=3. (**C**) Quantification of the percentage of pT371-positive U2OS cells depleted for 53BP1. Indirect immunofluorescence was performed with anti-pT371 antibody for >500 cells in n=3. (**D**) Quantification of the percentage of U2OS cells depleted for 53BP1 with Rap1 at APBs. Dual indirect immunofluorescence was performed with anti-Rap1 and anti-PML antibodies. Graph shows means for >500 cells in n=3.

Fig3.9

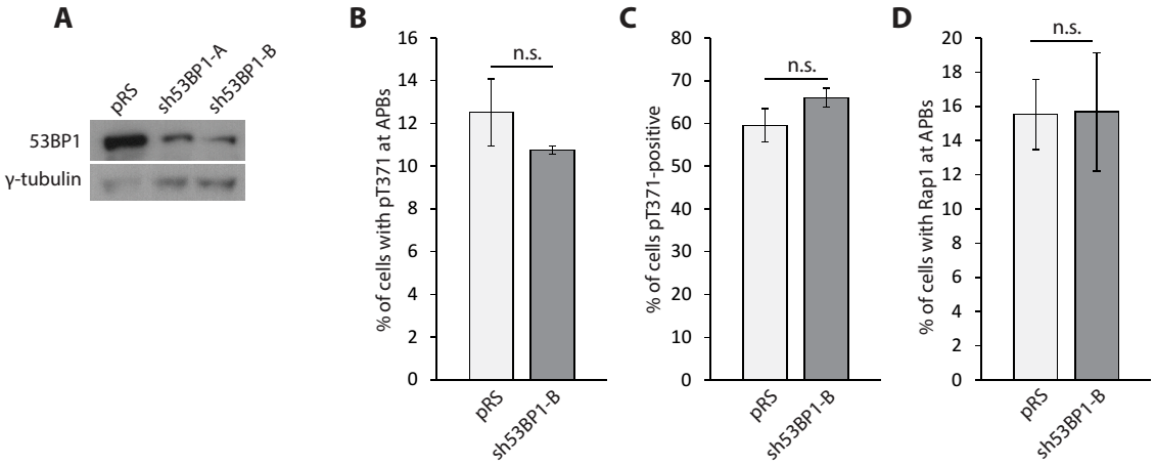
A
pRS
sh53BP1-A
sh53BP1-B
53BP1
γ-tubulin
B
% of cells with pT371 at APBs
n.s.
pRS
sh53BP1-B
C
% of cells pT371-positive
n.s.
pRS
sh53BP1-B
D
% of cells with Rap1 at APBs
n.s.
pRS
sh53BP1-B

Figure 3.10. The localization of phosphorylated (pT371)TRF1 to APBs in GM847 cells is dependent upon ATM and Mre11. (**A**) Western analysis of GM847 cells treated with various inhibitors for 1h. Immunoblotting was performed with anti-pT371, anti-TRF2 and anti-γ-tubulin antibodies. Samples were run on one gel. (**B**) Quantification of dual indirect immunofluorescence on inhibitor treated GM847 cells from (A), using anti-pT371 and anti-PML antibodies. The percentage of cells with (pT371)TRF1 at APBs is shown for >1000 cells in n=3. (**C**) Quantification of indirect immunofluorescence on inhibitor treated GM847 cells from (A) using anti-pT371 antibody. The percentage of pT371-positive cells is shown for >1000 cells in n=3. (**D**) Quantification of dual indirect immunofluorescence on inhibitor treated GM847 cells from (A), using anti-TRF1 and anti-PML antibodies. The percentage of cells with TRF1 at APBs is shown for >1000 cells in n=3. (**E**) Quantification of dual indirect immunofluorescence on inhibitor treated GM847 cells from (A), using anti-TRF2 and anti-PML antibodies. The percentage of cells with TRF2 at APBs is shown for >1000 cells in n=3. (**F**) Quantification of the percentage of cyclin A-positive GM847 cells from (A). Graph shows means for >1000 cells in n=3. (**G**) Quantification of the percentage of PML-positive GM847 cells from (A) for >1000 cells in n=3.

Fig3.10

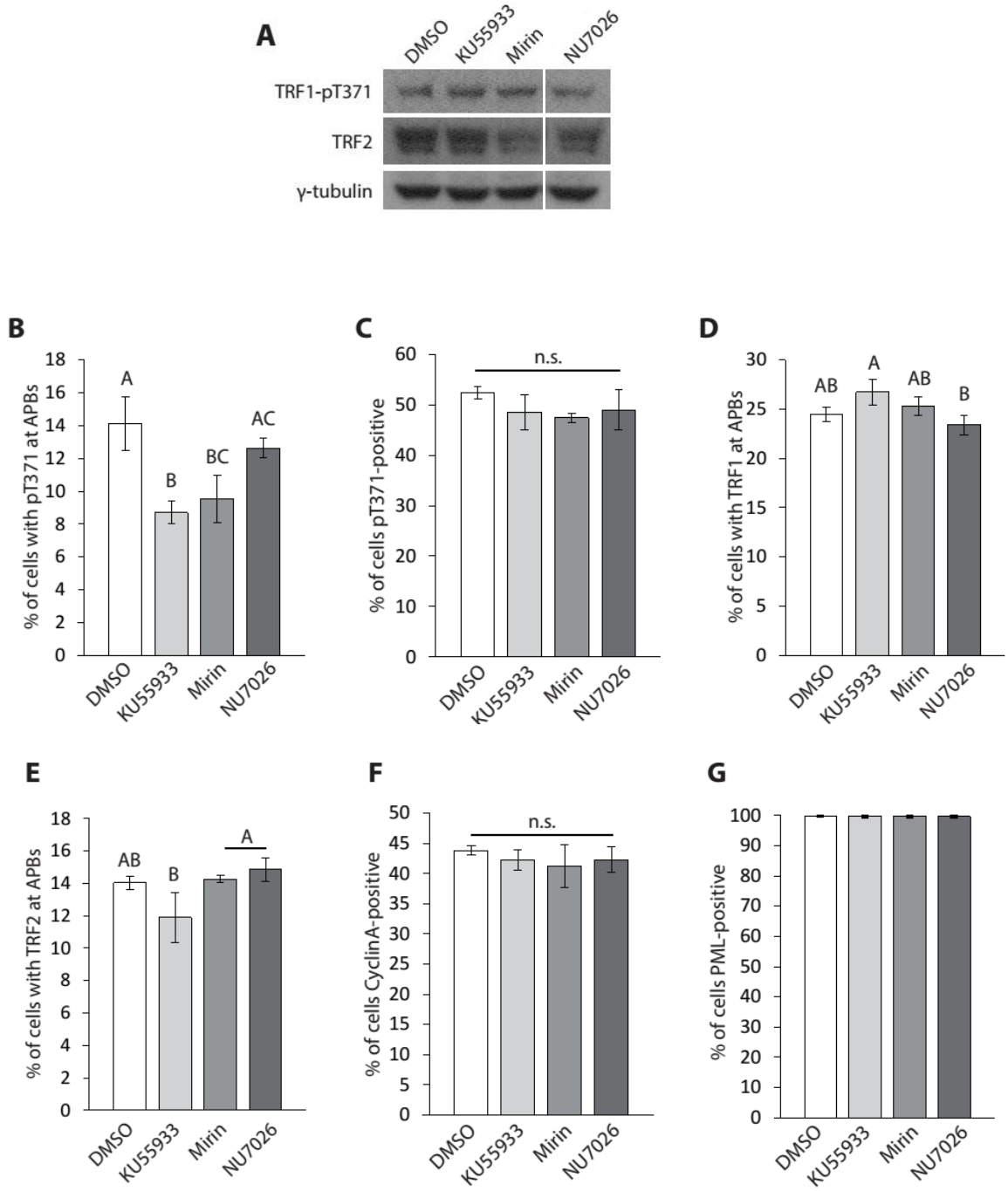
A
DMSO
KU55933
Mirin
NU7026
TRF1-pT371
TRF2
γ-tubulin
B
% of cells with pT371 at APBs
A
B
BC
AC
C
% of cells pT371-positive
n.s.
D
% of cells with TRF1 at APBs
AB
A
AB
B
E
% of cells with TRF2 at APBs
AB
B
A
F
% of cells CyclinA-positive
n.s.
G
% of cells PML-positive

Figure 3.11. The localization of phosphorylated (pT371)TRF1 to APBs in U2OS cells is dependent upon ATM and Mre11. (**A**) Western analysis of U2OS cells treated with various inhibitors for 1h, 2h or 4h. Immunoblotting was performed with anti-pT371 and anti-γ-tubulin antibodies. (**B**) Quantification of the percentage of U2OS cells with (pT371)TRF1 at APBs following a 1h treatment with KU55933 or a 4h treatment with Mirin. Cells we co-stained with anti-pT371 and anti-PML antibodies. Graph shows means for >500 cells in n=3. (**C**) Quantification of the percentage of pT371-positive U2OS cells following a 1h treatment with KU55933 or a 4h treatment with Mirin. Indirect immunofluorescence was performed with anti-pT371 antibody for >500 cells in n=3. (**D**) Quantification of the percentage of U2OS cells with Rap1 at APBs following a 1h treatment with KU55933 or a 4h treatment with Mirin. Dual indirect immunofluorescence was performed with anti-Rap1 and anti-PML antibodies for >500 cells in n=3.

Fig3.11

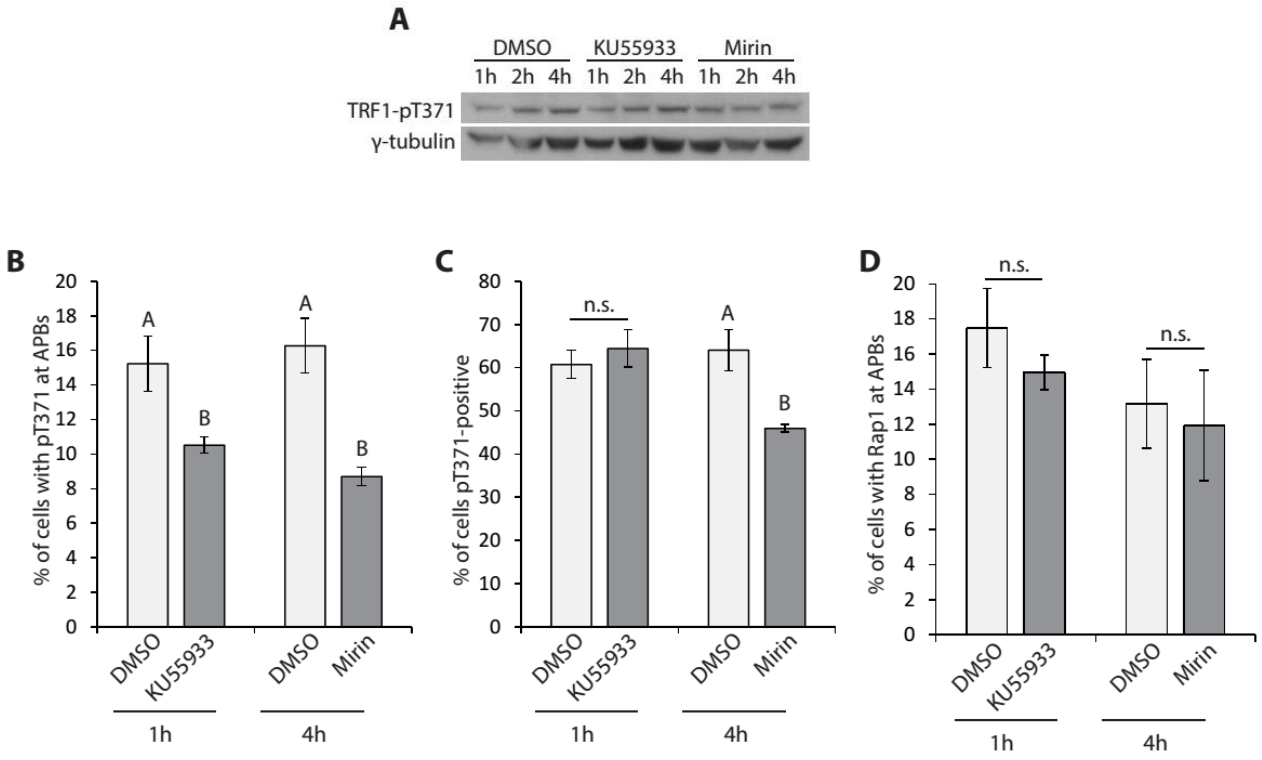
A
DMSO
KU55933
Mirin
1h 2h 4h 1h 2h 4h 1h 2h 4h
TRF1-pT371
γ-tubulin
B
% of cells with pT371 at APBs
A
B
A
B
DMSO
KU55933
DMSO
Mirin
1h
4h
C
% of cells pT371-positive
n.s.
A
B
D
% of cells with Rap1 at APBs
n.s.
n.s.

3.6 Phosphorylation at T371 of TRF1 is required for APB formation and C-circle production

To further investigate the association of phosphorylated (pT371)TRF1 with APBs, GM847 cells were depleted of endogenous TRF1 (Figure 3.12A and 3.12B) and complemented with Myc-tagged wild type TRF1, TRF1 with a nonphosphorylatable T371A (alanine) mutation or TRF1 with a phosphomimic T371D (aspartic acid) mutation (Figure 3.12C). A differential salt extraction of these cell lines showed that both wild type TRF1 and TRF1-T371A were found predominantly in the chromatin-bound fraction, whereas TRF1-T371D was distributed roughly equally between both the chromatin-free and chromatin-bound fractions (Figure 3.12D). This chromatin distribution of the TRF1-T371D mutant is similar to the distribution observed in GM847 parental cells with anti-pT371 antibody (Figure 3.3D). Both T371 mutants were able to form punctate pan-nuclear Myc foci (Figure 3.12E). Dual indirect immunofluorescence was performed on these cell lines using anti-Myc and anti-PML antibodies (Figure 3.12E). Quantification showed about a two-fold reduction in the localization of both T371A and T371D mutants to APBs compared to wild type TRF1 (Figure 3.12F), despite the percentage of Myc-positive cells being equal to or greater than wild type TRF1 (Figure 3.12G). Anti-pT371 antibody was unable to recognize TRF1 which had been mutated at T371 (Figure 3.13A), in line with the previous report (McKerlie & Zhu, 2011). Therefore, as expected the percentage of cells with phosphorylated (pT371)TRF1 at APBs was reduced for both cell lines expressing T371A and T371D mutants compared to wild type TRF1 (Figure 3.13B), although the percentage of pT371-positive cells was not significantly affected (Figure

3.13C). The localization of the shelterin proteins Rap1 (Figure 3.13D), TRF2 (Figure 3.13E) and TIN2 (Figure 3.13F) as well as the DNA repair factors Nbs1 (Figure 3.13G) and RPA (Figure 3.13H) at APBs was also significantly reduced in cells expressing T371A or T371D mutants, compared to wild type TRF1. The levels of these proteins were essentially unchanged across the different cell lines (Figure 3.13A). Taken together, these results suggest that the lack of phosphorylation at T371 of TRF1 impairs the localization of various shelterin proteins and DNA damage response factors to APBs.

C-circle formation was investigated in an attempt to understand the biological function of phosphorylated (pT371)TRF1 and to observe the effect that the T371 mutants might cause due to incomplete APB assembly. C-circle assays were performed using genomic DNA from the same GM847 cell lines as previously described (Figure 3.12C). Based on comparisons between the relative ratios of C-circles on the native gel (Figure 3.14A), a significant reduction in C-circle formation was observed in cells expressing the non-phosphorylatable T371A mutant compared to wild type TRF1 or the phosphomimic T371D mutant (Figure 3.14B). These results suggest that phosphorylation at T371 of TRF1 is important for the formation of C-circles.

Figure 3.12. The lack of phosphorylation at T371 impairs the ability of TRF1 to localize to APBs. (**A**) Western analysis of GM847 cells depleted for endogenous TRF1. Immunoblotting was performed with anti-TRF1 and anti-γ-tubulin antibodies. (**B**) Western analysis of GM847 cells depleted for endogenous TRF1. Immunoblotting was performed with anti-pT371 and anti-γ-tubulin antibodies. (**C**) Western analysis of GM847 cells depleted for endogenous TRF1 and complemented with Myc-tagged shTRF1-resistant wild type or mutant TRF1 proteins. Immunoblotting was performed with anti-Myc and anti-γ-tubulin antibodies. (**D**) Differential salt extraction of chromatin on GM847 cells from (C). Immunoblotting was performed with anti-Myc, anti-H2AX and anti-TRF2 antibodies. (**E**) Indirect immunofluorescence with anti-PML and anti-Myc antibodies on GM847 cells depleted of endogenous TRF1 and stably expressing Myc-tagged shTRF1-resistant TRF1 alleles as indicated. Cell nuclei were stained with DAPI in blue. (**F**) Quantification of the percentage of cells with Myc at APBs from (E). Graph shows results for >500 cells in n=6. (**G**) Quantification of the percentage of Myc-positive cells from (E). Graph shows means for >500 cells in n=6.

Fig3.12

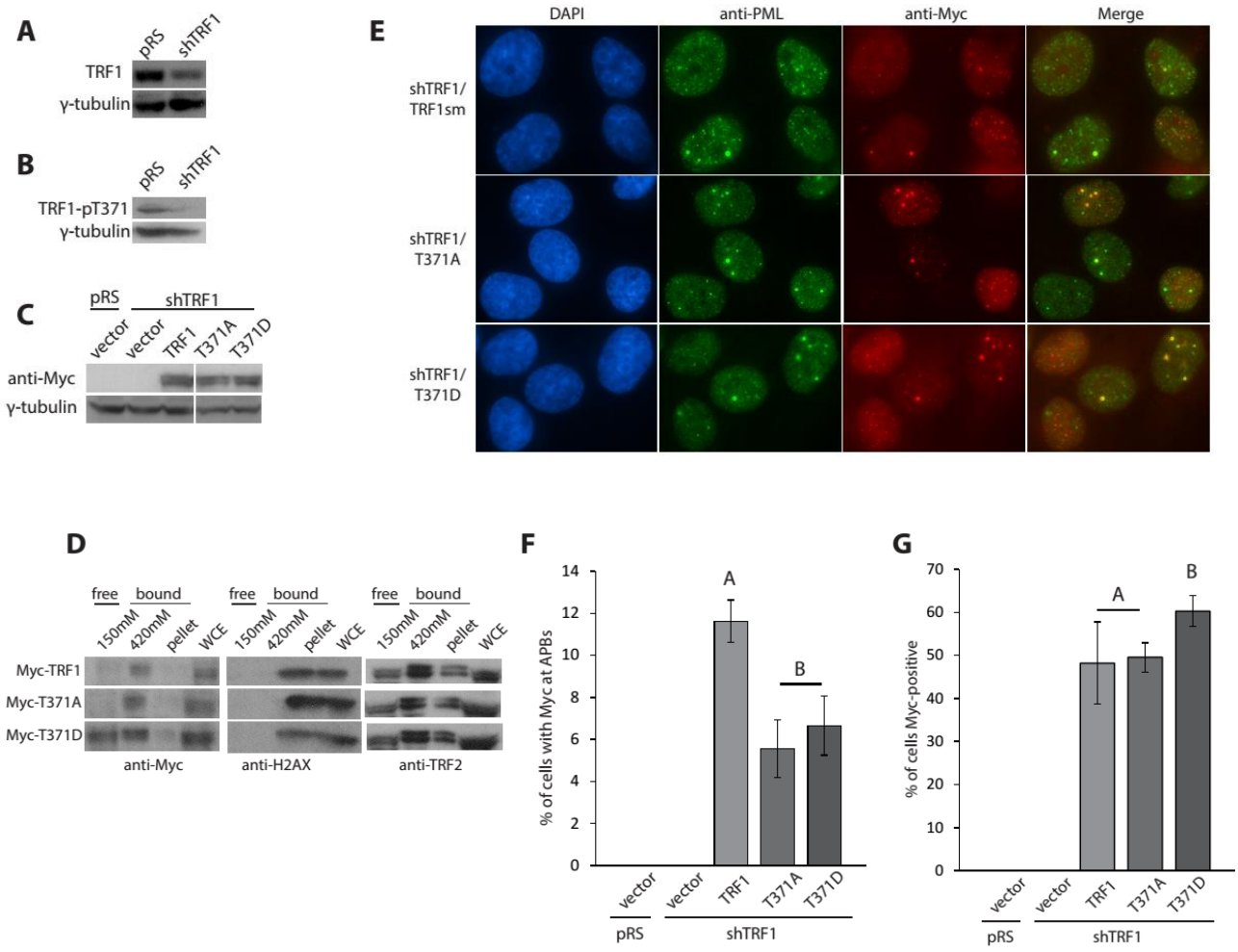
A
pRS
shTRF1
TRF1
γ-tubulin
B
pRS
shTRF1
TRF1-pT371
γ-tubulin
C
pRS
shTRF1
vector
vector
TRF1
T371A
T371D
anti-Myc
γ-tubulin
E
DAPI
anti-PML
anti-Myc
Merge
shTRF1/ TRF1sm
shTRF1/ T371A
shTRF1/ T371D
D
free
bound
150mM
420mM
pellet
WCE
Myc-TRF1
Myc-T371A
Myc-T371D
anti-Myc
anti-H2AX
anti-TRF2
F
% of cells with Myc at APBs
A
B
vector
vector
TRF1
T371A
T371D
pRS
shTRF1
G
% of cells Myc-positive
A
B
vector
vector
TRF1
T371A
T371D
pRS
shTRF1

Figure 3.13. The lack of phosphorylation at T371 of TRF1 impairs APB formation. (**A**) Western analysis of GM847 cells depleted of endogenous TRF1 and complemented with Myc-tagged shTRF1-resistant wild type or mutant TRF1 proteins. Immunoblotting was performed with the indicated antibodies. Asterisk indicates a non-specific band. (**B**) Quantification of the percentage of GM847 cells with (pT371)TRF1 at APBs for the various cell lines. Indirect immunofluorescence was performed with anti-pT371 and anti-PML antibodies for >500 cells in n=6. (**C**) Quantification of the percentage of pT371-positive GM847 cells for the various cell lines. Indirect immunofluorescence was performed with anti-pT371 antibody for >500 cells in n=6. (**D**) Quantification of the percentage of GM847 cells with Rap1 at APBs for the indicated cell lines. Indirect immunofluorescence was performed with anti-Rap1 and anti-PML antibodies for >500 cells in n=9. (**E**) Quantification of the percentage of GM847 cells with TRF2 at APBs for the indicated cell lines. Indirect immunofluorescence was performed with anti-TRF2 and anti-PML antibodies for >500 cells in n=6. (**F**) Quantification of the percentage of GM847 cells with TIN2 at APBs for the indicated cell lines. Indirect immunofluorescence was performed with anti-TIN2 and anti-PML antibodies for >500 cells in n=3. (**G**) Quantification of the percentage of GM847 cells with Nbs1 at APBs for the indicated cell lines. Indirect immunofluorescence was performed with anti-Nbs1 and anti-PML antibodies for >500 cells in n=6. (**H**) Quantification of the percentage of GM847 cells with RPA at APBs for the indicated cell lines. Indirect immunofluorescence was performed with anti-RPA32 and anti-PML antibodies for >500 cells in n=3.

Fig3.13

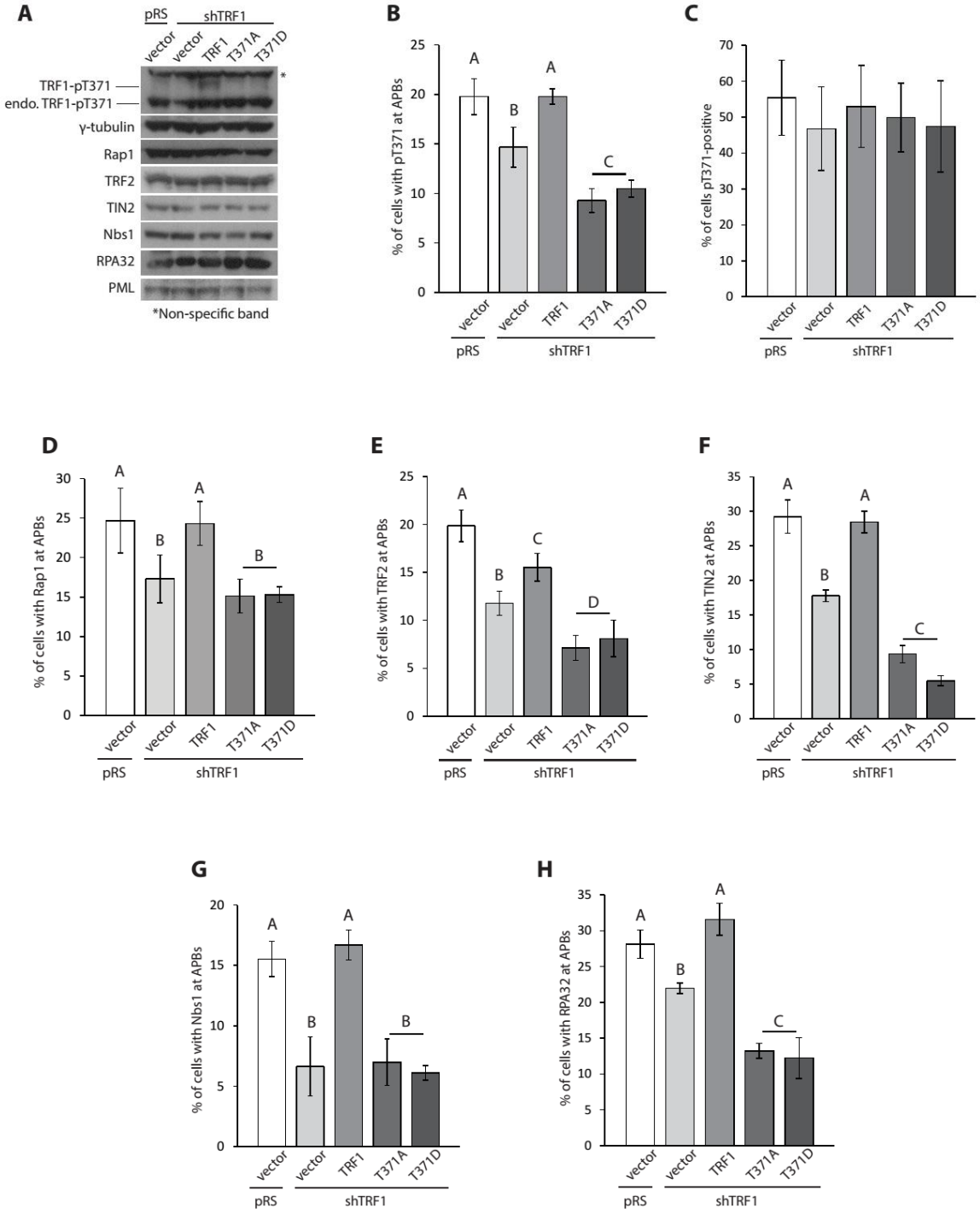
A
pRS
shTRF1
vector
vector
TRF1
T371A
T371D
TRF1-pT371
endo. TRF1-pT371
γ-tubulin
Rap1
TRF2
TIN2
Nbs1
RPA32
PML
*Non-specific band
B
% of cells with pT371 at APBs
C
% of cells pT371-positive
D
% of cells with Rap1 at APBs
E
% of cells with TRF2 at APBs
F
% of cells with TIN2 at APBs
G
% of cells with Nbs1 at APBs
H
% of cells with RPA32 at APBs

Figure 3.14. Phosphorylation at T371 of TRF1 is important for C-circle formation. (**A**) Native C-circle gel on GM847 cells stably depleted of endogenous TRF1 and complemented with Myc-tagged shTRF1-resistant wild type and mutant TRF1 proteins. The C-circle areas used for quantification in (B) are indicated. (**B**) Quantification of the relative ratio of C-circle volumes for ϕ29 lanes shown in the native gel in (A). The vector was set to 1. Graph shows mean ± SD for n=3.

Fig3.14

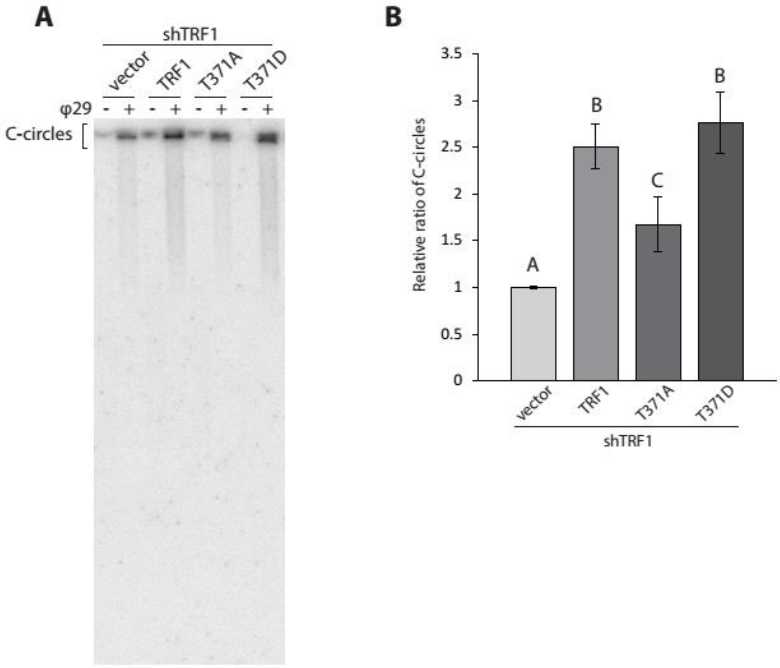
A
shTRF1
vector
TRF1
T371A
T371D
φ29
- + - + - + - +
C-circles
B
Relative ratio of C-circles
3.5
3
2.5
2
1.5
1
0.5
0
A
B
C
B
vector
TRF1
T371A
T371D
shTRF1

3.7 The dimerization domain of TRF1 is required for its localization to APBs

To further assess the function of phosphorylated (pT371)TRF1 in ALT cells, a series of TRF1 truncation mutants were generated to see if phosphorylation was still required when different domains of TRF1 were removed and also to investigate whether different domains have separate functions in APB formation. The truncation mutants include TRF1 with a deletion of the N-terminal acidic domain (ΔA), TRF1 with a deletion of the C-terminal Myb-like DNA binding domain (ΔM), TRF1 lacking both the acidic and Myb-like domains (ΔAΔM), TRF1 with only the linker and Myb-like domains (L-M) and TRF1 with only the linker domain (L) (Figure 3.15A). GM847 cells depleted of endogenous TRF1 were completed with Myc-tagged shTRF1-resistant wild type TRF1 and the various TRF1 truncation alleles described above, as well as TRF1 truncation alleles carrying either T371A or T371D mutations (Figure 3.15B). Unfortunately, lack of expression of the ΔA allele prevented it from being used in most experiments (Figure 3.15B). Despite many efforts, TRF1-ΔA could not be stably expressed in shTRF1 knockdown cells or through overexpression. Both Myc- and Flag-tagged ΔA constructs from different clones were tried to no avail (data not shown). A differential salt extraction of chromatin revealed that the truncation mutants ΔM, ΔAΔM, L-M and L were found predominantly in the chromatin-free fraction, compared to wild type TRF1 which was predominantly in the chromatin-bound fraction (Figure 3.15C). Consistent with this, indirect immunofluorescence using anti-Myc antibody revealed that none of the Myc-tagged truncation mutants were able to form telomere-like foci, whereas wild type TRF1 showed about 40% of cells with punctate Myc telomere-like foci (Figure 3.15D and

3.15E). Dual indirect immunofluorescence with anti-Myc and anti-PML antibodies showed that the truncation mutants ΔM, ΔAΔM and their corresponding T371 alleles were able to localize to APBs at a comparable level to wild type TRF1 (Figure 3.15F). On the other hand, all of the L-M alleles were significantly defective in their localization and none of the L alleles showed any detectable localization to APBs (Figure 3.15F). These differences were not due to a lack of Myc-positive cells (Figure 3.15G) or to a lack of protein expression (Figure 3.15H).

To summarize, only the TRF1 truncation mutants containing the TRFH homodimerization domain were able to fully localize to APBs, compared to full length wild type TRF1. These data therefore suggest that the dimerization domain of TRF1 is required for TRF1 to localize to APBs.

Figure 3.15. The dimerization domain of TRF1 is required for its localization to APBs. (**A**) A representative image of the domain structure of TRF1 and various TRF1 truncation mutants. The first and last amino acids (a.a.) of each protein are indicated. Diagram is not to scale. (**B**) Western analysis of GM847 cells depleted of endogenous TRF1 and complemented with Myc-tagged shTRF1-resistant wild type TRF1 and various TRF1 truncation alleles. Immunoblotting was performed with anti-Myc and anti-γ-tubulin antibodies. Samples were run on two separate 10% SDS-PAGE gels. Protein molecular weight markers (kDa) are labeled to the right of each blot. Arrows indicate approximate locations of each protein. Refer to main text for an explanation of protein abbreviations. (**C**) Differential salt extraction of TRF1-depleted GM847 cells expressing the indicated Myc-tagged shTRF1-resistant proteins. Immunoblotting was performed with anti-Myc and anti-TRF2 antibodies for samples run on a 10% SDS-PAGE gel, and anti-H2AX antibody was used for samples run on a 15% SDS-PAGE gel. (**D**) Indirect immunofluorescence analysis using anti-Myc and anti-PML antibodies on GM847 cells from (B). (**E**) Quantification of the percentage of cells with Myc telomere-like foci in GM847 cells from (B) as labeled. Immunofluorescence was performed with anti-Myc antibody for >500 cells in n=3. "V" represents the pRS/vector, "KD" represents the shTRF1/vector and "WT" represents shTRF1/TRF1sm. (**F**) Quantification of the percentage of cells with Myc at APBs for the indicated GM847 cell lines. Indirect immunofluorescence was performed with anti-Myc and anti-PML antibodies. Graph shows means for >500 cells in n=3. (**G**) Quantification of the percentage of Myc-positive cells for the indicated GM847 cell lines. Indirect immunofluorescence was performed

with anti-Myc antibody for >500 cells in n=3. (**H**) Western analysis of TRF1-depleted GM847 cells expressing various Myc-tagged TRF1 truncation mutant alleles. Immunoblotting was performed with anti-Myc and anti-γ-tubulin antibodies. Samples were run on a 10% SDS-PAGE gel. Protein molecular weight markers (kDa) are labeled to the right of each blot. Arrows indicate approximate locations of each protein.

Fig3.15

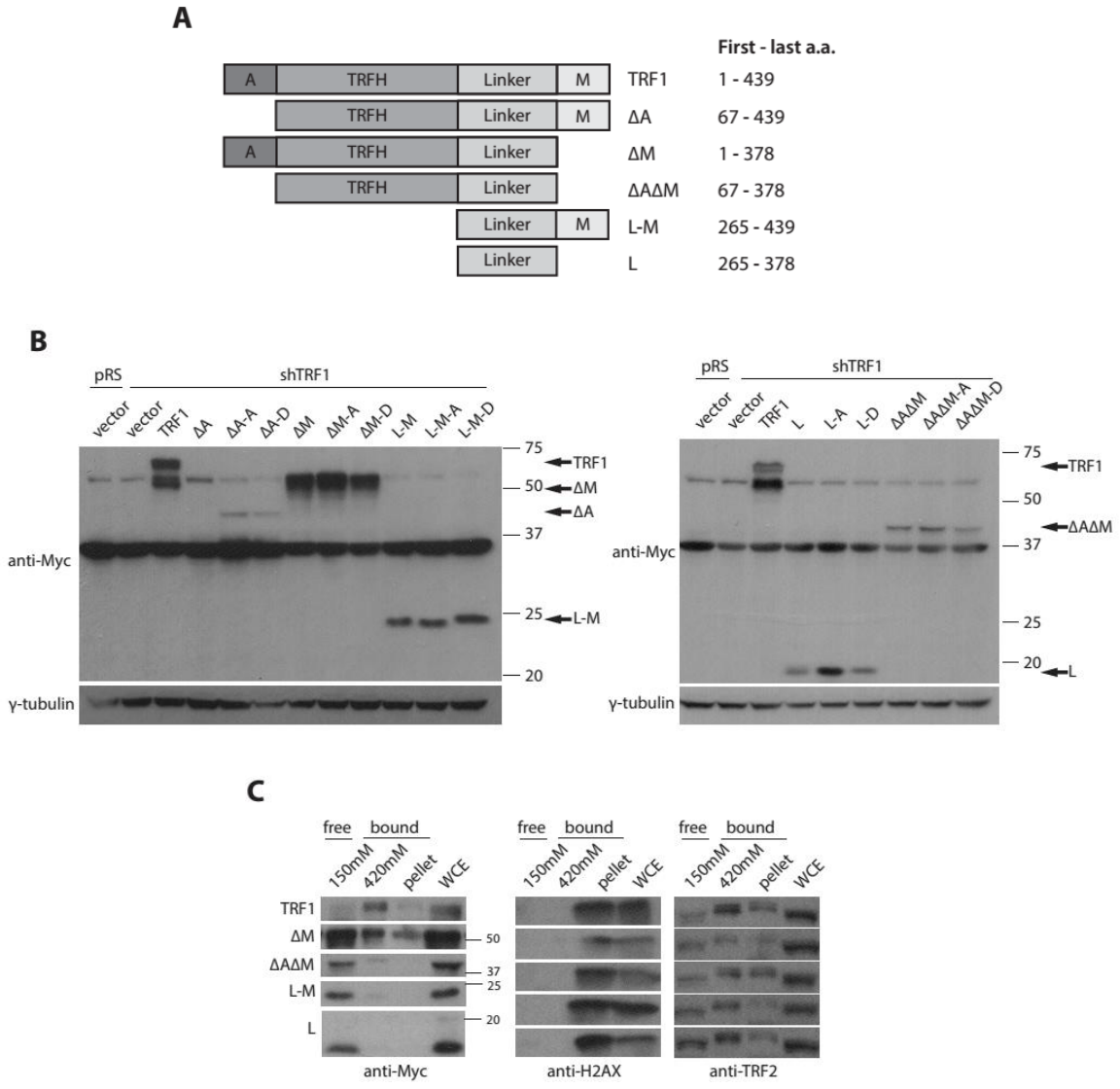
A
First - last a.a.
A
TRFH
Linker
M
TRF1
1 - 439
ΔA
67 - 439
ΔM
1 - 378
ΔAΔM
67 - 378
L-M
265 - 439
L
265 - 378
B
pRS
shTRF1
vector
vector
TRF1
ΔA
ΔA-A
ΔA-D
ΔM
ΔM-A
ΔM-D
L-M
L-M-A
L-M-D
anti-Myc
γ-tubulin
75
50
37
25
20
TRF1
ΔM
ΔA
L-M
L
ΔAΔM
ΔAΔM-A
ΔAΔM-D
C
free
bound
150mM
420mM
pellet
WCE
anti-Myc
anti-H2AX
anti-TRF2

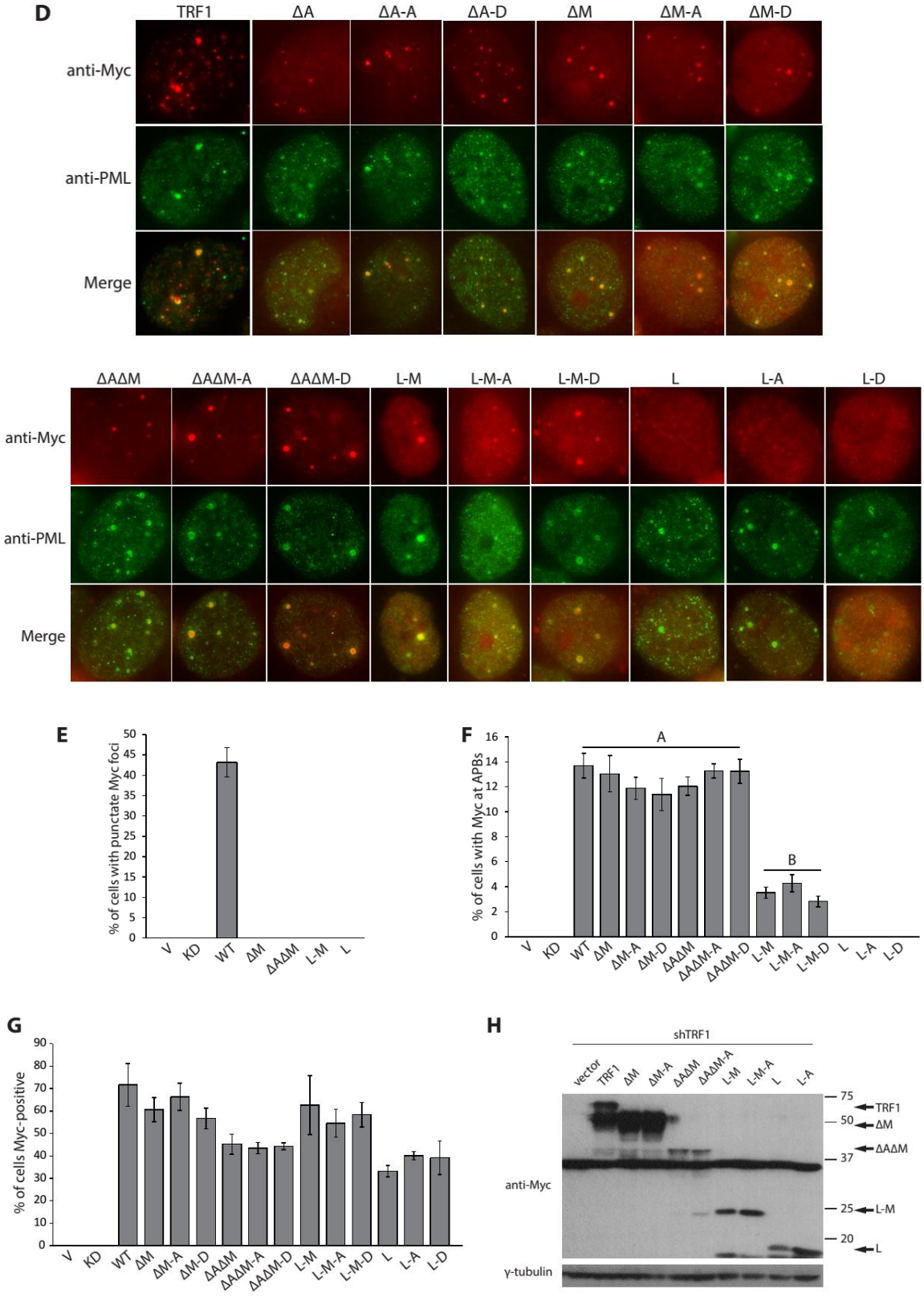
D
TRF1
ΔA
ΔA-A
ΔA-D
ΔM
ΔM-A
ΔM-D
anti-Myc
anti-PML
Merge
ΔAΔM
ΔAΔM-A
ΔAΔM-D
L-M
L-M-A
L-M-D
L
L-A
L-D
E
% of cells with punctate Myc foci
V
KD
WT
ΔM
ΔAΔM
L-M
L
F
% of cells with Myc at APBs
A
B
G
% of cells Myc-positive
H
shTRF1
vector
TRF1
ΔM
ΔM-A
ΔAΔM
ΔAΔM-A
L-M
L-M-A
L
L-A
anti-Myc
γ-tubulin
75
50
37
25
20

3.8 Full-length TRF1 and the DNA binding activity of TRF1 are required for the functional assembly of APBs

Based on the above results that some of the TRF1 truncation mutants were defective in their localization to APBs, the recruitment of other proteins to APBs was investigated in these cell lines. Dual indirect immunofluorescence using anti-PML antibody in conjunction with either anti-TRF2 or anti-TIN2 antibodies showed that only cells expressing the L-M truncation mutants were able to fully rescue the localization of these shelterin proteins to APBs compared to wild type TRF1 (Figure 3.16A and 3.16B). No significant differences were observed between the other truncation mutants and the shTRF1 vector control (Figure 3.16A and 3.16B). Analysis of the co-localization of Nbs1 and PML by indirect immunofluorescence revealed that none of the truncation mutant cell lines could fully recruit Nbs1 to APBs compared to wild type TRF1 (Figure 3.16C). An examination of the localization of RPA to APBs provided less clear-cut data, although the L-M and L-M-A mutants showed a higher level of co-localization compared to the other truncation mutants, which showed a similar level to the shTRF1 vector (Figure 3.16D). The percentage of pT371-positive cells was not significantly affected by expression of the various TRF1 truncation alleles compared to wild type TRF1 (Figure 3.16E). The percentage of cells in S and G2 phases as measured by cyclin A staining (Figure 3.16F) and the percentage of PML-positive cells (Figure 3.16G) were essentially unchanged for the cell lines investigated. The total protein levels of TRF2, TIN2 and RPA also showed little change (Figure 3.16H).

In summary, cells expressing the ΔM, ΔAΔM and L truncation mutant alleles were defective in their ability to recruit TRF2, TIN2, Nbs1 and RPA to APBs. However, cells expressing the L-M truncation mutant alleles showed similar levels of TRF2, TIN2 and RPA localization to APBs as full length TRF1, but these cells were also defective in recruiting Nbs1 to APBs. Collectively, these results suggest that only cells expressing full-length TRF1 are able to assemble complete APBs, as none of the truncation mutants were able to fully recruit all shelterin or DNA repair proteins that were investigated to APBs.

The differential salt extraction data discussed previously showed that the phosphomimic T371D mutant in full length TRF1 as well as all TRF1 truncation mutants were found predominantly in the chromatin-free fraction, compared to wild type TRF1 and the nonphosphorylatable T371A mutant which were mostly chromain-bound (Figure 3.12D and 3.15C). Neither cells expressing the T371 mutants nor the TRF1 truncation mutants were able to fully recruit all examined proteins to APBs. To further investigate whether the DNA-binding activity of TRF1 was required for the localization of TRF1 or other proteins to APBs, APBs were analysed in GM847 cells that were depleted of endogenous TRF1 and complemented with a series of TRF1 mutants unable to bind telomeric DNA. TRF1 carrying a single amino acid substitution of R425V in the Myb-like DNA binding domain is known to be defective in its ability to bind telomeric DNA (Fairall et al., 2001; McKerlie & Zhu, 2011; McKerlie et al., 2013). Therefore, Myc-tagged TRF1-R425V, as well as Myc-TRF1-R425V-T371A and Myc-TRF1-R425V-T371D were examined (Figure 3.17A). Differential salt extraction analysis showed that

TRF1-R425V, TRF1-R425V-T371A and TRF1-R425V-T371D were all found predominantly in the chromatin-free fraction, compared to chromatin-bound wild type TRF1 (Figure 3.17B). In line with this, the R425V mutants showed no punctate pan-nuclear Myc foci by indirect immunofluorescence (Figure 3.17C), consistent with previous reports that they are defective in forming telomere foci and in binding to telomeric DNA. Expression of the R425V mutants showed no significant effect on the co-localization of anti-Myc and anti-PML antibodies at APBs compared to wild type TRF1 (Figure 3.17D). The percentage of Myc-positive cells did not change significantly across cell lines (Figure 3.17E). However, the recruitment of TRF2, TIN2 and Nbs1 to APBs was observed to be defective for all three cell lines expressing R425V mutants, compared to wild type TRF1 (Figure 3.17F – 3.17H). These results suggest that the DNA binding ability of TRF1 is dispensable for its own localization to APBs, but that it is required for the recruitment of TRF2, TIN2 and Nbs1 to APBs.

Figure 3.16. Full-length TRF1 is required for complete APB assembly. (**A**) Quantification of the percentage of cells with TRF2 at APBs for the indicated GM847 cell lines. Indirect immunofluorescence was performed with anti-TRF2 and anti-PML antibodies for >500 cells in at least 6 trials. (**B**) Quantification of the percentage of cells with TIN2 at APBs for the indicated GM847 cell lines. Indirect immunofluorescence was performed with anti-TIN2 and anti-PML antibodies for >500 cells in at least 6 trials. (**C**) Quantification of the percentage of cells with Nbs1 at APBs for the indicated GM847 cell lines. Indirect immunofluorescence was performed with anti-Nbs1 and anti-PML antibodies. Graph shows mean ± SD for >500 cells in at least 6 trials. (**D**) Quantification of the percentage of cells with RPA at APBs for the indicated GM847 cell lines. Indirect immunofluorescence was performed with anti-RPA32 and anti-PML antibodies for >1000 cells in n=3. (**E**) Quantification of the percentage of pT371-positive GM847 cells for the indicated cell lines. Indirect immunofluorescence was performed with anti-pT371 antibody. Graph shows mean ± SD for >500 cells in n=3. (**F**) Quantification of the percentage of cyclin A-positive GM847 cells for the indicated cell lines. Indirect immunofluorescence was performed with anti-cyclin A antibody for >500 cells in n=3. (**G**) Quantification of the percentage of PML-positive GM847 cells for the indicated cell lines. Indirect immunofluorescence was performed with anti-PML antibody for >500 cells in n=3. (**H**) Western analysis of TRF1-depleted GM847 cells stably expressing the indicated cell lines. Immunoblotting was performed with anti-TRF2, anti-TIN2 and anti-RPA32 antibodies.

Fig3.16

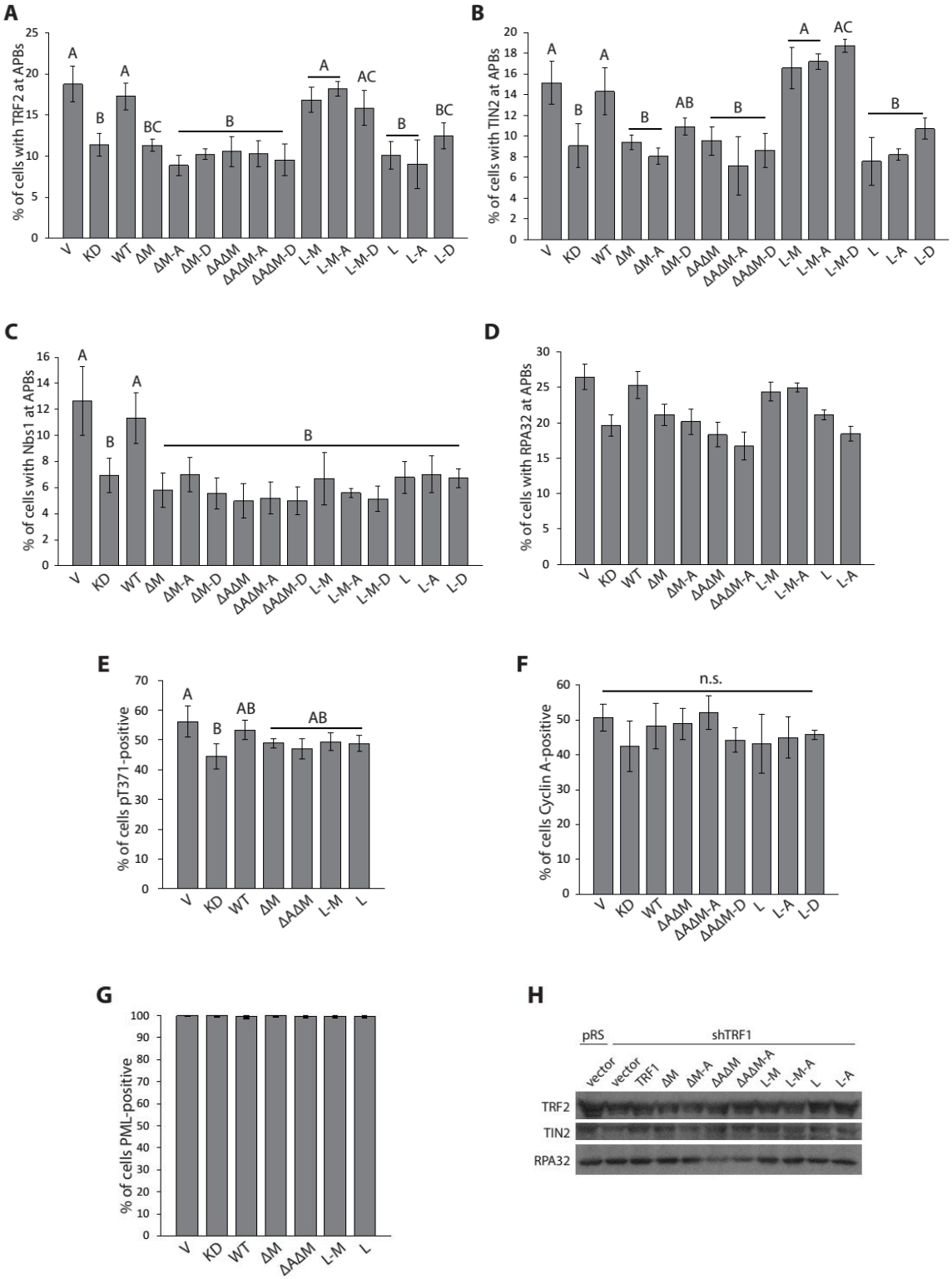
A
% of cells with TRF2 at APBs
B
% of cells with TIN2 at APBs
C
% of cells with Nbs1 at APBs
D
% of cells with RPA32 at APBs
E
% of cells pT371-positive
F
% of cells Cyclin A-positive
n.s.
G
% of cells PML-positive
H
pRS
shTRF1
vector
vector
TRF1
ΔM
ΔM-A
ΔAΔM
ΔAΔM-A
L-M
L-M-A
L
L-A
TRF2
TIN2
RPA32
V
KD
WT
ΔM
ΔM-A
ΔM-D
ΔAΔM
ΔAΔM-A
ΔAΔM-D
L-M
L-M-A
L-M-D
L
L-A
L-D

Figure 3.17. The DNA binding activity of TRF1 is important for APB formation. (**A**) Western analysis of GM847 cells stably depleted for endogenous TRF1 and complemented with Myc-tagged shTRF1-resistant wild type or mutant TRF1 proteins. Immunoblotting was performed with anti-Myc, anti-γ-tubulin, anti-TIN2, anti-TRF2, anti-Nbs1 and anti-PML antibodies. (**B**) Differential salt extraction of GM847 cells from (A) as labeled. Immunoblotting was performed with anti-Myc and anti-TRF2 antibodies. (**C**) Indirect immunofluorescence with anti-Myc and anti-PML antibodies on GM847 cells from (A) as labeled. (**D**) Quantification of the percentage of GM847 cells with Myc at APBs for the indicated cell lines as in (C). Graph shows mean ± SD for >1000 cells in n=3. (**E**) Quantification of the percentage of Myc-positive GM847 cells for the indicated cell lines as in (C). Graph shows mean ± SD for >1000 cells in n=3. (**F**) Quantification of the percentage of GM847 cells with TRF2 at APBs for the indicated cell lines. Indirect immunofluorescence was performed with anti-TRF2 and anti-PML antibodies for >1000 cells in n=3. (**G**) Quantification of the percentage of GM847 cells with TIN2 at APBs for the indicated cell lines. Indirect immunofluorescence was performed with anti-TIN2 and anti-PML antibodies. Graph shows mean ± SD for >1000 cells in n=3. (**H**) Quantification of the percentage of GM847 cells with Nbs1 at APBs for the indicated cell lines. Indirect immunofluorescence was performed with anti-Nbs1 and anti-PML antibodies for >1000 cells in n=3.

Fig3.17

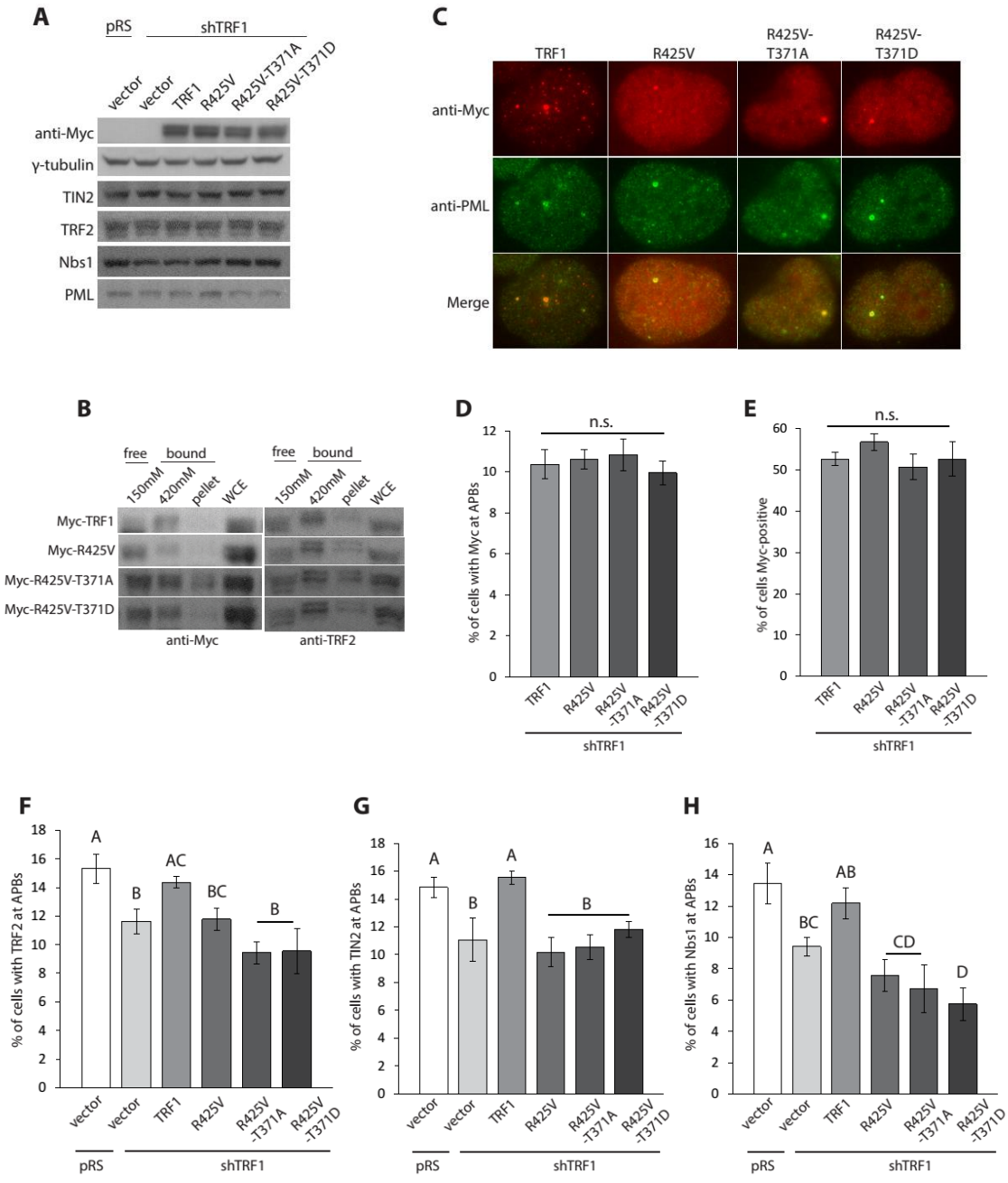
A
pRS
shTRF1
vector
vector
TRF1
R425V
R425V-T371A
R425V-T371D
anti-Myc
γ-tubulin
TIN2
TRF2
Nbs1
PML
C
TRF1
R425V
R425V-T371A
R425V-T371D
anti-Myc
anti-PML
Merge
B
free
bound
150mM
420mM
pellet
WCE
Myc-TRF1
Myc-R425V
Myc-R425V-T371A
Myc-R425V-T371D
anti-Myc
anti-TRF2
D
n.s.
% of cells with Myc at APBs
TRF1
R425V
R425V -T371A
R425V -T371D
shTRF1
E
n.s.
% of cells Myc-positive
TRF1
R425V
R425V -T371A
R425V -T371D
shTRF1
F
% of cells with TRF2 at APBs
A
B
AC
BC
B
vector
vector
TRF1
R425V
R425V -T371A
R425V -T371D
pRS
shTRF1
G
% of cells with TIN2 at APBs
A
B
A
B
vector
vector
TRF1
R425V
R425V -T371A
R425V -T371D
pRS
shTRF1
H
% of cells with Nbs1 at APBs
A
BC
AB
CD
D
vector
vector
TRF1
R425V
R425V -T371A
R425V -T371D
pRS
shTRF1

3.9 TRF1 truncation mutants do not have a significant effect on cell proliferation

To assess whether expression of the TRF1 truncation mutants and their inability to fully recruit proteins to APBs had an effect on cell proliferation, cells were cultured for over 50 days and population doublings (PDs) were recorded. No growth defects were observed, as the growth rates of all of the truncation mutant cell lines were essentially indistinguishable from cells expressing wild type TRF1 (Figure 3.18A and 3.18B). However, protein expression was slightly reduced for most cell lines by PD 30 to 40 (Figure 3.18C and 3.18D).

Figure 3.18. TRF1 truncation mutants do not have a significant effect on cell proliferation. (**A**) Growth curve of TRF1-depleted GM847 cells stably expressing various Myc-tagged TRF1 truncation constructs as indicated. The number of PDs was plotted against days in culture. (**B**) Growth curve of TRF1-depleted GM847 cells stably expressing various Myc-tagged TRF1 truncation constructs as indicated. The number of PDs was plotted against days in culture. (**C**) Western analysis of expression of various Myc-tagged TRF1 truncation mutants in early and late PDs, corresponding to the growth curve in (A). Samples were run on 2 separate 10% SDS-PAGE gels and immunoblotting was performed with anti-Myc and anti-γ-tubulin antibodies. (**D**) Western analysis of expression of various Myc-tagged TRF1 truncation mutants in early and late PDs, corresponding to the growth curve in (B). Samples were run on 2 separate 10% SDS-PAGE gels and immunoblotting was performed with anti-Myc and anti-γ-tubulin antibodies.

Fig3.18

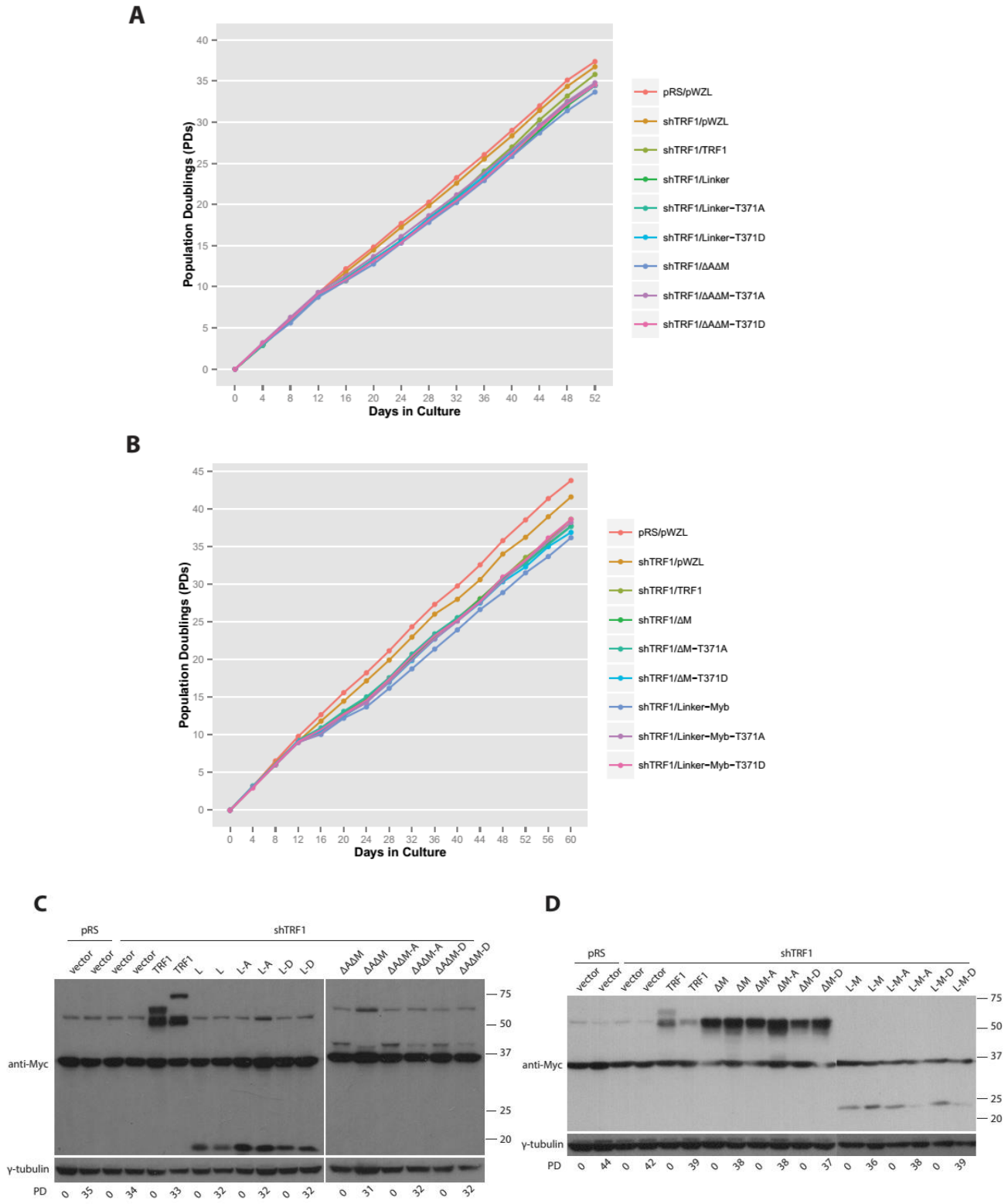
A
Population Doublings (PDs)
Days in Culture
pRS/pWZL
shTRF1/pWZL
shTRF1/TRF1
shTRF1/Linker
shTRF1/Linker−T371A
shTRF1/Linker−T371D
shTRF1/ΔAΔM
shTRF1/ΔAΔM−T371A
shTRF1/ΔAΔM−T371D
B
Population Doublings (PDs)
Days in Culture
pRS/pWZL
shTRF1/pWZL
shTRF1/TRF1
shTRF1/ΔM
shTRF1/ΔM−T371A
shTRF1/ΔM−T371D
shTRF1/Linker−Myb
shTRF1/Linker−Myb−T371A
shTRF1/Linker−Myb−T371D
C
pRS
shTRF1
anti-Myc
γ-tubulin
PD
D
pRS
shTRF1
anti-Myc
γ-tubulin
PD

CHAPTER 4 DISCUSSION

4.1 Preliminary analysis of phosphorylated (pT371)TRF1 in ALT cells

TRF1 is known to be involved in APB formation, including through its sumoylation by MMS21, its interaction with PML3 and its interaction with Nbs1 (Jiang et al., 2007; Potts & Yu, 2007; Yu et al., 2010). There are no reports that TRF1 is involved in other aspects of the canonical ALT pathway, such as in ECTR production, but the correlation between APBs and ECTRs suggests that TRF1 is likely important for other ALT roles. Consistent with this, the results presented here identify a role for TRF1 in C-circle production. There appears to be a direct relationship between the level of endogenous TRF1 and the relative amount of C-circles produced, as ALT cells depleted of TRF1 showed a significant decrease in C-circle production, whereas ALT cells overexpressing TRF1 showed a significant increase in C-circle production. The requirement for TRF1 in APB formation combined with this role in C-circle production raises the possibility that TRF1 is also involved in other ALT phenotypes, such as T-SCE and telomere length heterogeneity, which have yet to be investigated.

When TRF1 is not bound to telomeres it is typically degraded through the proteasome pathway (Chang et al., 2003; Lee et al., 2006). However, a fraction of endogenous pan-TRF1 can exist as a soluble pool that is not bound to telomeres. This portion is phosphorylated by Cdk1 at T371 and protects unbound TRF1 from degradation in telomerase-positive cells (McKerlie & Zhu, 2011). This telomere-free pool of TRF1 has been shown to faciliate HR-mediated DSB repair (McKerlie et al., 2013).

Phosphorylated (pT371)TRF1 was also found predominantly in the chromatin-free fraction in ALT cells, so it is likely that unbound (pT371)TRF1 is stabilized in ALT cells, allowing it to engage in other functions away from the telomere. The immunofluorescent staining pattern of (pT371)TRF1 differed from that of pan-TRF1, only staining telomeres in a subset of cells that were primarily in S and G2 phase of the cell cycle. The HR process is limited to S and G2 phases, whereas NHEJ is active throughout the cell cycle, favoured especially in G1 cells (Burma et al., 2006; Liang et al., 1998; Mao et al., 2008). In ALT cells, HR-mediated telomere regulation is thought to occur at APBs, which is also where phosphorylated (pT371)TRF1 is found. These preliminary findings prompted further investigations of the relationship between phosphorylated (pT371)TRF1 and the HR process in ALT cells.

Only 5% of endogenous TRF1 is phosphorylated at T371 (McKerlie & Zhu, 2011), so one might expect to see a reduction in the localization of phosphorylated (pT371)TRF1 to APBs compared to TRF1, but no significant difference was found. However, phosphorylated (pT371)TRF1 is unequally distributed in a cell population and is predominantly found in S and G2 phase cells, which is when cells are enriched with APBs (Wu et al., 2000a). If both phosphorylated (pT371)TRF1 and total TRF1 are able to localize to all of these APBs, then no difference would be observed when only looking at cells that contain APBs. Perhaps there is also an unequal distribution of phosphorylated (pT371)TRF1 within a cell, with an enrichment of soluble (pT371)TRF1 at APBs compared to at telomere foci. A possible explanation for this could be that phosphorylated (pT371)TRF1 is actively recruited to APBs to perform a specific function there.

4.2 Analysis of the relationship between phosphorylated (pT371)TRF1 and DNA damage response factors in ALT cells

As mentioned previously, γH2AX rapidly recognizes damaged DNA and facilitates the recruitment of appropriate repair factors. Based on the observation of co-localization between phosphorylated (pT371)TRF1 and γH2AX at APBs in interphase cells and, more importantly, at telomeres in metaphase cells could suggest that (pT371)TRF1 is also involved in this process, but further studies are needed to fully understand this mechanism. The presence of chromosome ends with weak or absent telomere signals and the enrichment of γH2AX signals at these locations supports previous evidence that ALT cells contain telomeres of heterogeneous length and that deprotected telomeres activate DNA damage response pathways (Bryan et al., 1995; Celli & de Lange, 2005; Kim et al., 2004; Rogan et al., 1995; Takai et al., 2003). Taken together, the results suggest that (pT371)TRF1 localizes to APBs with the HR repair proteins BRCA1 and RPA, which are proteins already known to be at APBs (Wu et al., 2003; Yeager et al., 1999). Whether (pT371)TRF1 plays a role in recruiting HR proteins to APBs is unknown.

Phosphorylated (pT371)TRF1 represents a subset of total TRF1 and has a different cellular distribution, different biochemical properties and a different function. Although the localization of (pT371)TRF1 to APBs was reduced by depletion or inhibition of ATM, Mre11 or BRCA1, the localization of total pan-TRF1 was not significantly affected. This suggests that the localization of (pT371)TRF1 to APBs is dependent on ATM, Mre11 and BRCA1, whereas pan-TRF1 appears to localize to APBs

independently of these factors. Only a small proportion of endogenous TRF1 is phosphorylated at T371, so while a significant reduction was observed with the anti-pT371 antibody at APBs, this difference may be masked when looking at pan-TRF1 with the anti-TRF1 antibody.

No significant change was observed in the percentage of cells with TRF1, TRF2 or Rap1 at APBs in cells depleted or inhibited for ATM, supporting previous reports that ATM does not play a direct role in APB formation (Nabetani et al., 2004; Osterwald et al., 2012). However, the localization of phosphorylated (pT371)TRF1 was significantly reduced following both ATM depletion and inhibition, suggesting that the presence and activity of ATM is required for this form of TRF1 to go to APBs.

A previous report has suggested that Mre11 is required for APB formation. This study used methionine restricted cells depleted for Mre11 and measured APBs by the co-localization of TRF2 and PML (Jiang et al., 2007). In the current experiments presented, Mirin was used to inhibit the nuclease activity of Mre11, simultaneously preventing the autophosphorylation of ATM on S1981. Mre11 nuclease activity is required for the processing of DNA ends during HR (Buis et al., 2008). Cells treated with Mirin did not show any significant change in the localization of TRF1, TRF2 or Rap1 to APBs, suggesting that the nuclease activity of Mre11 may not be required for APB formation. Depleting cells of Mre11 is ultimately different from inhibiting the nuclease activity of Mre11, since depletion uses siRNA to inhibit the formation of Mre11 protein, thus preventing Mre11 from engaging in any other functions or interactions. Mre11 nuclease activity was required for the localization of phosphorylated (pT371)TRF1 to APBs, which

suggests that this form of TRF1 requires the DNA processing activity of Mre11 to go to APBs. Unexpectedly, the percentage of pT371-positive U2OS cells was significantly reduced following a 4h Mirin treatment, but this difference was not observed in GM847 cells that were treated for 1h. The exact cause of this discrepancy is unknown, but the differences in treatment time may contribute to these results. Perhaps inhibiting Mre11 nuclease activity for a longer period of time interfered with the ability of TRF1 to be phosphorylated at T371, whereas a short term inhibition only affected its localization to APBs.

Although BRCA1 localizes to APBs and may be required for DNA synthesis at APBs (Wu et al., 2003), the clustering of telomeres in ALT cells appears to occur independently of BRCA1 (Cho et al., 2014). Cells depleted for BRCA1 showed no significant change in the localization of TRF1 or TRF2 to APBs, but were defective in localizing phosphorylated (pT371)TRF1 to APBs. These results suggest that APBs can form independently of BRCA1, but that the presence or activity of BRCA1 is necessary for (pT371)TRF1 to go to APBs.

Phosphorylated (pT371)TRF1 was also assessed in cells depleted for 53BP1 and in cells treated with a DNA-PK inhibitor to determine whether its localization was affected by NHEJ components. No significant differences were observed in these cells, suggesting that the localization of (pT371)TRF1 to APBs occurs independently of these factors.

Overall, it appears that the localization of phosphorylated (pT371)TRF1 to APBs depends on ATM, Mre11 and BRCA1, suggesting that regulation occurs through the HR

pathway. A similar dependence was previously established for the role of (pT371)TRF1 in HR-mediated DNA damage repair (McKerlie et al., 2013). The exact mechanism through which (pT371)TRF1 requires ATM, Mre11 and BRCA1 to localize to APBs is unknown. Various connections between TRF1, ATM, Mre11 and BRCA1 have been previously identified. It has been demonstrated that TRF1 and ATM interact both *in vivo* and *in vitro*, and that ATM can phosphorylate TRF1 in cells exposed to ionizing radiation and in undamaged cells (Kishi et al., 2001; Wu et al., 2007). TRF1 can interact with BRCA1, dependent upon DNA and the MRN complex (Ballal et al., 2009) and TRF1 has also been shown to interact with Nbs1 in a yeast two-hybrid assay (Wu et al., 2000a). Nbs1 plays an important role in APB formation and is required for the subsequent recruitment of Mre11, Rad50 and BRCA1 to APBs (Wu et al., 2003). In addition, ATM and MRN interact directly (Falck et al., 2005; You et al., 2005) and they are both found at telomeres in S and G2 phase cells (Verdun et al., 2005; Zhu et al., 2000). Therefore, there are numerous possibilities through which ATM, Mre11 and BRCA1 could regulate the localization of (pT371)TRF1 in ALT cells. It is possible that phosphorylated (pT371)TRF1 could rely on an interaction with ATM, the MRN complex or BRCA1 to localize to APBs, but further studies are needed to test this idea.

4.3 Investigation of the roles of the TRF1 phosphorylation site T371 in ALT cell functionality

TRF1 phosphorylation at T371 has previously been shown to be important for sister telomere resolution (McKerlie & Zhu, 2011) and HR-mediated DSB repair

(McKerlie et al., 2013). The findings presented here identify a novel role for phosphorylated (pT371)TRF1 in APB formation, which further demonstrates how a single phosphorylation site can have multiple functions.

Similarly to endogenous phosphorylated (pT371)TRF1, a portion of the Myc-tagged phosphomimic TRF1-T371D mutant was found in the soluble chromatin-free fraction of protein, whereas the nonphosphorylatable TRF1-T371A mutant was predominantly chromatin-bound. Despite these binding differences, both mutant proteins formed punctate pan-nuclear foci and APB foci, but they were both defective in their localization to APBs compared to wild type TRF1. These results suggest that the DNA binding differences between these mutants does not affect their localization to APBs. Although the lack of phosphorylation at T371 impairs the ability of Myc-tagged TRF1 to go to APBs, as shown by the T371A mutant, the phosphomimic mutant was unable to rescue this defect. Likewise, both the T371A and T371D mutants were defective in localization of Rap1, TRF2, TIN2, Nbs1 and RPA32 to APBs. Conversely, expression of the phosphomimic TRF1-T371D mutant in telomerase-positive cells produced results comparable to endogenous (pT371)TRF1 and was able to rescue the HR defects observed with the T371A mutant following DNA damage (McKerlie et al., 2013). There are several possible explanations for this discrepancy.

Unlike endogenously phosphorylated (pT371)TRF1, the aspartic acid substitution in the T371D mutant acts as a permanent phosphorylation. Based on the dynamic nature of phosphorylation events and the importance of dephosphorylation in biological functions, it is possible that only a temporary phosphorylation at T371 is important for

APB formation. Therefore, the inability of T371 to be dephosphorylated may interfere with its function. While aspartic acid may be chemically similar to phosphorylated threonine, it is possible that the protein conformation of TRF1 is altered in the constitutively phosphorylated T371D mutant, which may interfere with its activity, its ability to fold or its ability to interact with DNA and other proteins. If, for example, T371 phosphorylation or dephosphorylation is important for regulating TRF1 sumoylation, then APB formation will also be affected, since TRF1 sumoylation is required for APB formation (Potts & Yu, 2007). If the DNA binding activity and phosphorylation of TRF1 are both important for APB formation, the differences in chromatin-association between the T371A and T371D mutants may contribute to the results.

Collectively, these results suggest that the lack of phosphorylation at T371 of TRF1 impairs the ability of Myc-tagged TRF1, the shelterin proteins Rap1, TRF2 and TIN2, as well as the repair factors Nbs1 and RPA to localize to APBs.

It has been reproducibly shown that C-circle formation in ALT cells is dependent on TRF1 phosphorylation at T371, as cells expressing the nonphosphorylatable T371A mutant showed a significant reduction in C-circle formation compared to both wild type TRF1 and the T371D phosphomimic mutant. These results from the T371A mutant are consistent with the data obtained from APB studies, which further suggests that the inability of cells expressing the T371A mutant to form APBs may contribute to their inability to produce C-circles. However, the T371D mutant appears to be able to rescue the formation of C-circles even though it was unable to rescue APB formation. This suggests that the mechanism through which the T371D mutant operates may be different

for APB and C-circle formation. Since the T371D mutant mimics a constitutive phosphorylation, perhaps the removal of this phosphorylation is not important for C-circle formation, whereas it is important for APB formation. Further studies are needed to investigate if the function of phosphorylated (pT371)TRF1 differs for APB and C-circle formation.

4.4 Analysis of TRF1 domain structure and TRF1 DNA binding ability in APB formation

The phosphorylation site T371 is located within the linker region of TRF1, but other domains of TRF1 also appear crucial for APB formation. Only TRF1 truncation mutants containing the TRFH homodimerization domain were able to fully localize to APBs, suggesting that this domain is required for TRF1 to localize to APBs. However, both the dimerization and Myb-like domains are required for TRF1 to localize to telomeres and bind chromatin. This supports previous data that TRF1 binds DNA as a dimer, which requires both the dimerization and Myb domains (Bianchi et al., 1997). It therefore appears that the localization of TRF1 to APBs can occur independently of DNA.

The presence of Myc-tagged truncated TRF1 at APBs does not guarantee the recruitment of all proteins to APBs; for example, the ΔM truncation mutants showed a comparable level of Myc at APBs compared to wild type TRF1, but they were defective in localizing TRF2, TIN2, Nbs1 and RPA32 to APBs. Although the L-M truncation mutants were defective in their own localization to APBs and in Nbs1 localization, they were the only mutants able to rescue the localization of TRF2, TIN2 and RPA32 to APBs.

These results suggest that full-length TRF1 is required for the functional assembly of APBs, but that the Myb domain of TRF1 may be required to recruit TRF2, TIN2 and RPA32 to APBs. Therefore, the localization of other shelterin proteins to APBs does not seem to depend on TRF1 being at APBs, raising the possibility that shelterin proteins are recruited independently.

There are several explanations as to why cells expressing L-M truncation mutants could recruit TRF2, TIN2 and RPA32 to APBs, but were defective in the recruitment of Myc-tagged L-M. It is possible that the L-M mutants have some intrinsic DNA binding activity or may be loosely associated with chromatin at APBs, since the Myb domain is present. If the Myb domain or DNA binding activity of TRF1 is important for APB formation, this could explain the results observed. Previous work has suggested that TRF1 dimerization is a prerequisite for DNA binding, which requires two Myb motifs (Bianchi et al., 1997), but also that isolated Myb motifs of TRF1 can bind telomeric repeats in a South Western assay (Bilaud et al., 1996), so this model is not unrealistic. TRF1 is able to dimerize when it is not bound to telomeric DNA and these dimers are relatively stable (Bianchi et al., 1997). Since the L-M mutants lack the dimerization domain and are therefore unable to dimerize, unbound L-M monomers may somehow facilitate the localization of TRF2, TIN2 and RPA32 to APBs, perhaps through a signaling role. Since the TRFH domain of TRF1 is required to interact with TIN2 (Kim et al., 1999a), it is unlikely that the L-M mutants facilitate TIN2 recruitment to APBs through a direct interaction. Likewise, TRF1 and TRF2 cannot form heterodimers (Broccoli et al., 1997c; Fairall et al., 2001), so a direct interaction here is also improbable.

The recruitment of RPA32 to APBs may correlate with the presence of TRF2, which has been shown to physically associate with and stimulate the helicase activities of WRN and BLM, facilitating RPA coating of single stranded DNA (Opresko et al., 2002). It would be interesting to test this by investigating whether the L-M mutants are also able to recruit WRN and BLM proteins to APBs compared to the other truncation mutants.

Hypothetically, if the Myb domain of TRF1 is required for T371 phosphorylation to occur and this is required for APB formation as previously proposed, then L-M is the only truncation mutant able to fulfill this role. This may occur, for example, through an interaction between the Myb domain and Cdk1 or perhaps the Myb domain is required to relieve steric hindrance and allow Cdk1 to access and phosphorylate T371. However, the L-M-A truncation mutant is nonphosphorylatable at T371 and yet it produced similar APB results to the L-M mutant. Perhaps the presence of the Myb domain is sufficient to signal the recruitment of other proteins to APBs. It appears that phosphorylation at T371 becomes unimportant once TRF1 is truncated and is unable to bind telomeric DNA, as no significant differences were found between the truncation mutants alone compared to the truncation mutants with T371 mutations. Although the exact mechanism responsible for this is unknown, the chromatin-association of TRF1 may be a contributing factor. A portion of phosphorylated (pT371)TRF1 and a substantial amount of all of the truncation mutants are chromatin-free. If the chromatin binding properties of phosphorylated (pT371)TRF1 are important for its role at APBs, the constitutive inability of the truncation mutants to bind DNA may interfere with this function.

A previous report using GM847 cells expressing GFP-TRF1ΔMyb showed a slight increase in the percentage of cells with Nbs1 APB-like foci, suggesting that the recruitment of Nbs1 to APBs occurs independently of TRF1 (Wu et al., 2003). This experiment used immunofluorescence single staining of Nbs1 as an indicator of APB localization, rather than the ideal co-staining of Nbs1 and PML (Wu et al., 2003). However, the current data presented showed a significant reduction in Nbs1 at APBs in cells depleted for TRF1 and in cells expressing TRF1 truncation mutants, including TRF1-ΔM. It is known that the interaction between TRF1 and Nbs1 requires full length TRF1 and the C-terminus of Nbs1 (Wu et al., 2000a). The results presented here support a model in which full length TRF1 is required for Nbs1 localization to APBs, but whether this occurs through a direct interaction requires investigation. Since only full length TRF1 is chromatin-bound, it is possible that TRF1 must bind directly to telomeric DNA in order for Nbs1 to localize to APBs.

In support of the data obtained from the chromatin-free TRF1 truncation mutants, chromatin-free TRF1-R425V mutants were also unable to form complete APB structures, despite their own ability to localize to APBs. This further suggests that the telomeric DNA binding activity of TRF1 is dispensable for its localization to APBs, but that the localization of TRF2, TIN2 and Nbs1 to APBs requires TRF1 to be chromatin-bound. Therefore it appears that an intact and functional Myb domain of TRF1 is required for the functional assembly of APBs.

Also in line with the TRF1 truncation mutant results, it appears that phosphorylation at T371 becomes unimportant once TRF1 is unable to bind DNA, as the

R425V-T371A and R425V-T371D mutants produced similar results to the R425V mutant alone. This is in contrast to previous work in telomerase-positive cells where IR-induced DNA damage foci were unable to form in cells expressing the R425V-T371A mutant, compared to R425V and R425V-T371D mutants, suggesting that telomere-free TRF1 is still controlled by phosphorylation at T371 (McKerlie et al., 2013). It is likely that phosphorylated (pT371)TRF1 is regulated through a different mechanism in ALT cells compared to telomerase-positive cells. If TRF1 requires temporal changes in chromatin association for its role at APBs, the constitutive inability of the R425V mutants to bind DNA may interfere with this function.

The disruption of APB assembly in cells expressing TRF1 truncation mutants did not seem to influence their proliferation, so the biological significance of these truncations requires additional research. The impact of the truncation mutants on telomeric circle formation or overall telomere length has yet to be investigated.

CHAPTER 5 CONCLUSION

5.1 Overview of Findings and Future Directions

The work presented in this thesis has investigated functional and regulatory mechanisms of TRF1 in ALT cells using a variety of techniques, such as mutational analysis, the use of a phospho-specific antibody, immunofluorescence and C-circle amplification assays. The results have identified novel roles for TRF1 in ALT activity, including APB formation and C-circle production. The findings presented here suggest that the lack of phosphorylation at T371 of TRF1 impairs the functional assembly of APBs and impairs C-circle formation. Phosphorylated (pT371)TRF1 appears to be regulated in a cell cycle dependent manner in ALT cells, localizing predominantly to S and G2 phase cells. Phosphorylated (pT371)TRF1 is associated with γH2AX and HR proteins at APBs in interphase cells, and this localization is dependent on ATM, MRN and BRCA1 activity. Phosphorylated (pT371)TRF1 also co-localized with γH2AX at telomeres in metaphase cells, suggesting that this form of TRF1 may be involved in DNA damage signaling. While phosphorylation at T371 of TRF1 may be necessary for the assembly of APBs, only full length TRF1 is able to localize itself to APBs in addition to the recruitment of other proteins to these nuclear bodies.

Although there may be similarities between the role of phosphorylated (pT371)TRF1 in facilitating the HR-mediated repair of DSBs in telomerase-positive cells and in mediating APB formation in ALT cells, these mechanisms contain distinct features. Prior research has suggested that repair proteins, such as the MRN complex and Rad51, have separate associations with APBs compared to ionizing radiation-induced

foci, based on discrepancies in their localization at these structures (Wu et al., 2003). The phosphorylation site S343 of Nbs1 is important for DNA damage repair following ionizing radiation, but modifications at this site did not affect Nbs1 localization to APBs (Gatei et al., 2000; Lim et al., 2000; Wu et al., 2003, 2000b; Zhao et al., 2000). These results suggest that although HR-mediated telomere lengthening at APBs and HR-mediated repair of DSBs share similar features, these mechanisms operate independently and are not identical.

TRF1 is dynamically regulated at telomeres, moving between telomere-bound and unbound states (Mattern et al., 2004). It appears that both of these chromatin-bound and unbound pools of TRF1 are important for ALT activity. Phosphorylation at T371 of TRF1 creates a soluble fraction of TRF1 that localizes to APBs with HR factors and labels dysfunctional telomeres in metaphase. However, TRF1 must be able to dimerize to localize itself to APBs as well as associate with telomeric DNA through its Myb domain to form fully functional APBs. The use of TRF1 truncation mutants has allowed the different domains of TRF1 to be separated functionally. The homodimerization domain of TRF1 is required for complete localization of TRF1 to APBs, and an intact and functional Myb domain is required for TRF1 to bind DNA, which is necessary for the recruitment of TRF2, TIN2 and RPA32 to APBs. These two functions are independent, but both are essential for APB formation. As an example, the nonphosphorylatable T371A mutant in full length TRF1 was predominantly chromatin-bound but was defective in its own localization to APBs. On the other hand, the R425V mutant was unable to bind DNA but fully localized itself to APBs. However, neither T371A nor R425V were able to fully

recruit other proteins to APBs, demonstrating the importance of these individual functions.

Additionally, it appears that there may be two distinct roles for the Myb domain of TRF1. The first is DNA binding activity and the second is the ability to signal or interact with other proteins. When the DNA binding activity of the Myb domain was abrogated through an R425V point mutation, neither TRF2 nor TIN2 could localize to APBs, even though full length TRF1 was present. The removal of the Myb domain through truncation mutants also produced these results, despite the ability of TRF1 to localize itself to APBs. Even though the L-M truncation mutants appeared to be chromatin-free and were defective in localizing themselves to APBs, the Myb domain in this setting was able to facilitate the recruitment of TRF2, TIN2 and RPA32 to APBs. It is therefore likely that this occurs through an indirect signaling event or perhaps through direct protein-protein interactions. However, further investigations are required to test this model.

It is possible that there is an interaction between phosphorylated (pT371)TRF1 and the Myb domain of TRF1. Since a portion of (pT371)TRF1 is chromatin-free, one potential model is that the reduced affinity between (pT371)TRF1 and DNA may allow TRF1 to engage in other interactions, perhaps via its Myb domain. Phosphorylation at T371 may induce a conformational change in TRF1 allowing the Myb domain to access other substrates, which may help facilitate the recruitment of HR proteins to APBs.

TRF1 interacts with the proteins nucleostemin and guanine nucleotide-binding protein-like 3 at telomeres, and the interplay between these proteins regulates TRF1 function. When TRF1 is unbound from telomeres, it is generally ubiquitinated and

degraded by the proteasome-mediated pathway (Chang et al., 2003). The nucleolar GTP-binding protein nucleostemin (NS) interacts directly with TRF1 in the linker region and upregulates the degradation of TRF1 without affecting its ubiquitination (Meng et al., 2011; Tsai & Meng, 2009; Zhu et al., 2006). The exact amino acid position of the interaction between NS and the linker region of TRF1 is currently unknown. NS inhibits TRF1 homodimerization and consequently decreases the telomeric retention time of TRF1, but NS does not affect the overall amount of TRF1 bound to telomeres (Meng et al., 2011). In addition, NS overexpression can also reduce the level of TIF formation in U2OS cells expressing TRF2$^{\Delta B \Delta M}$, which contain an elevated level of dysfunctional telomeres, but the details of this mechanism are unknown (Meng et al., 2011; van Steensel et al., 1998). NS appears to be important for APB formation, perhaps by promoting the recruitment of telomeres to PML bodies from outside the nucleolus (Hsu et al., 2012). NS has also been shown to increase the sumoylation of TRF1 and promote its association with PML-IV (Hsu et al., 2012), which is required for APB formation (Potts & Yu, 2007). Therefore, it is possible that NS influences TRF1 function at APBs, regulating its ability to recruit HR proteins and facilitate the repair of dysfunctional telomeres (Meng et al., 2011). It would be interesting to investigate the relationship between phosphorylated (pT371)TRF1 and NS to determine whether phosphorylation at T371 could facilitate NS-TRF1 interactions, thereby promoting APB formation and HR-mediated telomere regulation in ALT cells. Co-immunoprecipitation analysis of TRF1-T371A, TRF1-T371D and NS would demonstrate whether phosphorylation at this site is important for TRF1-NS interaction.

A competitor of NS, guanine nucleotide-binding protein-like 3 (GNL3L), interacts with the TRFH domain of TRF1, promotes the dimerization and telomere binding of TRF1 (Zhu et al., 2009) and inhibits APB formation (Hsu et al., 2012). This regulation is therefore disrupted in the L-M truncation mutants since they are missing the TRFH domain, so presumably there will be less competition between NS and GNL3L on TRF1. It is possible that the L-M mutants exist as unbound monomers that are able to stimulate the repair of dysfunctional telomeres in ALT cells by promoting the localization of certain proteins to APBs, thus reducing DNA damage signaling. Similarly, phosphorylated (pT371)TRF1 also contributes to the unbound pool of TRF1 and may act in the same pathway by signaling or promoting the HR-mediated repair of dysfunctional telomeres and reducing DNA damage signaling.

To advance our understanding of the role of phosphorylated (pT371)TRF1 in ALT activity, research efforts should aim to establish the functional significance of this form of TRF1 in ALT cells. Although T371 phosphorylation may be important for APB and C-circle formation, whether the lack of phosphorylation at this site has any impact on cell proliferation, mean telomere length or cell survival following DNA damage requires investigation. A long term growth experiment using ALT cells depleted for endogenous TRF1 complemented with T371A and T371D mutants followed by pulsed-field gel electrophoresis could be used to assess cell proliferation and changes in telomere length over time. A colony survival assay on the same cells following exposure to ionizing radiation would determine whether the lack of phosphorylation at T371 compromises cell survival after DNA damage. Also, although the localization of (pT371)TRF1 to APBs

appears to depend on certain components of DNA repair pathways, the exact function of (pT371)TRF1 at APBs in unknown. Whether DNA synthesis at APBs is reduced in cells expressing the T371A mutant could be investigated by visualizing ssDNA at APBs by BrdU incorporation. A metaphase spread analysis of ALT cells expressing Myc-tagged T371A could be used to assess whether the lack of phosphorylation at this site affects the localization of TRF1 to telomeres, which may shed light on the mechanism through which phosphorylated (pT371)TRF1 may facilitate the functional assembly of APBs. To assess how phosphorylated (pT371)TRF1 is recruited to APBs, co-immunoprecipitations could be performed to examine interactions between (pT371)TRF1 and candidate proteins such as ATM, Mre11 and BRCA1, since these factors appear to be important for the localization of (pT371)TRF1 to APBs.

An assessment of the impact of TRF1 truncation mutants on ALT activity and cell survival following DNA damage should also be investigated. It would be interesting to test whether C-circle levels are affected in the truncation mutants, as well as DNA synthesis at APBs. Although the truncation mutants did not affect cell proliferation, an assessment of mean telomere length could be used as a functional readout for the impact of these mutations.

5.2 Implications and Significance

TRF1 is known to have a variety of important cellular roles which are required for genomic stability. These roles include, but are not limited to, telomere protection, telomerase-dependent telomere length regulation, sister telomere resolution in mitosis and facilitation of HR-mediated DSB repair of non-telomeric DNA. Although the role of

TRF1 in telomerase-positive cells has been studied extensively, how TRF1 functions in ALT cells is still not well understood. ALT tumours typically have poor prognosis due to a lack of treatment options, since our understanding of ALT mechanisms is limited. Therefore, any additional information that could further our knowledge of ALT cell regulation will be valuable in developing therapeutic strategies. The work presented here has identified novel roles for TRF1 in regulating APB formation and C-circle production in ALT cells. This information regarding TRF1 phosphorylation, TRF1 domain structure and HR signaling events in ALT cell functionality could potentially be exploited for the development of anti-cancer therapies.

5.3 References

Abreu, E., Aritonovska, E., Reichenbach, P., Cristofari, G., Culp, B., Terns, R. M., Lingner, J., & Terns, M. P. (2010). TIN2-tethered TPP1 recruits human telomerase to telomeres in vivo. *Molecular and cellular biology*, *30*(12), 2971–2982.

Alani, E., Griffith, J. D., Kolodner, D., Carolina, N., & Hill, C. (1992). Characterization of DNA-binding and Strand-exchange Stimulation Properties of y-RPA , a Yeast Protein DNA-binding Properties, 54–71.

Allsopp, R. C., Vaziri, H., Patterson, C., Goldstein, S., Younglai, E. V, Futcher, A. B., Greider, C. W., & Harley, C. B. (1992). Telomere length predicts replicative capacity of human fibroblasts. *Proceedings of the National Academy of Sciences of the United States of America*, *89*(21), 10114–10118.

Amiard, S., Doudeau, M., Pinte, S., Poulet, A., Lenain, C., Faivre-Moskalenko, C., Angelov, D., Hug, N., Vindigni, A., Bouvet, P., Paoletti, J., Gilson, E., & Giraud-Panis, M.-J. (2007). A topological mechanism for TRF2-enhanced strand invasion. *Nature structural & molecular biology*, *14*(2), 147–54.

Ancelin, K., Brunori, M., Bauwens, S., Koering, C.-E., Brun, C., Ricoul, M., Pommier, J.-P., Sabatier, L., & Gilson, E. (2002). Targeting assay to study the cis functions of human telomeric proteins: evidence for inhibition of telomerase by TRF1 and for activation of telomere degradation by TRF2. *Molecular and cellular biology*, *22*(10), 3474–3487.

Andrews, E. A., Palecek, J., Sergeant, J., Lehmann, A. R., & Watts, F. Z. (2005). Nse2, a Component of the Smc5-6 Complex, Is a SUMO Ligase Required for the Response to DNA Damage. *Molecular and cellular biology*, *25*(1), 185–196.

Bae, N. S., & Baumann, P. (2007). A RAP1/TRF2 complex inhibits nonhomologous end-joining at human telomeric DNA ends. *Molecular cell*, *26*(3), 323–34.

Baird, D. M., & Kipling, D. (2004). The Extent and Significance of Telomere Loss with Age. *Annals New York Academy of Sciences*, *1019*, 265–268.

Ballal, R. D., Saha, T., Fan, S., Haddad, B. R., & Rosen, E. M. (2009). BRCA1 localization to the telomere and its loss from the telomere in response to DNA damage. *The Journal of biological chemistry*, *284*(52), 36083–98.

Bartek, J., & Lukas, J. (2003). Chk1 and Chk2 kinases in checkpoint control and cancer. *Cancer Cell*, *3*, 421–429.

Batenburg, N. L., Mitchell, T. R. H., Leach, D. M., Rainbow, A. J., & Zhu, X.-D. (2012). Cockayne Syndrome group B protein interacts with TRF2 and regulates telomere length and stability. *Nucleic acids research*, *40*(19), 9661–74.

Baumann, P., & Cech, T. R. (2001). Pot1, the Putative Telomere End-Binding Protein in Fission Yeast and Humans. *Science*, *292*, 1171–1175.

Baumann, P., & West, S. C. (1998). Role of the human RAD51 protein in homologous recombination and double-stranded-break repair. *Trends in biochemical sciencess*, *23*(7).

Bechter, O. E., Shay, J. W., & Wright, W. E. (2004). The Frequency of Homologous Recombination in Human ALT Cells. *Cell cycle*, *3*(5), 547–549.

Bechter, O. E., Zou, Y., Shay, J. W., & Wright, W. E. (2003). Homologous recombination in human telomerase-positive and ALT cells occurs with the same frequency. *EMBO reports*, *4*(12), 1138–43.

Benetti, R., Garcı-Cao, M., & Blasco, M. A. (2007a). Telomere length regulates the epigenetic status of mammalian telomeres and subtelomeres. *Nature genetics*, *39*(2), 243–250.

Benetti, R., Gonzalo, S., Jaco, I., Schotta, G., Klatt, P., Jenuwein, T., & Blasco, M. a. (2007b). Suv4-20h deficiency results in telomere elongation and derepression of telomere recombination. *The Journal of cell biology*, *178*(6), 925–36.

Bhanot, M., & Smith, S. (2012). TIN2 stability is regulated by the E3 ligase Siah2. *Molecular and cellular biology*, *32*(2), 376–84.

Bianchi, A., Smith, S., Chong, L., Elias, P., & de Lange, T. (1997). TRF1 is a dimer and bends telomeric DNA. *The EMBO journal*, *16*(7), 1785–94.

Bianchi, A., Stansel, R. M., Fairall, L., Griffith, J. D., Rhodes, D., & de Lange, T. (1999). TRF1 binds a bipartite telomeric site with extreme spatial flexibility. *The EMBO journal*, *18*(20), 5735–44.

Bilaud, T., Koering, C. E., Binet-Brasselet, E., Ancelin, K., Pollice, A., Gasser, S. M., & Gilson, E. (1996). The telobox, a Myb-related telomeric DNA binding motif found in proteins from yeast, plants and human. *Nucleic acids research*, *24*(7), 1294–1303.

Blackburn, E. H., Greider, C. W., Henderson, E., Lee, M. S., Shampay, J., & Shippen-Lentz, D. (1989). Recognition and elongation of telomeres by telomerase. *Genome*, *31*(2), 553–60.

Blasco, M. a, Lee, H. W., Hande, M. P., Samper, E., Lansdorp, P. M., DePinho, R. a, & Greider, C. W. (1997). Telomere shortening and tumor formation by mouse cells lacking telomerase RNA. *Cell*, *91*(1), 25–34.

Bouwman, P., Aly, A., Escandell, J. M., Pieterse, M., Bartkova, J., van der Gulden, H., Hiddingh, S., Thanasoula, M., Kulkarni, A., Yang, Q., Haffty, B. G., Tommiska, J., Blomqvist, C., Drapkin, R., Adams, D. J., Nevanlinna, H., Bartek, J., Tarsounas, M., Ganesan, S., & Jonkers, J. (2010). 53BP1 loss rescues BRCA1 deficiency and is associated with triple-negative and BRCA-mutated breast cancers. *Nature structural & molecular biology*, *17*(6), 688–95.

Broccoli, D., Chong, L., Oelmann, S., Fernald, a a, Marziliano, N., van Steensel, B., Kipling, D., Le Beau, M. M., & de Lange, T. (1997a). Comparison of the human and mouse genes encoding the telomeric protein, TRF1: chromosomal localization, expression and conserved protein domains. *Human molecular genetics*, *6*(1), 69–76.

Broccoli, D., Smogorzewska, A., Chong, L., & de Lange, T. (1997b). Human telomeres contain two distinct Myb-related proteins, TRF1 and TRF2. *Nature Genetics*, *17*, 231–235.

Broccoli, D., Smogorzewska, A., Chong, L., & de Lange, T. (1997c). Human telomeres contain two discint Myb-related proteins, TRF1 and TRF2. *Nature genetics*, *17*, 231–235.

Broccoli, D., Young, J. W., & de Lange, T. (1995). Telomerase activity in normal and malignant hematopoietic cells. *Proceedings of the National Academy of Sciences of the United States of America*, *92*, 9082–9086.

Brouwer, A. K., Schimmel, J., Wiegant, J. C. A. G., Vertegaal, A. C. O., Tanke, H. J., & Dirks, R. W. (2009). Telomeric DNA Mediates De Novo PML Body Formation. *Molecular Biology of the Cell*, *20*, 4804–4815.

Bryan, T. M., Englezou, A., Gupta, J., Bacchetti, S., & Reddel, R. R. (1995). Telomere elongation in immortal human cells without detectable telomerase activity. *The EMBO journal*, *14*(17), 4240–8.

Buis, J., Wu, Y., Deng, Y., Leddon, J., Westfield, G., Eckersdorff, M., Sekiguchi, J. M., Chang, S., & Ferguson, D. O. (2008). Mre11 nuclease activity has essential roles in DNA repair and genomic stability distinct from ATM activation. *Cell*, *135*(1), 85–96.

Bunting, S. F., Callén, E., Wong, N., Chen, H.-T., Polato, F., Gunn, A., Bothmer, A., Feldhahn, N., Fernandez-Capetillo, O., Cao, L., Xu, X., Deng, C.-X., Finkel, T., Nussenzweig, M., Stark, J. M., & Nussenzweig, A. (2010). 53BP1 inhibits homologous recombination in Brca1-deficient cells by blocking resection of DNA breaks. *Cell*, *141*(2), 243–54.

Burma, S., Chen, B. P. C., & Chen, D. J. (2006). Role of non-homologous end joining (NHEJ) in maintaining genomic integrity. *DNA repair*, *5*(9-10), 1042–8.

Burma, S., Chen, B. P., Murphy, M., Kurimasa, a, & Chen, D. J. (2001). ATM phosphorylates histone H2AX in response to DNA double-strand breaks. *The Journal of biological chemistry*, *276*(45), 42462–7.

Cao, L., Xu, X., Bunting, S. F., Liu, J., Wang, R.-H., Cao, L. L., Wu, J. J., Peng, T.-N., Chen, J., Nussenzweig, A., Deng, C.-X., & Finkel, T. (2009). A selective requirement for 53BP1 in the biological response to genomic instability induced by Brca1 deficiency. *Molecular cell*, *35*(4), 534–41.

Carson, C. T., Schwartz, R. A., Stracker, T. H., Lilley, C. E., Lee, D. V, & Weitzman, M. D. (2003). The Mre11 complex is required for ATM activation and the G2/M checkpoint. *The EMBO journal*, *22*(24).

Celli, G. B., & de Lange, T. (2005). DNA processing is not required for ATM-mediated telomere damage response after TRF2 deletion. *Nature cell biology*, *7*(7), 712–8.

Celli, G. B., Denchi, E. L., & de Lange, T. (2006). Ku70 stimulates fusion of dysfunctional telomeres yet protects chromosome ends from homologous recombination. *Nature cell biology*, *8*(8), 885–90.

Cerone, M. a, Autexier, C., Londoño-Vallejo, J. A., & Bacchetti, S. (2005). A human cell line that maintains telomeres in the absence of telomerase and of key markers of ALT. *Oncogene*, *24*(53), 7893–901.

Cesare, A. J., & Griffith, J. D. (2004). Telomeric DNA in ALT Cells Is Characterized by Free Telomeric Circles and Heterogeneous t-Loops. *Molecular and cellular biology*, *24*(22).

Cesare, A. J., Kaul, Z., Cohen, S. B., Napier, C. E., Pickett, H. a, Neumann, A. a, & Reddel, R. R. (2009). Spontaneous occurrence of telomeric DNA damage response in the absence of chromosome fusions. *Nature structural & molecular biology*, *16*(12), 1244–51.

Cesare, A. J., & Reddel, R. R. (2010). Alternative lengthening of telomeres: models, mechanisms and implications. *Nature reviews. Genetics*, *11*(5), 319–30.

Chang, W., Dynek, J. N., & Smith, S. (2003). TRF1 is degraded by ubiquitin-mediated proteolysis after release from telomeres. *Genes & development*, *17*(11), 1328–33.

Chapman, J. R., Taylor, M. R. G., & Boulton, S. J. (2012). Playing the end game: DNA double-strand break repair pathway choice. *Molecular cell*, *47*(4), 497–510.

Chen, L., Nievera, C. J., Lee, A. Y.-L., & Wu, X. (2008a). Cell cycle-dependent complex formation of BRCA1.CtIP.MRN is important for DNA double-strand break repair. *The Journal of biological chemistry*, *283*(12), 7713–20.

Chen, Y. M., Kappel, C., Beaudouin, J., Eils, R., & Spector, D. L. (2008b). Live Cell Dynamics of Promyelocytic Leukemia Nuclear Bodies upon Entry into and Exit from Mitosis. *Molecular Biology of the Cell*, *19*(July), 3147–3162.

Chen, Y., Yang, Y., van Overbeek, M., Donigian, J. R., Baciu, P., de Lange, T., & Lei, M. (2008c). A Shared Docking Motif in TRF1 and TRF2 Used for Differential Recruitment of Telomeric Proteins. *Science*, *319*(February), 1092–1096.

Chen, Y.-C., Teng, S.-C., & Wu, K.-J. (2009). Phosphorylation of telomeric repeat binding factor 1 (TRF1) by Akt causes telomere shortening. *Cancer investigation*, *27*(1), 24–8.

Cheng, J.-F., Smith, C. L., & Cantor, C. R. (1989). Isolation and characterization of a human telomere. *Nucleic acids research*, *17*(15), 6109–6127.

Cho, N. W., Dilley, R. L., Lampson, M. A., & Greenberg, R. A. (2014). Interchromosomal Homology Searches Drive Directional ALT Telomere Movement and Synapsis. *Cell*, *159*(1), 108–121.

Chong, L., Steensel, B. Van, Broccoli, D., Erdjument-bromage, H., Hanish, J., Tempst, P., & Lange, T. De. (1995). A Human Telomeric Protein. *Science*, *270*(5242), 1663–1667.

Chow, T. T., Zhao, Y., Mak, S. S., Shay, J. W., & Wright, W. E. (2012). Early and late steps in telomere overhang processing in normal human cells: the position of the final RNA primer drives telomere shortening. *Genes & development*, *26*(11), 1167–78.

Chung, I., Leonhardt, H., & Rippe, K. (2011). De novo assembly of a PML nuclear subcompartment occurs through multiple pathways and induces telomere elongation. *Journal of cell science*, *124*(Pt 21), 3603–18.

Chung, I., Osterwald, S., Deeg, K., & Rippe, K. (2012). PML body meets telomere - The beginning of an ALTernate ending. *Nucleus*, *3*(3), 263–275.

Cifuentes-Rojas, C., & Shippen, D. E. (2012). Telomerase regulation. *Mutation research*, *730*(1), 20–27.

Conomos, D., Pickett, H. a, & Reddel, R. R. (2013). Alternative lengthening of telomeres: remodeling the telomere architecture. *Frontiers in oncology*, *3*(February), 27.

Conomos, D., Reddel, R. R., & Pickett, H. a. (2014). NuRD-ZNF827 recruitment to telomeres creates a molecular scaffold for homologous recombination. *Nature structural & molecular biology*, (August).

Conomos, D., Stutz, M. D., Hills, M., Neumann, A. a, Bryan, T. M., Reddel, R. R., & Pickett, H. a. (2012). Variant repeats are interspersed throughout the telomeres and recruit nuclear receptors in ALT cells. *The Journal of cell biology*, *199*(6), 893–906.

Constantinou, A., Davies, A. a, & West, S. C. (2001). Branch Migration and Holliday Junction Resolution Catalyzed by Activities from Mammalian Cells. *Cell*, *104*(2), 259–268.

Cook, B. D., Dynek, J. N., Chang, W., Shostak, G., & Smith, S. (2002). Role for the Related Poly (ADP-Ribose) Polymerases Tankyrase 1 and 2 at Human Telomeres. *Molecular and cellular biology*, *22*(1), 332–342.

Cooper, J., Nimmo, E., Allshire, R. C., & Cech, T. R. (1997). Regulation of telomere length and function by a Myb-domain protein in fission yeast. *Letters to Nature*, *385*.

Counter, C. M., Avilion, A. A., Lefeuvrel, C. E., Stewart, N. G., Greider, C. W., Harley, C. B., & Bacchettil, S. (1992). Telomere shortening associated with chromosome instability is arrested in immortal cells which express telomerase activity, *1*(5).

Coverley, D., Kenny, M. K., Lane, D. P., & Wood, R. D. (1992). A role for the human single-stranded DNA bnding protein HSSB / RPA in an early stage of nucleotide excision repair. *Nucleic acids research*, *20*(15), 3873–3880.

Darefsky, A. S., King, J. T., & Dubrow, R. (2012). Adult glioblastoma multiforme survival in the temozolomide era: a population-based analysis of Surveillance, Epidemiology, and End Results registries. *Cancer*, *118*(8), 2163–72.

De Lange, T. (2005). Shelterin: the protein complex that shapes and safeguards human telomeres. *Genes & development*, *19*(18), 2100–10.

De Lange, T., Shiue, L., Myers, R. M., Cox, D. R., Naylor, S. L., Killery, A. M., & Varmus, H. E. (1990). Structure and Variability of Human Chromosome Ends. *Molecular and cellular biology*, *10*(2).

Denchi, E. L., & de Lange, T. (2007). Protection of telomeres through independent control of ATM and ATR by TRF2 and POT1. *Nature*, *448*(7157), 1068–71.

Dimitrova, N., Chen, Y.-C. M., Spector, D. L., & de Lange, T. (2008). 53BP1 promotes non-homologous end joining of telomeres by increasing chromatin mobility. *Nature*, *456*(7221), 524–8.

Doksani, Y., Wu, J. Y., de Lange, T., & Zhuang, X. (2013). Super-resolution fluorescence imaging of telomeres reveals TRF2-dependent T-loop formation. *Cell*, *155*(2), 345–56.

Doucas, V., Tini, M., Egan, D. A., & Evans, R. M. (1999). Modulation of CREB binding protein function by the promyelocytic (ML) oncoprotein suggests a role for nuclear bodies in hormone signaling. *Proceedings of the National Academy of Sciences of the United States of America*, *96*(March), 2627–2632.

Draskovic, I., Arnoult, N., Steiner, V., Bacchetti, S., Lomonte, P., & Londoño-Vallejo, A. (2009). Probing PML body function in ALT cells reveals spatiotemporal requirements for telomere recombination. *Proceedings of the National Academy of Sciences of the United States of America*, *106*(37), 15726–31.

Duckett, D. R., Murchie, A. I. H., Diekmann, S., von Kitzing, E., Kemper, B., & Lilley, D. M. J. (1988). The structure of the holliday junction, and its resolution. *Cell*, *55*(1), 79–89.

Dunham, M. a, Neumann, a a, Fasching, C. L., & Reddel, R. R. (2000). Telomere maintenance by recombination in human cells. *Nature genetics*, *26*(4), 447–50.

Dupré, A., Boyer-Chatenet, L., Sattler, R. M., Modi, A. P., Lee, J.-H., Nicolette, M. L., Kopelovich, L., Jasin, M., Baer, R., Paull, T. T., & Gautier, J. (2008). A forward chemical genetic screen reveals an inhibitor of the Mre11-Rad50-Nbs1 complex. *Nature chemical biology*, *4*(2), 119–25.

Dynan, W. S., & Yoo, S. (1998). Interaction of Ku protein and DNA-dependent protein kinase catalytic subunit with nucleic acids. *Nucleic Acids Research*, *26*(7), 1551–1559.

Dynek, J. N., & Smith, S. (2004). Resolution of sister telomere association is required for progression through mitosis. *Science*, *304*.

Easton, D. F., Bishop, D. T., Ford, D., Crockford, G. P., & Linkage, C. (1993). Genetic Linkage Analysis in Familial Breast and Ovarian Cancer : Results from 214 Families Consortium ', 678–701.

Escribano-Díaz, C., Orthwein, A., Fradet-Turcotte, A., Xing, M., Young, J. T. F., Tkáč, J., Cook, M. a, Rosebrock, A. P., Munro, M., Canny, M. D., Xu, D., & Durocher, D. (2013). A cell cycle-dependent regulatory circuit composed of 53BP1-RIF1 and BRCA1-CtIP controls DNA repair pathway choice. *Molecular cell*, *49*(5), 872–83.

Everett, R. D., Lomonte, P., Sternsdorf, T., van Driel, R., & Orr, A. (1999). Cell cycle regulation of PML modification and ND10 composition. *Journal of cell science*, *112*, 4581–8.

Fairall, L., Chapman, L., Moss, H., de Lange, T., & Rhodes, D. (2001). Structure of the TRFH dimerization domain of the human telomeric proteins TRF1 and TRF2. *Molecular cell*, *8*(2), 351–61.

Falck, J., Coates, J., & Jackson, S. P. (2005). Conserved modes of recruitment of ATM, ATR and DNA-PKcs to sites of DNA damage. *Nature*, *434*(7033), 605–11.

Falzon, M., Fewell, J. W., & Kuff, E. L. (1993). EBP-80 , a Transcription Factor Closely Resembling the Human Autoantigen Ku , Recognizes Single- to Double-Strand. *The Journal of biological chemistry*, *268*(14), 10546–10552.

Fasching, C. L., Neumann, A. a, Muntoni, A., Yeager, T. R., & Reddel, R. R. (2007). DNA damage induces alternative lengthening of telomeres (ALT) associated promyelocytic leukemia bodies that preferentially associate with linear telomeric DNA. *Cancer research*, *67*(15), 7072–7.

Feng, X., Luo, Z., Jiang, S., Li, F., Han, X., Hu, Y., Wang, D., Zhao, Y., Ma, W., Liu, D., Huang, J., & Songyang, Z. (2013). The telomere-associated homeobox-containing protein TAH1/HMBOX1 participates in telomere maintenance in ALT cells. *Journal of cell science*, *126*(Pt 17), 3982–9.

Gatei, M., Young, D., Cerosaletti, K. M., Desai-Mehta, a, Spring, K., Kozlov, S., Lavin, M. F., Gatti, R. a, Concannon, P., & Khanna, K. (2000). ATM-dependent phosphorylation of nibrin in response to radiation exposure. *Nature genetics*, *25*(1), 115–9.

Gong, Y., & de Lange, T. (2010). A Shld1-controlled POT1a provides support for repression of ATR signaling at telomeres through RPA exclusion. *Molecular cell*, *40*(3), 377–87.

Gonzalo, S., Jaco, I., Fraga, M. F., Chen, T., Li, E., Esteller, M., & Blasco, M. a. (2006). DNA methyltransferases control telomere length and telomere recombination in mammalian cells. *Nature cell biology*, *8*(4), 416–24.

Gottlieb, T. M., & Jackson, S. P. (1993). The DNA-Dependent Protein Kinase: Requirement for DNA Ends and Association with Ku Antigen. *Cell*, *72*, 131–142.

Gravel, S., Chapman, J. R., Magill, C., & Jackson, S. P. (2008). DNA helicases Sgs1 and BLM promote DNA double-strand break resection. *Genes & development*, *22*(20), 2767–72.

Grawunder, U., Wilm, M., Wu, X., Kulesza, P., Wilson, T. E., Mann, M., & Lieber, M. R. (1997). Activity of DNA ligase IV stimulated by complex formation with XRCC4 protein in mammalian cells. *Letters to Nature*, *388*(July), 3–6.

Greider, C., & Blackburn, E. H. (1985). Identification of a specific telomere terminal transferase activity in Tetrahymena extracts. *Cell*, *43*(2 Pt 1).

Greider, C. W., & Blackburn, E. H. (1987). The telomere terminal transferase of Tetrahymena is a ribonucleoprotein enzyme with two kinds of primer specificity. *Cell*, *51*(6), 887–98.

Greider, C. W., & Blackburn, E. H. (1989). A telomeric sequence in the RNA of Tetrahymena telomerase required for telomere repeat synthesis. *Nature*, *337*(6205), 405–13.

Griffith, J., Bianchi, a, & de Lange, T. (1998). TRF1 promotes parallel pairing of telomeric tracts in vitro. *Journal of molecular biology*, *278*(1), 79–88.

Griffith, J. D., Comeau, L., Rosenfield, S., Stansel, R. M., Bianchi, a, Moss, H., & de Lange, T. (1999). Mammalian telomeres end in a large duplex loop. *Cell*, *97*(4), 503–14.

Grobelny, J. V, Godwin, a K., & Broccoli, D. (2000). ALT-associated PML bodies are present in viable cells and are enriched in cells in the G(2)/M phase of the cell cycle. *Journal of cell science*, *113 Pt 24*, 4577–85.

Guo, X., Deng, Y., Lin, Y., Cosme-Blanco, W., Chan, S., He, H., Yuan, G., Brown, E. J., & Chang, S. (2007). Dysfunctional telomeres activate an ATM-ATR-dependent DNA damage response to suppress tumorigenesis. *The EMBO journal*, *26*(22), 4709–19.

Hakin-Smith, V., Jellinek, D. A., Levy, D., Carroll, T., Teo, M., Timperley, W. R., McKay, M. J., Reddel, R. R., & Royds, J. A. (2003). Alternative lengthening of telomeres and survival in patients with glioblastoma multiforme. *The Lancet*, *361*, 836–838.

Harley, C. B., Futcher, A. B., & Greider, C. W. (1990). Telomeres shorten during ageing of human fibroblasts. *Letters to Nature*, *345*.

Hastie, N. D., Dempster, M., Dunlop, M. G., Thompson, A. M., Green, D. K., & Allshire, R. C. (1990). Telomere reduction in human colorectal carcinoma and with ageing. *Letters to Nature*, *346*.

Hayflick, L. (1965). The Limited in vitro Lifetime of Human Diploid Cell Strains. *Experimental cell research*, *37*, 614–636.

Heaphy, C. M., Wilde, R. F. De, Jiao, Y., Klein, A. P., Edil, B. H., Shi, C., Bettegowda, C., Rodriguez, F. J., Charles, G., Hebbar, S., Offerhaus, G. J., Mclendon, R., Ahmed, B., He, Y., Yan, H., Bigner, D. D., Oba-shinjo, S. M., Kazue, S., Marie, N., Riggins, G. J., Kinzler, K. W., Vogelstein, B., Ralph, H., Maitra, A., Papadopoulos, N., & Meeker, A. K. (2011). Altered telomeres in tumors with ATRX and DAXX mutations. *Science*, *333*(6041).

Hecker, C.-M., Rabiller, M., Haglund, K., Bayer, P., & Dikic, I. (2006). Specification of SUMO1- and SUMO2-interacting motifs. *The Journal of biological chemistry*, *281*(23), 16117–27.

Hemann, M. T., Strong, M. a, Hao, L. Y., & Greider, C. W. (2001). The shortest telomere, not average telomere length, is critical for cell viability and chromosome stability. *Cell*, *107*(1), 67–77.

Henderson, E. R., & Blackburn, E. H. (1989). An overhanging 3' terminus is a conserved feature of telomeres. *Molecular and cellular biology*, *9*(1), 345–8.

Henson, J. D., Cao, Y., Huschtscha, L. I., Chang, A. C., Au, A. Y. M., Pickett, H. a, & Reddel, R. R. (2009). DNA C-circles are specific and quantifiable markers of alternative-lengthening-of-telomeres activity. *Nature biotechnology*, *27*(12), 1181–5.

Henson, J. D., Hannay, J. A., Mccarthy, S. W., Royds, J. A., Yeager, T. R., Robinson, R. A., Wharton, S. B., Jellinek, D. A., Arbuckle, S. M., Yoo, J., Robinson, B. G., Learoyd, D. L., Stalley, P. D., Bonar, S. F., Yu, D., Pollock, R. E., & Reddel, R. R. (2005). A Robust Assay for Alternative Lengthening of Telomeres in Tumors Shows the Significance of Alternative Lengthening of Telomeres in Sarcomas and Astrocytomas. *Clinical Cancer Research*, *11*, 217–225.

Henson, J. D., Neumann, A. A., Yeager, T. R., & Reddel, R. R. (2002). Alternative lengthening of telomeres in mammalian cells. *Oncogene*, *21*, 598–610.

Henson, J. D., & Reddel, R. R. (2010). Assaying and investigating Alternative Lengthening of Telomeres activity in human cells and cancers. *FEBS letters*, *584*(17), 3800–11.

Her, Y. R., & Chung, I. K. (2009). Ubiquitin Ligase RLIM Modulates Telomere Length Homeostasis through a Proteolysis of TRF1. *The Journal of biological chemistry*, *284*(13), 8557–66.

Heyer, W.-D., Ehmsen, K. T., & Liu, J. (2010). Regulation of homologous recombination in eukaryotes. *Annual review of genetics*, *44*, 113–39.

Hickson, I., Zhao, Y., Richardson, C. J., Green, S. J., Martin, N. M. B., Orr, A. I., Reaper, P. M., Jackson, S. P., Curtin, N. J., & Smith, G. C. M. (2004). Identification and Characterization of a Novel and Specific Inhibitor of the Ataxia-Telangiectasia Mutated Kinase ATM. *Cancer research*, *64*, 9152–9159.

Hockemeyer, D., Palm, W., Else, T., Daniels, J.-P., Takai, K. K., Ye, J. Z.-S., Keegan, C. E., de Lange, T., & Hammer, G. D. (2007). Telomere protection by mammalian Pot1 requires interaction with Tpp1. *Nature structural & molecular biology*, *14*(8), 754–61.

Hockemeyer, D., Sfeir, A. J., Shay, J. W., Wright, W. E., & de Lange, T. (2005). POT1 protects telomeres from a transient DNA damage response and determines how human chromosomes end. *The EMBO journal*, *24*(14), 2667–78.

Houghtaling, B. R., Cuttonaro, L., Chang, W., & Smith, S. (2004). A Dynamic Molecular Link between the Telomere Length Regulator TRF1 and the Chromosome End Protector TRF2. *Current Biology*, *14*, 1621–1631.

Hsu, J. K., Lin, T., & Tsai, R. Y. L. (2012). Nucleostemin prevents telomere damage by promoting PML-IV recruitment to SUMOylated TRF1. *The Journal of cell biology*, *197*(5), 613–24.

Huen, M. S. Y., Grant, R., Manke, I., Minn, K., Yu, X., Yaffe, M. B., & Chen, J. (2007). RNF8 transduces the DNA-damage signal via histone ubiquitylation and checkpoint protein assembly. *Cell*, *131*(5), 901–14.

Iwano, T., Tachibana, M., Reth, M., & Shinkai, Y. (2004). Importance of TRF1 for functional telomere structure. *The Journal of biological chemistry*, *279*(2), 1442–8.

Jazayeri, A., Falck, J., Lukas, C., Bartek, J., Smith, G. C. M., Lukas, J., & Jackson, S. P. (2006). ATM- and cell cycle-dependent regulation of ATR in response to DNA double-strand breaks. *Nature cell biology*, *8*(1), 37–45.

Jiang, W.-Q., Zhong, Z.-H., Henson, J. D., Neumann, A. A., Chang, A. C., & Reddel, R. R. (2005). Suppression of Alternative Lengthening of Telomeres by Sp100-Mediated Sequestration of the MRE11/RAD50/NBS1 Complex. *Molecular and cellular biology*, *25*(7), 2708–2721.

Jiang, W.-Q., Zhong, Z.-H., Henson, J. D., & Reddel, R. R. (2007). Identification of candidate alternative lengthening of telomeres genes by methionine restriction and RNA interference. *Oncogene*, *26*(32), 4635–47.

Karlseder, J. (1999). p53- and ATM-Dependent Apoptosis Induced by Telomeres Lacking TRF2. *Science*, *283*(5406), 1321–1325.

Karlseder, J., Kachatrian, L., Takai, H., Mercer, K., Hingorani, S., Jacks, T., & de Lange, T. (2003). Targeted Deletion Reveals an Essential Function for the Telomere Length Regulator Trf1. *Molecular and cellular biology*, *23*(18), 6533–6541.

Karlseder, J., Smogorzewska, A., & de Lange, T. (2002, March 29). Senescence induced by altered telomere state, not telomere loss. *Science (New York, N.Y.)*.

Kelleher, C., Kurth, I., & Lingner, J. (2005). Human Protection of Telomeres 1 (POT1) Is a Negative Regulator of Telomerase Activity In Vitro. *Molecular and cellular biology*, *25*(2), 808–818.

Kennelly, P. J., & Krebs, E. G. (1991). Consensus Sequences as Substrate Specificity Determinants for Protein Kinases and Protein Phosphatases. *The Journal of biological chemistry*, *266*(24), 15555–15556.

Kim, M. K., Kang, M. R., Nam, H. W., Bae, Y.-S., Kim, Y. S., & Chung, I. K. (2008). Regulation of telomeric repeat binding factor 1 binding to telomeres by casein kinase 2-mediated phosphorylation. *The Journal of biological chemistry*, *283*(20), 14144–52.

Kim, N. W., Piatyszek, M. a, Prowse, K. R., Harley, C. B., West, M. D., Ho, P. L., Coviello, G. M., Wright, W. E., Weinrich, S. L., & Shay, J. W. (1994). Specific association of human telomerase activity with immortal cells and cancer. *Science (New York, N.Y.)*, *266*(5193), 2011–5.

Kim, S., Beausejour, C., Davalos, A. R., Kaminker, P., Heo, S.-J., & Campisi, J. (2004). TIN2 mediates functions of TRF2 at human telomeres. *The Journal of biological chemistry*, *279*(42), 43799–804.

Kim, S. H., Kaminker, P., & Campisi, J. (1999a). TIN2, a new regulator of telomere length in human cells. *Nature genetics*, *23*(4), 405–12.

Kim, S.-T., Lim, D.-S., Canman, C. E., & Kastan, M. B. (1999b). Substrate Specificities and Identification of Putative Substrates of ATM Kinase Family Members. *Journal of Biological Chemistry*, *274*(53), 37538–37543.

Kishi, S., Zhou, X. Z., Ziv, Y., Khoo, C., Hill, D. E., Shiloh, Y., & Lu, K. P. (2001). Telomeric protein Pin2/TRF1 as an important ATM target in response to double strand DNA breaks. *The Journal of biological chemistry*, *276*(31), 29282–91.

Lallemand-Breitenbach, V., & de Thé, H. (2010). PML nuclear bodies. *Cold Spring Harbor perspectives in biology*, *2*(5), a000661.

LaMorte, V. J., Dyck, J. A., Ochs, R. L., & Evans, R. M. (1998). Localization of nascent RNA and CREB binding protein with the PML-containing nuclear body. *Proceedings of the National Academy of Sciences of the United States of America*, *95*(April), 4991–4996.

Lang, M., Jegou, T., Chung, I., Richter, K., Münch, S., Udvarhelyi, A., Cremer, C., Hemmerich, P., Engelhardt, J., Hell, S. W., & Rippe, K. (2010). Three-dimensional organization of promyelocytic leukemia nuclear bodies. *Journal of cell science*, *123*(Pt 3), 392–400.

Laud, P. R., Multani, A. S., Bailey, S. M., Wu, L., Ma, J., Kingsley, C., Lebel, M., Pathak, S., DePinho, R. a, & Chang, S. (2005). Elevated telomere-telomere recombination in WRN-deficient, telomere dysfunctional cells promotes escape from senescence and engagement of the ALT pathway. *Genes & development*, *19*(21), 2560–70.

Lee, H.-W., Blasco, M. A., Gottlieb, G. J., Ii, J. W. H., Greider, C. W., & Depinho, R. A. (1998). Essential role of mouse telomerase in highly proliferative organs. *Nature*, *392*, 569–574.

Lee, J.-H., & Paull, T. T. (2004). Direct activation of the ATM protein kinase by the Mre11-Rad50-Nbs1 complex. *Science*, *304*.

Lee, J.-H., & Paull, T. T. (2005). ATM activation by DNA double-strand breaks through the Mre11-Rad50-Nbs1 complex. *Science*, *308*.

Lee, T. H., Perrem, K., Harper, J. W., Lu, K. P., & Zhou, X. Z. (2006). The F-box protein FBX4 targets PIN2/TRF1 for ubiquitin-mediated degradation and regulates telomere maintenance. *The Journal of biological chemistry*, *281*(2), 759–68.

Lee, T. H., Tun-Kyi, A., Shi, R., Lim, J., Soohoo, C., Finn, G., Balastik, M., Pastorino, L., Wulf, G., Zhou, X. Z., & Lu, K. P. (2009). Essential role of Pin1 in regulation of TRF1 stability and telomere maintenance. *Nature cell biology*, *11*(1), 97–105.

Lei, M., Podell, E. R., & Cech, T. R. (2004). Structure of human POT1 bound to telomeric single-stranded DNA provides a model for chromosome end-protection. *Nature structural & molecular biology*, *11*(12), 1223–9.

Levy, M. Z., Allsopp, R. C., Futcher, A. B., Greider, C. W., & Harley, C. B. (1992). Telomere end-replication problem and cell aging. *Journal of Molecular Biology*, *225*(4), 951–960.

Li, B., Jog, S. P., Reddy, S., & Comai, L. (2008). WRN controls formation of extrachromosomal telomeric circles and is required for TRF2DeltaB-mediated telomere shortening. *Molecular and cellular biology*, *28*(6), 1892–904.

Li, B., & Lange, T. De. (2003). Rap1 Affects the Length and Heterogeneity of Human. *Molecular Biology of the Cell*, *14*(December), 5060–5068.

Li, B., & Lustig, A. J. (1996). A novel mechanism for telomere size control in Saccharomyces cerevisiae. *Genes & Development*, *10*(11), 1310–1326.

Li, B., Oestreich, S., & de Lange, T. (2000). Identification of human Rap1: implications for telomere evolution. *Cell*, *101*(5), 471–83.

Li, X., Stith, C. M., Burgers, P. M., & Heyer, W.-D. (2009). PCNA is required for initiation of recombination-associated DNA synthesis by DNA polymerase delta. *Molecular cell*, *36*(4), 704–13.

Liang, F., Han, M., Romanienko, P. J., & Jasin, M. (1998). Homology-directed repair is a major double-strand break repair pathway in mammalian cells. *Proceedings of the National Academy of Sciences of the United States of America*, *95*, 5172–5177.

Lieber, M. R. (2010). NHEJ and its backup pathways in chromosomal translocations. *Nature structural & molecular biology*, *17*(4), 393–5.

Lim, D.-S., Kim, S.-T., Xu, B., Maser, R. S., Lin, J., Petrini, J. H. J., & Kastan, M. B. (2000). ATM phosphorylates p95/nbs1 in an S-phase checkpoint pathway. *Letters to Nature*, *404*(April), 613–617.

Liu, D., O'Connor, M. S., Qin, J., & Songyang, Z. (2004a). Telosome, a mammalian telomere-associated complex formed by multiple telomeric proteins. *The Journal of biological chemistry*, *279*(49), 51338–42.

Liu, D., Safari, A., O'Connor, M. S., Chan, D. W., Laegeler, A., Qin, J., & Songyang, Z. (2004b). PTOP interacts with POT1 and regulates its localization to telomeres. *Nature cell biology*, *6*(7), 673–80.

Liu, J., Doty, T., Gibson, B., & Heyer, W.-D. (2010). Human BRCA2 protein promotes RAD51 filament formation on RPA-covered single-stranded DNA. *Nature structural & molecular biology*, *17*(10), 1260–2.

Liu, Y., Masson, J.-Y., Shah, R., O'Regan, P., & West, S. C. (2004c). RAD51C is required for Holliday Junction processing in mammalian cells. *Science*, *303*.

Loayza, D., & Lange, T. De. (2003). POT1 as a terminal transducer of TRF1 telomere length control. *Letters to Nature*, *75*, 1013–1018.

Loayza, D., Parsons, H., Donigian, J., Hoke, K., & de Lange, T. (2004). DNA binding features of human POT1: a nonamer 5'-TAGGGTTAG-3' minimal binding site, sequence specificity, and internal binding to multimeric sites. *The Journal of biological chemistry*, *279*(13), 13241–8.

Londoño-Vallejo, J. A., Der-sarkissian, H., Cazes, L., Bacchetti, S., & Reddel, R. R. (2004). Alternative Lengthening of Telomeres Is Characterized by High Rates of Telomeric Exchange. *Cancer research*, *64*, 2324–2327.

Lu, K. P., Hanes, S. D., & Hunter, T. (1996). A human peptidyl-prolyl isomerase essential for regulation of mitosis. *Letters to Nature*, *380*.

Lukas, C., Melander, F., Stucki, M., Falck, J., Bekker-Jensen, S., Goldberg, M., Lerenthal, Y., Jackson, S. P., Bartek, J., & Lukas, J. (2004). Mdc1 couples DNA double-strand break recognition by Nbs1 with its H2AX-dependent chromatin retention. *The EMBO journal*, *23*(13), 2674–83.

Lundblad, V., & Blackburn, E. H. (1993). An alternative pathway for yeast telomere maintenance rescues est1- senescence. *Cell*, *73*(2), 347–60.

Lustig, A. J. (2003). Clues to catastrophic telomere loss in mammals from yeast telomere rapid deletion. *Nature reviews. Genetics*, *4*(11), 916–23.

Ma, Y., Pannicke, U., Schwarz, K., & Lieber, M. R. (2002). Hairpin Opening and Overhang Processing by an Artemis/DNA-Dependent Protein Kinase Complex in Nonhomologous End Joining and V(D)J Recombination. *Cell*, *108*(6), 781–794.

Makarov, V. L., Hirose, Y., & Langmore, J. P. (1997). Long G tails at both ends of human chromosomes suggest a C strand degradation mechanism for telomere shortening. *Cell*, *88*(5), 657–66.

Mao, Z., Bozzella, M., Seluanov, A., & Gorbunova, V. (2008). Comparison of nonhomologous end joining and homologous recombination in human cells. *DNA repair*, *7*(10), 1765–71.

Marcand, S. (1997). A Protein-Counting Mechanism for Telomere Length Regulation in Yeast. *Science*, *275*(5302), 986–990.

Martínez, P., Thanasoula, M., Muñoz, P., Liao, C., Tejera, A., McNees, C., Flores, J. M., Fernández-Capetillo, O., Tarsounas, M., & Blasco, M. (2009). Increased telomere fragility and fusions resulting from TRF1 deficiency lead to degenerative pathologies and increased cancer in mice. *Genes & development*, *23*(17), 2060–75.

Mattern, K. A., Swiggers, S. J. J., Nigg, A. L., Lo, B., Houtsmuller, A. B., & Zijlmans, J. M. J. M. (2004). Dynamics of Protein Binding to Telomeres in Living Cells : Implications for Telomere Structure and Function. *Molecular and cellular biology*, *24*(12), 5587–5594.

Maul, G. G., Guldner, H. H., & Spivack, J. G. (1993). Modification of discrete nuclear domains induced by herpes simplex virus type 1 immediate early gene 1 product (ICP0). *Journal of General Virology*, *74*(12), 2679–2690.

McElligott, R., & Wellinger, R. J. (1997). The terminal DNA structure of mammalian chromosomes. *The EMBO journal*, *16*(12), 3705–14.

McKerlie, M., Lin, S., & Zhu, X.-D. (2012). ATM regulates proteasome-dependent subnuclear localization of TRF1, which is important for telomere maintenance. *Nucleic acids research*, *40*(9), 3975–89.

McKerlie, M., Walker, J. R., Mitchell, T. R. H., Wilson, F. R., & Zhu, X.-D. (2013). Phosphorylated (pT371)TRF1 is recruited to sites of DNA damage to facilitate homologous recombination and checkpoint activation. *Nucleic acids research*, *41*(22), 10268–82.

McKerlie, M., & Zhu, X.-D. (2011). Cyclin B-dependent kinase 1 regulates human TRF1 to modulate the resolution of sister telomeres. *Nature communications*, *2*, 371.

Mekeel, K. L., Tang, W., Kachnic, L. a, Luo, C. M., DeFrank, J. S., & Powell, S. N. (1997). Inactivation of p53 results in high rates of homologous recombination. *Oncogene*, *14*(15), 1847–57.

Meng, L., Hsu, J. K., Zhu, Q., Lin, T., & Tsai, R. Y. L. (2011). Nucleostemin inhibits TRF1 dimerization and shortens its dynamic association with the telomere. *Journal of cell science*, *124*(Pt 21), 3706–14.

Meyne, J., Ratliff, R. L., & Moyzis, R. K. (1989). Conservation of the human telomere sequence (TTAGGG)n among vertebrates. *Proceedings of the National Academy of Sciences of the United States of America*, *86*(18), 7049–53.

Milne, G. T., & Weaver, D. T. (1993). Dominant negative alleles of RAD52 reveal a DNA repair/recombination complex including Rad51 and Rad52. *Genes & Development*, *7*(9), 1755–1765.

Mitchell, T. R. H., Glenfield, K., Jeyanthan, K., & Zhu, X.-D. (2009). Arginine methylation regulates telomere length and stability. *Molecular and cellular biology*, *29*(18), 4918–34.

Modesti, M., Hesse, J. E., & Gellert, M. (1999). DNA binding of Xrcc4 protein is associated with V (D)J recombination but not with stimulation of DNA ligase IV activity. *The EMBO journal*, *18*(7), 2008–2018.

Morin, G. B. (1989). The human telomere terminal transferase enzyme is a ribonucleoprotein that synthesizes TTAGGG repeats. *Cell*, *59*(3), 521–9.

Moshous, D., Callebaut, I., de Chasseval, R., Corneo, B., Cavazzana-Calvo, M., Le Deist, F., Tezcan, I., Sanal, O., Bertrand, Y., Philippe, N., Fischer, A., & de Villartay, J.-P. (2001). Artemis, a Novel DNA Double-Strand Break Repair/V(D)J Recombination Protein, Is Mutated in Human Severe Combined Immune Deficiency. *Cell*, *105*(2), 177–186.

Moynahan, M. E., Chiu, J. W., Koller, B. H., & Jasin, M. (1999). Brca1 Controls Homology-Directed DNA Repair. *Molecular Cell*, *4*, 511–518.

Moynahan, M. E., & Jasin, M. (2010). Mitotic homologous recombination maintains genomic stability and suppresses tumorigenesis. *Nature reviews. Molecular cell biology*, *11*(3), 196–207.

Moyzis, R. K., Buckingham, J. M., Crams, L. S., Dani, M., Larry, L., Jones, M. D., Meyne, J., Ratliff, R. L., Wu, J., & Rich, A. (1988). j ~ iA (J, *85*(September), 6622–6626.

Müller, S., Hoege, C., Pyrowolakis, G., & Jentsch, S. (2001). SUMO, Ubiquitin's mysterious cousin. *Nature Reviews*, *2*, 202–210.

Muntoni, A., & Reddel, R. R. (2005). The first molecular details of ALT in human tumor cells. *Human Molecular Genetics*, *14*.

Nabetani, A., & Ishikawa, F. (2011). Alternative lengthening of telomeres pathway: recombination-mediated telomere maintenance mechanism in human cells. *Journal of biochemistry*, *149*(1), 5–14.

Nabetani, A., Yokoyama, O., & Ishikawa, F. (2004). Localization of hRad9, hHus1, hRad1, and hRad17 and caffeine-sensitive DNA replication at the alternative

lengthening of telomeres-associated promyelocytic leukemia body. *The Journal of biological chemistry*, *279*(24), 25849–57.

Naka, K., Ikeda, K., & Motoyama, N. (2002). Recruitment of NBS1 into PML oncogenic domains via interaction with SP100 protein. *Biochemical and Biophysical Research Communications*, *299*(5), 863–871.

Nakamura, K., Sakai, W., Kawamoto, T., Bree, R. T., Lowndes, N. F., Takeda, S., & Taniguchi, Y. (2006). Genetic dissection of vertebrate 53BP1: a major role in non-homologous end joining of DNA double strand breaks. *DNA repair*, *5*(6), 741–9.

Nakamura, M., Zhou, X. Z., Kishi, S., & Ã, K. P. L. (2002). Involvement of the telomeric protein Pin2 / TRF1 in the regulation of the mitotic spindle, *514*, 193–198.

Natarajan, S., & McEachern, M. J. (2002). Recombinational Telomere Elongation Promoted by DNA Circles. *Molecular and cellular biology*, *22*(13).

New, J. H., Sugiyama, T., Zaitseva, E., & Kowalczykowski, S. C. (1998). Rad52 protein stimulates DNA strand exchange by Rad51 and replication protein A. *Nature*, *391*(January), 407–410.

Nimonkar, A. V, Genschel, J., Kinoshita, E., Polaczek, P., Campbell, J. L., Wyman, C., Modrich, P., & Kowalczykowski, S. C. (2011). BLM-DNA2-RPA-MRN and EXO1-BLM-RPA-MRN constitute two DNA end resection machineries for human DNA break repair. *Genes & development*, *25*(4), 350–62.

O'Connor, M. S., Safari, A., Xin, H., Liu, D., & Songyang, Z. (2006). A critical role for TPP1 and TIN2 interaction in high-order telomeric complex assembly. *Proceedings of the National Academy of Sciences of the United States of America*, *103*(32), 11874–9.

O'Sullivan, R. J., Arnoult, N., Lackner, D. H., Oganesian, L., Haggblom, C., Corpet, A., Almouzni, G., & Karlseder, J. (2014). Rapid induction of alternative lengthening of telomeres by depletion of the histone chaperone ASF1. *Nature structural & molecular biology*, *21*(2), 167–74.

Ohishi, T., Hirota, T., Tsuruo, T., & Seimiya, H. (2010). TRF1 mediates mitotic abnormalities induced by Aurora-A overexpression. *Cancer research*, *70*(5), 2041–52.

Okazaki, R., Okazaki, T., Sakabe, K., Kazunori, S., & Sugino, A. (1968). Mechanism of DNA chain growth, I. Possible discontinuity and unusual secondary structure of newly synthesized chains. *Biochemistry*, *59*, 598–605.

Olovnikov, A. M. (1971). Principle of marginotomy in template synthesis of polynucleotides. *Doklady Akademii nauk SSSR*, *201*(6), 1496–9.

Olovnikov, A. M. (1973). A Theory of Marginotomy The Incomplete Copying of Template Margin in Enzymic Synthesis of Polym & otides and Biological Significance of the Phenomenon. *Journal of Theoretical Biology*, *41*, 181–190.

Opresko, P. L., Mason, P. a, Podell, E. R., Lei, M., Hickson, I. D., Cech, T. R., & Bohr, V. a. (2005). POT1 stimulates RecQ helicases WRN and BLM to unwind telomeric DNA substrates. *The Journal of biological chemistry*, *280*(37), 32069–80.

Opresko, P. L., von Kobbe, C., Laine, J.-P., Harrigan, J., Hickson, I. D., & Bohr, V. a. (2002). Telomere-binding protein TRF2 binds to and stimulates the Werner and Bloom syndrome helicases. *The Journal of biological chemistry*, *277*(43), 41110–9.

Osterwald, S., Wörz, S., Reymann, J., Sieckmann, F., Rohr, K., Erfle, H., & Rippe, K. (2012). A three-dimensional colocalization RNA interference screening platform to elucidate the alternative lengthening of telomeres pathway. *Biotechnology journal*, *7*(1), 103–16.

Pagano, M., Pepperkok, R., Verde, F., Ansorge, W., & Draetta, G. (1992). Cyclin A is required at two points in the human cell cycle. *The EMBO journal*, *1*(3), 961–971.

Palm, W., & de Lange, T. (2008). How shelterin protects mammalian telomeres. *Annual review of genetics*, *42*, 301–34.

Paull, T. T. (2010). Making the best of the loose ends: Mre11/Rad50 complexes and Sae2 promote DNA double-strand break resection. *DNA repair*, *9*(12), 1283–91.

Paull, T. T., Rogakou, E. P., Yamazaki, V., Kirchgessner, C. U., Gellert, M., & Bonner, W. M. (2000). A critical role for histone H2AX in recruitment of repair factors to nuclear foci after DNA damage. *Current Biology*, *10*(15), 886–895.

Perrem, K., Bryan, T. M., Englezou, A., Hackl, T., Moy, E. L., & Reddel, R. R. (1999). Repression of an alternative mechanism for lengthening of telomeres in somatic cell hybrids. *Oncogene*, *18*, 3383–3390.

Perrem, K., Colgin, L. M., Neumann, A. A., Yeager, R., & Reddel, R. R. (2001). Coexistence of Alternative Lengthening of Telomeres and Telomerase in Coexistence of Alternative Lengthening of Telomeres and Telomerase in hTERT-Transfected GM847 Cells. *Molecular and cellular biology*, *21*(12), 3862–3875.

Petrini, J. H. J. (1999). The Mammalian Mre11-Rad50-Nbs1 Protein Complex : Integration of Functions in the Cellular DNA – Damage Response. *The American Journal of Human Genetics*, *64*, 1264–1269.

Petukhova, G., Van Komen, S., Vergano, S., Klein, H., & Sung, P. (1999). Yeast Rad54 Promotes Rad51-dependent Homologous DNA Pairing via ATP Hydrolysis-driven Change in DNA Double Helix Conformation. *Journal of Biological Chemistry*, *274*(41), 29453–29462.

Pickett, H. a, Cesare, A. J., Johnston, R. L., Neumann, A. a, & Reddel, R. R. (2009). Control of telomere length by a trimming mechanism that involves generation of t-circles. *The EMBO journal*, *28*(7), 799–809.

Potts, P. R., & Yu, H. (2005). Human MMS21/NSE2 Is a SUMO Ligase Required for DNA Repair. *Molecular and cellular biology*, *25*(16).

Potts, P. R., & Yu, H. (2007). The SMC5/6 complex maintains telomere length in ALT cancer cells through SUMOylation of telomere-binding proteins. *Nature structural & molecular biology*, *14*(7), 581–90.

R Core Team (2014). R: A language and environment for statistical computing. R Foundation for Statistical Computing, Vienna, Austria. URL http://www.R-project.org/

Radding, C. M. (1978). Genetic Recombination: Strand transfer and mismatch repair. *Annual review of biochemistry*, *47*(1).

Rogakou, E. P., Pilch, D. R., Orr, a. H., Ivanova, V. S., & Bonner, W. M. (1998). DNA Double-stranded Breaks Induce Histone H2AX Phosphorylation on Serine 139. *Journal of Biological Chemistry*, *273*(10), 5858–5868.

Rogan, E. M., Bryan, T. M., Hukku, B., Maclean, K., Chang, A. C., Moy, E. L., Englezou, A., Warneford, S. G., Dalla-Pozza, L., & Reddel, R. R. (1995). Alterations in p53 and p16INK4 expression and telomere length during spontaneous immortalization of Li-Fraumeni syndrome fibroblasts. *Molecular and cellular biology*, *15*(9).

Rouet, P., Smih, F., & Jasin, M. (1994). Introduction of Double-Strand Breaks into the Genome of Mouse Cells by Expression of a Rare-Cutting Endonuclease. *Molecular and cellular biology*, *14*(12).

San Filippo, J., Sung, P., & Klein, H. (2008). Mechanism of eukaryotic homologous recombination. *Annual review of biochemistry*, *77*, 229–57.

Sarthy, J., Bae, N. S., Scrafford, J., & Baumann, P. (2009). Human RAP1 inhibits non-homologous end joining at telomeres. *The EMBO journal*, *28*(21), 3390–9.

Sartori, A. a, Lukas, C., Coates, J., Mistrik, M., Fu, S., Bartek, J., Baer, R., Lukas, J., & Jackson, S. P. (2007). Human CtIP promotes DNA end resection. *Nature*, *450*(7169), 509–14.

Schultz, L. B., Chehab, N. H., Malikzay, A., & Halazonetis, T. D. (2000). p53 Binding Protein 1 (53BP1) Is an Early Participant in the Cellular Response to DNA Double-Strand Breaks. *The Journal of cell biology*, *151*(7), 1381–1390.

Schwartzentruber, J., Korshunov, A., Liu, X.-Y., Jones, D. T. W., Pfaff, E., Jacob, K., Sturm, D., Fontebasso, A. M., Quang, D.-A. K., Tönjes, M., Hovestadt, V., Albrecht, S., Kool, M., Nantel, A., Konermann, C., Lindroth, A., Jäger, N., Rausch, T., Ryzhova, M., Korbel, J. O., Hielscher, T., Hauser, P., Garami, M., Klekner, A., Bognar, L., Ebinger, M., Schuhmann, M. U., Scheurlen, W., Pekrun, A., Frühwald, M. C., Roggendorf, W., Kramm, C., Dürken, M., Atkinson, J., Lepage, P., Montpetit, A., Zakrzewska, M., Zakrzewski, K., Liberski, P. P., Dong, Z., Siegel, P., Kulozik, A. E., Zapatka, M., Guha, A., Malkin, D., Felsberg, J., Reifenberger, G., von Deimling, A., Ichimura, K., Collins, V. P., Witt, H., Milde, T., Witt, O., Zhang, C., Castelo-Branco, P., Lichter, P., Faury, D., Tabori, U., Plass, C., Majewski, J., Pfister, S. M., & Jabado, N. (2012). Driver mutations in histone H3.3 and chromatin remodelling genes in paediatric glioblastoma. *Nature*, *482*(7384), 226–31.

Scully, R., Chen, J., Plug, A., Xiao, Y., Weaver, D., Feunteun, J., Ashley, T., & Livingston, D. M. (1997). Association of BRCA1 with Rad51 in Mitotic and Meiotic Cells. *Cell*, *88*(2), 265–275.

Sfeir, A., & de Lange, T. (2012). Removal of shelterin reveals the telomere end-protection problem. *Science (New York, N.Y.)*, *336*(6081), 593–7.

Sfeir, A., Kabir, S., van Overbeek, M., Celli, G. B., & de Lange, T. (2010). Loss of Rap1 induces telomere recombination in absence of NHEJ or a DNA damage signal. *National Institutes of Health*, *327*(5973), 1657–1661.

Sfeir, A., Kosiyatrakul, S. T., Hockemeyer, D., MacRae, S. L., Karlseder, J., Schildkraut, C. L., & de Lange, T. (2009). Mammalian telomeres resemble fragile sites and require TRF1 for efficient replication. *Cell*, *138*(1), 90–103.

Shay, J. W., & Bacchetti, S. (1997). A survey of telomerase activity in human cancer. *European Journal of Cancer*, *33*(5), 787–791.

Shen, M., Haggblom, C., Vogt, M., Hunter, T., & Lu, K. P. (1997). Characterization and cell cycle regulation of the related human telomeric proteins Pin2 and TRF1 suggest

a role in mitosis. *Proceedings of the National Academy of Sciences of the United States of America*, *94*(25), 13618–23.

Shen, M., Stukenberg, P. T., Kirschner, M. W., & Lu, K. P. (1998). The essential mitotic peptidyl-prolyl isomerase Pin1 binds and regulates mitosis-specific phosphoproteins. *Genes & Development*, *12*(5), 706–720.

Shen, Z., Cloud, K. G., Chen, D. J., & Park, M. S. (1996). Specific Interactions between the Human RAD51 and RAD52 Proteins. *Journal of Biological Chemistry*, *271*(1), 148–152.

Shiloh, Y. (2003). ATM and related protein kinases: safeguarding genome integrity. *Nature reviews. Cancer*, *3*(3), 155–68.

Sijbers, A. M., de Laat, W. L., Ariza, R. R., Biggerstaff, M., Wei, Y.-F., Moggs, J. G., Carter, K. C., Shell, B. K., Evans, E., de Jong, M. C., Rademakers, S., de Rooij, J., Jaspers, N. G. ., Hoeijmakers, J. H. ., & Wood, R. D. (1996). Xeroderma Pigmentosum Group F Caused by a Defect in a Structure-Specific DNA Repair Endonuclease. *Cell*, *86*(5), 811–822.

Smith, S. (1998). Tankyrase, a Poly(ADP-Ribose) Polymerase at Human Telomeres. *Science*, *282*(5393), 1484–1487.

Smith, S., & de Lange, T. (2000). Tankyrase promotes telomere elongation in human cells. *Current biology : CB*, *10*(20), 1299–302.

Smogorzewska, A., & de Lange, T. (2004). Regulation of telomerase by telomeric proteins. *Annual review of biochemistry*, *73*, 177–208.

Smogorzewska, A., Steensel, B. Van, Bianchi, A., Oelmann, S., Schaefer, M. R., Schnapp, G., & de Lange, T. (2000). Control of Human Telomere Length by TRF1 and TRF2. *Molecular and cellular biology*, *20*(5), 1659–1668.

Solinger, J. A., Kiianitsa, K., & Heyer, W. (2002). Rad54 , a Swi2/Snf2-like Recombinational Repair Protein , Disassembles Rad51:dsDNA Filaments. *Molecular cell*, *10*, 1175–1188.

Stampfer, M. R., Garbe, J., Nijjar, T., Wigington, D., Swisshelm, K., & Yaswen, P. (2003). Loss of p53 function accelerates acquisition of telomerase activity in indefinite lifespan human mammary epithelial cell lines. *Oncogene*, *22*(34), 5238–51.

Stansel, R. M., de Lange, T., & Griffith, J. D. (2001). T-loop assembly in vitro involves binding of TRF2 near the 3' telomeric overhang. *The EMBO journal*, *20*(19), 5532–40.

Sternsdorf, T., Jensen, K., & Will, H. (1997). Evidence for Covalent Modification of the Nuclear Dot–associated Proteins PML and Sp100 by PIC1/SUMO-1. *The Journal of cell biology*, *139*(7), 1621–1634.

Stucki, M., Clapperton, J. a, Mohammad, D., Yaffe, M. B., Smerdon, S. J., & Jackson, S. P. (2005). MDC1 directly binds phosphorylated histone H2AX to regulate cellular responses to DNA double-strand breaks. *Cell*, *123*(7), 1213–26.

Takai, H., Smogorzewska, A., & de Lange, T. (2003). DNA Damage Foci at Dysfunctional Telomeres. *Current Biology*, *13*(17), 1549 – 1556.

Takai, K. K., Hooper, S., Blackwood, S., Gandhi, R., & de Lange, T. (2010). In vivo stoichiometry of shelterin components. *The Journal of biological chemistry*, *285*(2), 1457–67.

Takai, K. K., Kibe, T., Donigian, J. R., Frescas, D., & de Lange, T. (2011). Telomere protection by TPP1/POT1 requires tethering to TIN2. *Molecular cell*, *44*(4), 647–59.

Tan, T. L. R., Essers, J., Citterio, E., Swagemakers, S. M. a., de Wit, J., Benson, F. E., Hoeijmakers, J. H. J., & Kanaar, R. (1999). Mouse Rad54 affects DNA conformation and DNA-damage-induced Rad51 foci formation. *Current Biology*, *9*(6), 325–328.

Tarsounas, M., Davies, A. a, & West, S. C. (2004). RAD51 localization and activation following DNA damage. *Philosophical transactions of the Royal Society of London. Series B, Biological sciences*, *359*(1441), 87–93.

Tirkkonen, M., Johannsson, O., Agnarsson, B. A., Ingvarsson, S., Karhu, R., Tanner, M., Isola, J., Barkardottir, R. B., Borg, A., & Kallioniemi, O.-P. (1997). Distinct Somatic Genetic Changes Associated with Tumor Progression in Carriers of BRCA1 and BRCA2 Germ-line Mutations. *Cancer research*, *57*, 1222–1227.

Tomlinson, G. E., Chen, T. T., Stastny, V. A., Virmani, A. K., Spillman, M. A., Tonk, V., Blum, J. L., Schneider, N. R., Wistuba, I. I., Shay, J. W., Minna, J. D., & Gazdar, A. F. (1998). Characterization of a Breast Cancer Cell Line Derived from a Germ-Line BRCA1 Mutation Carrier. *Cancer research*, *58*, 3237–3242.

Tsai, R. Y. L., & Meng, L. (2009). Nucleostemin: a latecomer with new tricks. *The international journal of biochemistry & cell biology*, *41*(11), 2122–4.

Uziel, T., Lerenthal, Y., Moyal, L., Andegeko, Y., Mittelman, L., & Shiloh, Y. (2003). Requirement of the MRN complex for ATM activation by DNA damage, *22*(20).

Vallian, S., Ga, J. A., Trayner, I. D., Gingold, E. B., Kouzarides, T., Chang, K., & Farzaneh, F. (1997). Transcriptional Repression by the Promyelocytic Leukemia Protein, PML. *Experimental cell research*, *382*(237), 371–382.

Van Steensel, B., & de Lange, T. (1997). Control of telomere length by the human telomeric protein TRF1. *Nature*, *385*, 740–743.

Van Steensel, B., Smogorzewska, a, & de Lange, T. (1998). TRF2 protects human telomeres from end-to-end fusions. *Cell*, *92*(3), 401–13.

Vaziri, H., West, M. D., Allsopp, R. C., Davison, T. S., Wu, Y. S., Arrowsmith, C. H., Poirier, G. G., & Benchimol, S. (1997). ATM-dependent telomere loss in aging human diploid fibroblasts and DNA damage lead to the post-translational activation of p53 protein involving poly(ADP-ribose) polymerase. *The EMBO journal*, *16*(19), 6018–33.

Verdun, R. E., Crabbe, L., Haggblom, C., & Karlseder, J. (2005). Functional human telomeres are recognized as DNA damage in G2 of the cell cycle. *Molecular cell*, *20*(4), 551–61.

Veuger, S. J., Curtin, N. J., Smith, G. C. M., & Durkacz, B. W. (2004). Effects of novel inhibitors of poly(ADP-ribose) polymerase-1 and the DNA-dependent protein kinase on enzyme activities and DNA repair. *Oncogene*, *23*(44), 7322–9.

Walker, J. R., Corpina, R. A., & Goldberg, J. (2001). Structure of the Ku heterodimer bound to DNA and its implications for double-strand break repair. *Nature*, *412*, 607–614.

Walker, J. R., & Zhu, X.-D. (2012). Post-translational modifications of TRF1 and TRF2 and their roles in telomere maintenance. *Mechanisms of ageing and development*, *133*(6), 421–34.

Wang, C., Xiao, H., Ma, J., Zhu, Y., Yu, J., Sun, L., Sun, H., Liu, Y., Jin, C., & Huang, H. (2013). The F-box protein β-TrCP promotes ubiquitination of TRF1 and regulates the ALT-associated PML bodies formation in U2OS cells. *Biochemical and biophysical research communications*, *434*(4), 728–34.

Wang, F., Podell, E. R., Zaug, A. J., Yang, Y., Baciu, P., Cech, T. R., & Lei, M. (2007). The POT1-TPP1 telomere complex is a telomerase processivity factor. *Nature*, *445*(7127), 506–10.

Wang, R. C., Smogorzewska, A., & de Lange, T. (2004). Homologous recombination generates T-loop-sized deletions at human telomeres. *Cell*, *119*(3), 355–68.

Wang, Y., Erdmann, N., Giannone, R. J., Wu, J., Gomez, M., & Liu, Y. (2005). An increase in telomere sister chromatid exchange in murine embryonic stem cells possessing critically shortened telomeres. *Proceedings of the National Academy of Sciences of the United States of America*, *102*(29), 10256–60.

Wright, W. E., Tesmer, V. M., Huffman, K. E., Levene, S. D., & Shay, J. W. (1997). Normal human chromosomes have long G-rich telomeric overhangs at one end. *Genes & Development*, *11*(21), 2801–2809.

Wu, G., Jiang, X., Lee, W.-H., & Chen, P.-L. (2003). Assembly of Functional ALT-associated Promyelocytic Leukemia Bodies Requires Nijmegen Breakage Syndrome 1. *Cancer research*, *63*, 2589–2595.

Wu, G., Lee, W. H., & Chen, P. L. (2000a). NBS1 and TRF1 colocalize at promyelocytic leukemia bodies during late S/G2 phases in immortalized telomerase-negative cells. Implication of NBS1 in alternative lengthening of telomeres. *The Journal of biological chemistry*, *275*(39), 30618–22.

Wu, L., Multani, A. S., He, H., Cosme-Blanco, W., Deng, Y., Deng, J. M., Bachilo, O., Pathak, S., Tahara, H., Bailey, S. M., Deng, Y., Behringer, R. R., & Chang, S. (2006). Pot1 deficiency initiates DNA damage checkpoint activation and aberrant homologous recombination at telomeres. *Cell*, *126*(1), 49–62.

Wu, X., Ranganathan, V., Weisman, D. S., Heine, W. F., Ciccone, D. N., Neill, T. B. O., Crick, K. E., Pierce, K. A., Lane, W. S., Rathbun, G., Livingston, D. M., & Weaver, D. T. (2000b). ATM phosphorylation of Nijmegen breakage syndrome protein is required in a DNA damage response. *Letters to Nature*, *405*, 477–482.

Wu, Y., Xiao, S., & Zhu, X.-D. (2007). MRE11-RAD50-NBS1 and ATM function as co-mediators of TRF1 in telomere length control. *Nature structural & molecular biology*, *14*(9), 832–40.

Wu, Z.-Q., Yang, X., Weber, G., & Liu, X. (2008). Plk1 phosphorylation of TRF1 is essential for its binding to telomeres. *The Journal of biological chemistry*, *283*(37), 25503–13.

Xie, K., Lambie, E. J., & Snyder, M. (1993). Nuclear Dot Antigens May Specify Transcriptional Domains in the Nucleus. *Molecular and cellular biology*, *13*(10).

Xin, H., Liu, D., Wan, M., Safari, A., Kim, H., Sun, W., O'Connor, M. S., & Songyang, Z. (2007). TPP1 is a homologue of ciliate TEBP-beta and interacts with POT1 to recruit telomerase. *Nature*, *445*(7127), 559–62.

Xu, X., Qiao, W., Linke, S. P., Cao, L., Li, W., Furth, P. A., Harris, C. C., & Deng, C. (2001). Genetic interactions between tumor suppressors Brca1 and p53 in apoptosis , cell cycle and tumorigenesis. *Nature Genetics*, *28*.

Ye, J. Z.-S., & de Lange, T. (2004). TIN2 is a tankyrase 1 PARP modulator in the TRF1 telomere length control complex. *Nature genetics*, *36*(6), 618–23.

Ye, J. Z.-S., Donigian, J. R., van Overbeek, M., Loayza, D., Luo, Y., Krutchinsky, A. N., Chait, B. T., & de Lange, T. (2004a). TIN2 binds TRF1 and TRF2 simultaneously and stabilizes the TRF2 complex on telomeres. *The Journal of biological chemistry*, *279*(45), 47264–71.

Ye, J. Z.-S., Hockemeyer, D., Krutchinsky, A. N., Loayza, D., Hooper, S., Chait, B. T., & de Lange, T. (2004b). POT1-interacting protein PIP1: a telomere length regulator that recruits POT1 to the TIN2/TRF1 complex. *Genes & development*, *18*(14), 1649–54.

Yeager, T. R., Neumann, A. A., Englezou, A., Huschtscha, L. I., Noble, J. R., & Reddel, R. R. (1999). Telomerase-negative Immortalized Human Cells Contain a Novel Type of Promyelocytic Leukemia (PML) Body. *Cancer research*, *59*, 4175–4179.

You, Z., Chahwan, C., Bailis, J., Russell, P., & Hunter, T. (2005). ATM Activation and Its Recruitment to Damaged DNA Require Binding to the C Terminus of Nbs1. *Molecular and cellular biology*, *25*(13), 5363–5379.

Yu, J., Lan, J., Wang, C., Wu, Q., Zhu, Y., Lai, X., Sun, J., Jin, C., & Huang, H. (2010). PML3 interacts with TRF1 and is essential for ALT-associated PML bodies assembly in U2OS cells. *Cancer letters*, *291*(2), 177–86.

Yu, X., & Chen, J. (2004). DNA Damage-Induced Cell Cycle Checkpoint Control Requires CtIP , a Phosphorylation-Dependent Binding Partner of BRCA1 C-Terminal Domains. *Molecular and cellular biology*, *24*(21).

Yu, X., Fu, S., Lai, M., Baer, R., & Chen, J. (2006). BRCA1 ubiquitinates its phosphorylation-dependent binding partner CtIP. *Genes & development*, *20*(13), 1721–6.

Zaug, A. J., Podell, E. R., & Cech, T. R. (2005). Human POT1 disrupts telomeric G-quadruplexes allowing telomerase extension in vitro. *Proceedings of the National Academy of Sciences of the United States of America*, *102*(31), 10864–9.

Zhao, S., Weng, Y.-C., Yuan, S.-S. F., Lin, Y.-T., Zdzienicka, Â. Z., Gatti, R. A., Shay, J. W., Ziv, Y., Shiloh, Y., & Lee, E. Y. P. (2000). Functional link between ataxia-telangiectasia and Nijmegen breakage syndrome gene products. *Letters to Nature*, *405*(May), 473–477.

Zhao, X., & Blobel, G. (2005). A SUMO ligase is part of a nuclear multiprotein complex that affects DNA repair and chromosomal organization. *Proceedings of the National Academy of Sciences of the United States of America*, *102*(25).

Zhong, F. L., Batista, L. F. Z., Freund, A., Pech, M. F., Venteicher, A. S., & Artandi, S. E. (2012). TPP1 OB-fold domain controls telomere maintenance by recruiting telomerase to chromosome ends. *Cell*, *150*(3), 481–94.

Zhong, Z.-H., Jiang, W.-Q., Cesare, A. J., Neumann, A. a, Wadhwa, R., & Reddel, R. R. (2007). Disruption of telomere maintenance by depletion of the MRE11/RAD50/NBS1 complex in cells that use alternative lengthening of telomeres. *The Journal of biological chemistry*, *282*(40), 29314–22.

Zhou, B. S., & Elledge, S. J. (2000). The DNA damage response - Putting checkpoints in perspective. *Nature review*, *408*(November), 433–439.

Zhu, Q., Meng, L., Hsu, J. K., Lin, T., Teishima, J., & Tsai, R. Y. L. (2009). GNL3L stabilizes the TRF1 complex and promotes mitotic transition. *The Journal of cell biology*, *185*(5), 827–39.

Zhu, Q., Yasumoto, H., & Tsai, R. Y. L. (2006). Nucleostemin delays cellular senescence and negatively regulates TRF1 protein stability. *Molecular and cellular biology*, *26*(24), 9279–90.

Zhu, X.-D., Küster, B., Mann, M., Petrini, J. H. J., & Lange, T. De. (2000). Cell-cycle-regulated association of RAD50/MRE11/NBS1 with TRF2 and human telomeres. *Nature genetics*, *25*, 347–352.

Zhu, X.-D., Niedernhofer, L., Kuster, B., Mann, M., Hoeijmakers, J. H. J., & de Lange, T. (2003). ERCC1/XPF removes the 3' overhang from uncapped telomeres and represses formation of telomeric DNA-containing double minute chromosomes. *Molecular cell*, *12*(6), 1489–98.

APPENDIX I STATISTICAL RESULTS

One-way ANOVA and Tukey HSD (multiple comparisons of means, 95% family-wise confidence level) tests were performed using the statistical software R (R Core Team, 2014). Presented below are the results from these tests for the indicated figures. Significant differences ($p<0.05$) are displayed on the graphs as different letters above columns. The significance codes (Sig) are: 0 '***' 0.001 '**' 0.01 '*' 0.05 '.' 0.1 ' ' 1.

	ANOVA			
Fig3.1	***Df* (groups, residuals)**	***F* value**	***p***	**Sig**
3.1A pRS, shTRF1				
Small, medium & large	1,4	1.401	0.302	
Medium & large	1,4	15.84	0.0164	*
Large	1,4	0.25	0.643	
3.1B Vector, shTRF1	1,4	4.907	0.0911	.

	ANOVA			
Fig3.2	***Df* (groups, residuals)**	***F* value**	***p***	**Sig**
3.2B Vector, shTRF1	1,8	39.27	0.000241	***
3.2E Vector, TRF1	1,6	13.77	0.00996	**

Fig3.3	***Df* (groups, residuals)**	***F* value**	***p***	**Sig**
3.3B TRF1, pT371	1,4	1170	4.36×10^{-6}	***

	ANOVA				Tukey HSD
Fig3.5	***Df* (groups, residuals)**	***F* value**	***p***	**Sig**	
3.5A TRF1, pT371	1,4	0.695	0.451		
3.5B pRS, shTRF1	1,4	8.653	0.0423	*	
3.5D pRS/vector (V), shTRF1/vector (KD), shTRF1/TRF1 (WT)	2,15	19.55	6.63×10^{-5}	***	KD-V 0.0002024 WT-V 0.9998479 WT-KD 0.0001962

	ANOVA				Tukey HSD	
Fig3.8	***Df* (groups, residuals)**	***F* value**	***p***	**Sig**		
3.8D	4,10	18.97	0.000116	***	shATM-pRS	0.0011584
					shBRCA1-pRS	0.0016886
					sh53BP1.A-pRS	0.4356198
					sh53BP1.B-pRS	0.9472110
					shBRCA1-shATM	0.9983837
					sh53BP1.A-shATM	0.0146486
					sh53BP1.B-shATM	0.0004616
					sh53BP1.A-shBRCA1	0.0225419
					sh53BP1.B-shBRCA1	0.0006566
					sh53BP1.B-sh53BP1.A	0.1674682
3.8E	4,10	6.585	0.00729	**	shATM-pRS	0.9855893
					shBRCA1-pRS	0.0781081
					sh53BP1.A-pRS	0.0370576
					sh53BP1.B-pRS	0.9874765

					shBRCA1-shATM 0.1656002 sh53BP1.A-shATM 0.0802900 sh53BP1.B-shATM 0.8583555 sh53BP1.A-shBRCA1 0.9874132 sh53BP1.B-shBRCA1 0.0370952 sh53BP1.B-sh53BP1.A 0.0176397
3.8F	4,10	2.166	0.147		
3.8G	4,10	0.54	0.71		

	ANOVA			
Fig3.9 pRS, sh53BP1-B	***Df* (groups, residuals)**	***F* value**	***p***	**Sig**
3.9B	1,4	3.689	0.127	
3.9C	1,4	6.222	0.0672	.

	ANOVA				**Tukey HSD**
Fig10	***Df* (groups, residuals)**	***F* value**	***p***	**Sig**	**DMSO, KU55933 (KU), Mirin, NU7026**
3.10B	3,8	14.02	0.0015	**	KU-DMSO 0.0022132 Mirin-DMSO 0.0063800 NU7026-DMSO 0.4580858 Mirin-KU 0.8127623 NU7026-KU 0.0149352 NU7026-Mirin 0.0504170
3.10C	3,8	1.867	0.213		
3.10D	3,8	5.708	0.0218	*	KU-DMSO 0.1023994 Mirin-DMSO 0.7463265 NU7026-DMSO 0.5827446 Mirin-KU 0.3920333 NU7026-KU 0.0165800 NU7026-Mirin 0.1716062
3.10E	3,8	6.43	0.0159	*	KU-DMSO 0.0708504 Mirin-DMSO 0.9832384 NU7026-DMSO 0.6743473 Mirin-KU 0.0428200 NU7026-KU 0.0145634 NU7026-Mirin 0.8580916

	ANOVA			
Fig3.11	***Df* (groups, residuals)**	***F* value**	***p***	**Sig**
3.11B				
DMSO, KU55933	1,4	23.81	0.00817	**
DMSO, Mirin	1,4	57.78	0.00161	**
3.11C				
DMSO, KU55933	1,4	1.4	0.302	
DMSO, Mirin	1,4	12.91	0.0229	*

	ANOVA				**Tukey HSD**
Fig3.12	***Df* (groups, residuals)**	***F* value**	***p***	**Sig**	**shTRF1/TRF1 (WT), shTRF1/T371A (A), shTRF1/T371D (D)**
3.12F	2,15	38.6	1.22×10^{-6}	***	A-WT 0.0000017 D-WT 0.0000181 D-A 0.3285973
3.12G	2,15	6.861	0.00766	**	A-WT 0.9228424 D-WT 0.0107735

					D-A 0.0230120

	ANOVA				Tukey HSD
Fig3.13	***Df* (groups, residuals)**	***F* value**	***p***	**Sig**	**pRS/vector (V), shTRF1/vector (KD), shTRF1/TRF1 (WT), shTRF1/T371A (A), shTRF1/T371D (D)**
3.13B	4,25	70.65	$2.96x10^{-13}$	***	KD-V 0.0000162 WT-V 1.0000000 A-V 0.0000000 D-V 0.0000000 WT-KD 0.0000155 A-KD 0.0000155 D-KD 0.0002711 A-WT 0.0000000 D-WT 0.0000000 D-A 0.7856349
3.13D	4,40	21.76	$1.35x10^{-9}$	***	KD-V 0.0000842 WT-V 0.9992524 A-V 0.0000007 D-V 0.0000010 WT-KD 0.0001781 A-KD 0.5697049 D-KD 0.6509529 A-WT 0.0000015 D-WT 0.0000023 D-A 0.9999330
3.13E	4,25	71.92	$2.41x10^{-13}$	***	KD-V 0.0000000 WT-V 0.0004185 A-V 0.0000000 D-V 0.0000000 WT-KD 0.0022524 A-KD 0.0001640 D-KD 0.0027398 A-WT 0.0000000 D-WT 0.0000001 D-A 0.7981311
3.13F	4,10	158.1	$5.42x10^{-9}$	***	KD-V 0.0000212 WT-V 0.9680324 A-V 0.0000001 D-V 0.0000000 WT-KD 0.0000391 A-KD 0.0002979

					D-KD 0.0000111 A-WT 0.0000002 D-WT 0.0000000 D-A 0.0600046
3.13G	4,25	60.06	$1.86x10^{-12}$	***	KD-V 0.0000000 WT-V 0.7391048 A-V 0.0000000 D-V 0.0000000 WT-KD 0.0000000 A-KD 0.9955741 D-KD 0.9805472 A-WT 0.0000000 D-WT 0.0000000 D-A 0.8838568
3.13H	4,10	60.07	$5.9x10^{-7}$	***	KD-V 0.0193902 WT-V 0.2639492 A-V 0.0000208 D-V 0.0000116 WT-KD 0.0008761 A-KD 0.0018008 D-KD 0.0007852 A-WT 0.0000031 D-WT 0.0000019 D-A 0.9672442

	ANOVA				**Tukey HSD**
Fig3.14	***Df* (groups, residuals)**	***F* value**	***p***	**Sig**	
3.14B	3,8	31.28	$9.07x10^{-5}$	***	TRF1-vector 0.0003508 T371A-vector 0.0435961 T371D-vector 0.0001137 T371A-TRF1 0.0146622 T371D-TRF1 0.6071839 T371D-T371A 0.0030046

	ANOVA				**Tukey HSD**
Fig3.15	***Df* (groups, residuals)**	***F* value**	***p***	**Sig**	**WT (TRF1), ΔM (M), ΔM-A (MA), ΔM-D (MD), ΔAΔM (AM), ΔAΔM-A (AMA), ΔAΔM-D (AMD), L-M (LM), L-M-A (LMA), L-M-D (LMD)**
3.15F	9,20	22.86	$1.22x10^{-8}$	***	AM-TRF1 0.9559551 AMA-TRF1 0.9999993 AMD-TRF1 0.9999985

					M-TRF1 0.9999563 MA-TRF1 0.9249933 MD-TRF1 0.7631554 LM-TRF1 0.0000080 LMA-TRF1 0.0000247 LMD-TRF1 0.0000029 AMA-AM 0.9928927 AMD-AM 0.9941890 M-AM 0.9986057 MA-AM 1.0000000 MD-AM 0.9999503 LM-AM 0.0000980 LMA-AM 0.0003279 LMD-AM 0.0000328 AMD-AMA 1.0000000 M-AMA 1.0000000 MA-AMA 0.9835887 MD-AMA 0.9019423 LM-AMA 0.0000145 LMA-AMA 0.0000458 LMD-AMA 0.0000052 M-AMD 1.0000000 MA-AMD 0.9861065 MD-AMD 0.9109212 LM-AMD 0.0000153 LMA-AMD 0.0000484 LMD-AMD 0.0000054 MA-M 0.9956929 MD-M 0.9543586 LM-M 0.0000210 LMA-M 0.0000672 LMD-M 0.0000074 MD-MA 0.9999955 LM-MA 0.0001267

					LMA-MA 0.0004266 LMD-MA 0.0000421 LM-MD 0.0002804 LMA-MD 0.0009609 LMD-MD 0.0000913 LMA-LM 0.9998447 LMD-LM 0.9999138 LMD-LMA 0.9789153

	ANOVA				**Tukey HSD**
Fig3.16	***Df* (groups, residuals)**	***F* value**	***p***	**Sig**	**V (pWZL), KD (shTRF1), WT (TRF1), ΔM (M), ΔM-A (MA), ΔM-D (MD), ΔAΔM (AM), ΔAΔM-A (AMA), ΔAΔM-D (AMD), L-M (LM), L-M-A (LMA), L-M-D (LMD)**
3.16A	14,66	22.35	$<2x10^{-16}$	***	shTRF1-pWZL 0.0000000 TRF1-pWZL 0.9036742 L-pWZL 0.0000000 LA-pWZL 0.0000000 LD-pWZL 0.0000006 AM-pWZL 0.0000000 AMA-pWZL 0.0000000 AMD-pWZL 0.0000000 M-pWZL 0.0000041 MA-pWZL 0.0000000 MD-pWZL 0.0000001 LM-pWZL 0.9581714 LMA-pWZL 0.9999999 LMD-pWZL 0.5198961 TRF1-shTRF1 0.0000002 L-shTRF1 0.9882156 LA-shTRF1 0.4473201 LD-shTRF1 0.9986668 AM-shTRF1 0.9998815 AMA-shTRF1 0.9976644 AMD-shTRF1 0.8156343 M-shTRF1 1.0000000 MA-shTRF1 0.7180176 MD-shTRF1 0.9995436 LM-shTRF1 0.0019918 LMA-shTRF1 0.0000382 LMD-shTRF1 0.0282624

					L-TRF1 0.0000000 LA-TRF1 0.0000000 LD-TRF1 0.0003004 AM-TRF1 0.0000001 AMA-TRF1 0.0000000 AMD-TRF1 0.0000000 M-TRF1 0.0004872 MA-TRF1 0.0000002 MD-TRF1 0.0000151 LM-TRF1 1.0000000 LMA-TRF1 0.9999827 LMD-TRF1 0.9975144 LA-L 0.9991030 LD-L 0.6385144 AM-L 1.0000000 AMA-L 1.0000000 AMD-L 0.9999997 M-L 0.9997233 MA-L 0.9995673 MD-L 1.0000000 LM-L 0.0001318 LMA-L 0.0000025 LMD-L 0.0022138 LD-LA 0.0922839 AM-LA 0.9735782 AMA-LA 0.9950100 AMD-LA 0.9999999 M-LA 0.8873265 MA-LA 1.0000000 MD-LA 0.9997490 LM-LA 0.0000047 LMA-LA 0.0000001 LMD-LA 0.0000989 AM-LD 0.8898469 AMA-LD 0.7628864 AMD-LD 0.2822760 M-LD 0.9998820 MA-LD 0.2669507 MD-LD 0.9100303 LM-LD 0.0558996

					LMA-LD 0.0024304 LMD-LD 0.3284674 AMA-AM 1.0000000 AMD-AM 0.9995799 M-AM 0.9999992 MA-AM 0.9894980 MD-AM 1.0000000 LM-AM 0.0004920 LMA-AM 0.0000104 LMD-AM 0.0072635 AMD-AMA 0.9999866 M-AMA 0.9999661 MA-AMA 0.9979049 MD-AMA 1.0000000 LM-AMA 0.0002344 LMA-AMA 0.0000047 LMD-AMA 0.0037359 M-AMD 0.9853226 MA-AMD 0.9999997 MD-AMD 0.9999998 LM-AMD 0.0000241 LMA-AMD 0.0000004 LMD-AMD 0.0004589 MA-M 0.9338611 MD-M 0.9999824 LM-M 0.0243242 LMA-M 0.0014030 LMD-M 0.1452424 MD-MA 0.9997959 LM-MA 0.0000771 LMA-MA 0.0000025 LMD-MA 0.0009361 LM-MD 0.0021937 LMA-MD 0.0000904 LMD-MD 0.0195833 LMA-LM 0.9998813 LMD-LM 0.9999951 LMD-LMA 0.9617145
3.16B	14,66	20.48	$<2x10^{-16}$	***	shTRF1-pWZL 0.0000001 TRF1-pWZL 0.9996286

					L-pWZL 0.0000000 LA-pWZL 0.0000001 LD-pWZL 0.0017378 AM-pWZL 0.0000194 AMA-pWZL 0.0000000 AMD-pWZL 0.0000004 M-pWZL 0.0011514 MA-pWZL 0.0000200 MD-pWZL 0.0587146 LM-pWZL 0.9968326 LMA-pWZL 0.9317522 LMD-pWZL 0.2147689 TRF1-shTRF1 0.0000070 L-shTRF1 0.9615937 LA-shTRF1 0.9998459 LD-shTRF1 0.9249208 AM-shTRF1 0.9999999 AMA-shTRF1 0.7895300 AMD-shTRF1 1.0000000 M-shTRF1 1.0000000 MA-shTRF1 0.9999467 MD-shTRF1 0.9694573 LM-shTRF1 0.0000048 LMA-shTRF1 0.0000007 LMD-shTRF1 0.0000000 L-TRF1 0.0000002 LA-TRF1 0.0000025 LD-TRF1 0.0281985 AM-TRF1 0.0005135 AMA-TRF1 0.0000000 AMD-TRF1 0.0000138 M-TRF1 0.0114055 MA-TRF1 0.0002710 MD-TRF1 0.2850611 LM-TRF1 0.8575858 LMA-TRF1 0.5470123 LMD-TRF1 0.0396802 LA-L 0.9999989 LD-L 0.1905285 AM-L 0.8593271 AMA-L 1.0000000

					AMD-L 0.9995038 M-L 0.9833243 MA-L 1.0000000 MD-L 0.3952504 LM-L 0.0000002 LMA-L 0.0000000 LMD-L 0.0000000 LD-LA 0.5411430 AM-LA 0.9938521 AMA-LA 0.9994478 AMD-LA 1.0000000 M-LA 0.9997984 MA-LA 1.0000000 MD-LA 0.7305288 LM-LA 0.0000013 LMA-LA 0.0000002 LMD-LA 0.0000000 AM-LD 0.9984474 AMA-LD 0.0727910 AMD-LD 0.8025050 M-LD 0.9993710 MA-LD 0.7647701 MD-LD 1.0000000 LM-LD 0.0020793 LMA-LD 0.0003986 LMD-LD 0.0000045 AMA-AM 0.6119755 AMD-AM 0.9998927 M-AM 1.0000000 MA-AM 0.9978877 MD-AM 0.9989874 LM-AM 0.0000778 LMA-AM 0.0000129 LMD-AM 0.0000001 AMD-AMA 0.9843095 M-AMA 0.9113400 MA-AMA 0.9999901 MD-AMA 0.2141639 LM-AMA 0.0000000 LMA-AMA 0.0000000 LMD-AMA 0.0000000

					M-AMD 0.9999990 MA-AMD 1.0000000 MD-AMD 0.8990496 LM-AMD 0.0000049 LMA-AMD 0.0000008 LMD-AMD 0.0000000 MA-M 0.9998673 MD-M 0.9993577 LM-M 0.0007977 LMA-M 0.0001831 LMD-M 0.0000037 MD-MA 0.8401882 LM-MA 0.0000290 LMA-MA 0.0000060 LMD-MA 0.0000001 LM-MD 0.0229738 LMA-MD 0.0065652 LMD-MD 0.0001887 LMA-LM 1.0000000 LMD-LM 0.9829391 LMD-LMA 0.9994122
3.16C	14,93	20.63	$<2x10^{-16}$	***	shTRF1-pWZL 0.0000000 TRF1-pWZL 0.7471509 L-pWZL 0.0000000 LA-pWZL 0.0000000 LD-pWZL 0.0000000 AM-pWZL 0.0000000 AMA-pWZL 0.0000000 AMD-pWZL 0.0000000 M-pWZL 0.0000000 MA-pWZL 0.0000000 MD-pWZL 0.0000000 LM-pWZL 0.0000000 LMA-pWZL 0.0000000 LMD-pWZL 0.0000000 TRF1-shTRF1 0.0000001 L-shTRF1 1.0000000 LA-shTRF1 1.0000000 LD-shTRF1 1.0000000 AM-shTRF1 0.4540793 AMA-shTRF1 0.6519023

					AMD-shTRF1 0.4668487 M-shTRF1 0.9806942 MA-shTRF1 1.0000000 MD-shTRF1 0.9031666 LM-shTRF1 1.0000000 LMA-shTRF1 0.9207692 LMD-shTRF1 0.6069179 L-TRF1 0.0000102 LA-TRF1 0.0000358 LD-TRF1 0.0000072 AM-TRF1 0.0000000 AMA-TRF1 0.0000000 AMD-TRF1 0.0000000 M-TRF1 0.0000000 MA-TRF1 0.0000329 MD-TRF1 0.0000000 LM-TRF1 0.0000061 LMA-TRF1 0.0000000 LMD-TRF1 0.0000000 LA-L 1.0000000 LD-L 1.0000000 AM-L 0.7990974 AMA-L 0.9115817 AMD-L 0.8081028 M-L 0.9989189 MA-L 1.0000000 MD-L 0.9885828 LM-L 1.0000000 LMA-L 0.9915584 LMD-L 0.8906062 LD-LA 1.0000000 AM-LA 0.6323011 AMA-LA 0.7904843 AMD-LA 0.6435340 M-LA 0.9905955 MA-LA 1.0000000 MD-LA 0.9502269 LM-LA 1.0000000 LMA-LA 0.9598011 LMD-LA 0.7572715

					AM-LD 0.8371665 AMA-LD 0.9342238 AMD-LD 0.8452302 M-LD 0.9994837 MA-LD 1.0000000 MD-LD 0.9930751 LM-LD 1.0000000 LMA-LD 0.9950313 LMD-LD 0.9168245 AMA-AM 1.0000000 AMD-AM 1.0000000 M-AM 0.9998423 MA-AM 0.6447480 MD-AM 0.9999984 LM-AM 0.8532318 LMA-AM 0.9999963 LMD-AM 1.0000000 AMD-AMA 1.0000000 M-AMA 0.9999963 MA-AMA 0.8006613 MD-AMA 1.0000000 LM-AMA 0.9431440 LMA-AMA 1.0000000 LMD-AMA 1.0000000 M-AMD 0.9998717 MA-AMD 0.6559036 MD-AMD 0.9999989 LM-AMD 0.8608352 LMA-AMD 0.9999973 LMD-AMD 1.0000000 MA-M 0.9917102 MD-M 1.0000000 LM-M 0.9996415 LMA-M 1.0000000 LMD-M 0.9999901 MD-MA 0.9543261 LM-MA 1.0000000 LMA-MA 0.9633029 LMD-MA 0.7681564 LM-MD 0.9945852

					LMA-MD 1.0000000 LMD-MD 1.0000000 LMA-LM 0.9961719 LMD-LM 0.9273338 LMD-LMA 0.9999999
3.16D	10,22	14.29	$1.93x10^{-7}$	***	shTRF1-pWZL 0.0005021 TRF1-pWZL 0.9956192 L-pWZL 0.0089814 LA-pWZL 0.0000620 AM-pWZL 0.0000487 AMA-pWZL 0.0000030 M-pWZL 0.0089453 MA-pWZL 0.0014801 LM-pWZL 0.8102213 LMA-pWZL 0.9739467 TRF1-shTRF1 0.0044629 L-shTRF1 0.9672293 LA-shTRF1 0.9963927 AM-shTRF1 0.9915612 AMA-shTRF1 0.4457366 M-shTRF1 0.9675310 MA-shTRF1 0.9999906 LM-shTRF1 0.0252948 LMA-shTRF1 0.0081493 L-TRF1 0.0705649 LA-TRF1 0.0005296 AM-TRF1 0.0004130 AMA-TRF1 0.0000226 M-TRF1 0.0703101 MA-TRF1 0.0129821 LM-TRF1 0.9991970 LMA-TRF1 1.0000000 LA-L 0.5378499 AM-L 0.4720567 AMA-L 0.0482494 M-L 1.0000000 MA-L 0.9990540 LM-L 0.2887181 LMA-L 0.1187131 AM-LA 1.0000000 AMA-LA 0.9331221

					M-LA 0.5389475 MA-LA 0.9367276 LM-LA 0.0031242 LMA-LA 0.0009709 AMA-AM 0.9589608 M-AM 0.4731150 MA-AM 0.9031378 LM-AM 0.0024335 LMA-AM 0.0007563 M-AMA 0.0484302 MA-AMA 0.2189597 LM-AMA 0.0001241 LMA-AMA 0.0000402 MA-M 0.9990719 LM-M 0.2879102 LMA-M 0.1183102 LM-MA 0.0684278 LMA-MA 0.0233150 LMA-LM 0.9999809
3.16E	6,14	3.734	0.0198	*	KD-V 0.0149491 WT-V 0.9468357 M-V 0.2146005 AM-V 0.0690056 LM-V 0.2664583 L-V 0.1925778 WT-KD 0.0888478 M-KD 0.7215044 AM-KD 0.9745923 LM-KD 0.6385822 L-KD 0.7596990 M-WT 0.7122119 AM-WT 0.3364918 LM-WT 0.7899951 L-WT 0.6723366 AM-M 0.9914153 LM-M 0.9999989 L-M 1.0000000 LM-AM 0.9773598

					L-AM 0.9951434 L-LM 0.9999882
3.16F	8,18	1.164	0.372		

	ANOVA				**Tukey HSD**
Fig3.17	***Df* (groups, residuals)**	***F* value**	***p***	**Sig**	**pRS/pWZL (V), shTRF1/pWZL (KD), shTRF1/TRF1sm (WT), shTRF1/R425V (RV), shTRF1/R425V-T371A (RVA), shTRF1/R425V-T371D (RVD)**
3.17D	3,8	1.04	0.426		
3.17E	3,8	2.312	0.153		
3.17F	5,12	18.86	$2.6x10^{-5}$	***	KD-V 0.0053265 WT-V 0.8267039 RV-V 0.0075187 RVA-V 0.0000889 RVD-V 0.0001054 WT-KD 0.0401710 RV-KD 0.9999291 RVA-KD 0.1353455 RVD-KD 0.1650561 RV-WT 0.0569886 RVA-WT 0.0004784 RVD-WT 0.0005776 RVA-RV 0.0969642 RVD-RV 0.1190484 RVD-RVA 0.9999938
3.17G	5,12	17.5	$3.83x10^{-5}$	***	KD-V 0.0039434 WT-V 0.9391393 RV-V 0.0006697 RVA-V 0.0013612 RVD-V 0.0202175 WT-KD 0.0009532 RV-KD 0.8582608 RVA-KD 0.9822586 RVD-KD 0.9151931 RV-WT 0.0001828 RVA-WT 0.0003532 RVD-WT 0.0045050 RVA-RV 0.9965795 RVD-RV 0.3410757 RVD-RVA 0.5842676
3.17H	5,12	22.76	$9.73x10^{-6}$	***	KD-V 0.0084141

					WT-V	0.7346887
					RV-V	0.0003515
					RVA-V	0.0001043
					RVD-V	0.0000258
					WT-KD	0.0859213
					RV-KD	0.3796775
					RVA-KD	0.1054880
					RVD-KD	0.0170434
					RV-WT	0.0029147
					RVA-WT	0.0007481
					RVD-WT	0.0001555
					RVA-RV	0.9460368
					RVD-RV	0.4132151
					RVD-RVA	0.8758271